Variational Principles for Circle Patterns

vorgelegt von
Dipl.-Math. Boris A. Springborn

von der Fakultät II – Mathematik und Naturwissenschaften
der Technischen Universität Berlin
zur Erlangung des akademischen Grades

Doktor der Naturwissenschaften
– Dr. rer. nat. –

genehmigte Dissertation

Promotionsausschuss

Vorsitzender: Prof. Dr. Michael E. Pohst
Gutachter/Berichter: Prof. Dr. Alexander I. Bobenko
Prof. Dr. Günter M. Ziegler

Tag der wissenschaftlichen Aussprache: 27. November 2003

Abstract

A Delaunay cell decomposition of a surface with constant curvature gives rise to a circle pattern, consisting of the circles which are circumscribed to the facets. We treat the problem whether there exists a Delaunay cell decomposition for a given (topological) cell decomposition and given intersection angles of the circles, whether it is unique and how it may be constructed. Somewhat more generally, we allow cone-like singularities in the centers and intersection points of the circles. We prove existence and uniqueness theorems for the solution of the circle pattern problem using a variational principle. The functionals (one for the euclidean, one for the hyperbolic case) are convex functions of the radii of the circles. The critical points correspond to solutions of the circle pattern problem. The analogous functional for the spherical case is not convex, hence this case is treated by stereographic projection to the plane. From the existence and uniqueness of circle patterns in the sphere, we derive a strengthened version of Steinitz' theorem on the geometric realizability of abstract polyhedra.

We derive the variational principles of Colin de Verdière, Brägger, and Rivin for circle packings and circle patterns from our variational principles. In the case of Brägger's and Rivin's functionals, this requires a Legendre transformation of our euclidean functional. The respective Legendre transformations of the hyperbolic and spherical functionals lead to new variational principles. The variables of the transformed functionals are certain angles instead of radii. The transformed functionals may be interpreted geometrically as volumes of certain three-dimensional polyhedra in hyperbolic space. Leibon's functional for hyperbolic circle patterns cannot be derived from our functionals. But we construct yet another functional from which both Leibon's and our functionals can be derived. By applying the inverse Legendre transformation to Leibon's functional, we obtain a new variational principle for hyperbolic circle patterns.

We present Java software to compute and visualize circle patterns.

Zusammenfassung

Eine Delaunay-Zellzerlegung einer Fläche konstanter Krümmung liefert ein Kreismuster, welches aus den Kreisen besteht, die den Facetten umschrieben sind. Wir betrachten das Problem, ob es für eine vorgegebene (topologische) Zellzerlegung und vorgegebene Schnittwinkel zwischen den Kreisen eine entsprechende Delaunay-Zellzerlegung gibt, ob sie eindeutig ist, und wie sie zu konstruieren ist. Etwas allgemeiner lassen wir auch kegelartige Singularitäten in den Mittel- und Schnittpunkten der Kreise zu. Wir beweisen Existenz- und Eindeutigkeitssätze für die Lösung des Kreismusterproblems mit Hilfe von Variationsprinzipien. Die Funktionale (eins für den euklidischen, eins für den hyperbolischen Fall) sind konvexe Funktionen der Radien der Kreise. Kritische Punkte entsprechen Lösungen des Kreismusterproblems. Das analoge Funktional für den sphärischen Fall ist nicht konvex, deshalb wird dieser Fall durch stereographische Projektion in die Ebene erledigt. Aus der Existenz und Eindeutigkeit von Kreismustern in der Sphäre folgern wir eine verschärfte Version des Satzes von Steinitz über die geometrische Realisierbarkeit von abstrakten Polyedern.

Wir leiten die Variationsprinzipien von Colin de Verdière, Brägger und Rivin für Kreispackungen bzw. Kreismuster aus unseren Variationsprinzipien ab. Im Fall der Funktionale von Brägger und Rivin erfordert dies eine Legendretransformation unseres euklidischen Funktionals. Entsprechende Legendretransformationen des hyperbolischen und des sphärischen Funktionals liefern neue Variationsprinzipien. Die Variablen der transformierten Funktionale sind nicht Radien, sondern bestimmte Winkel. Die transformierten Funktionale besitzen eine geometrische Interpretation als Volumen von bestimmten dreidimensionalen Polyedern im hyperbolischen Raum. Leibons Funktional für hyperbolische Kreismuster lässt sich nicht aus unseren Funktionalen herleiten. Wir konstruieren jedoch ein weiteres Funktional, aus dem sowohl Leibon's als auch unser Funktional hergeleitet werden kann. Durch die umgekehrte Legendretransformation von Leibons Funktional erhalten wir ein neues Variationsprinzip für hyperbolische Kreismuster.

Wir präsentieren Java Software zur Berechnung und Visualisierung von Kreismustern.

Contents

Introduction

1.1. Existence and uniqueness theorems

A *circle packing* is a configuration of circular discs in a surface such that the discs may touch but not overlap. We consider only circle packings in surfaces of constant curvature. Connecting the centers of touching discs by geodesics as in figure 1.1, one obtains an embedded graph, the *adjacency graph* of the packing. Consider the case when the adjacency graph triangulates the surface as in figure 1.1 (*left*). The following theorem of Koebe [**26**] answers the question: Given an abstract triangulation of the sphere, does there exist a circle packing whose adjacency graph is a geometric realization of the abstract triangulation?

THEOREM 1.1 (Koebe). *For every abstract triangulation of the sphere there is a circle packing whose adjacency graph is a geometric realization of the triangulation. The circle packing corresponding to a triangulation is unique up to Möbius transformations of the sphere.*

Now consider the case when the adjacency graph of a circle packing gives rise to a cell decomposition whose faces are not necessarily triangles, as in figure 1.1 (*right*). To characterize the cell decompositions of the sphere which correspond to circle packings, we need the following definition.

DEFINITION. A cell complex is called *regular* if the characteristic maps, that map closed discs onto the closed cells, are homeomorphisms. A cell complex is called *strongly regular* if it is regular and the intersection of two closed cells is empty or equal to a single closed cell.

REMARK. Suppose a cell complex Σ is in fact a cell decomposition of a compact surface without boundary. One obtains the following conditions for Σ being regular and strongly regular.

The cell decomposition Σ is regular if and only if the following conditions hold.

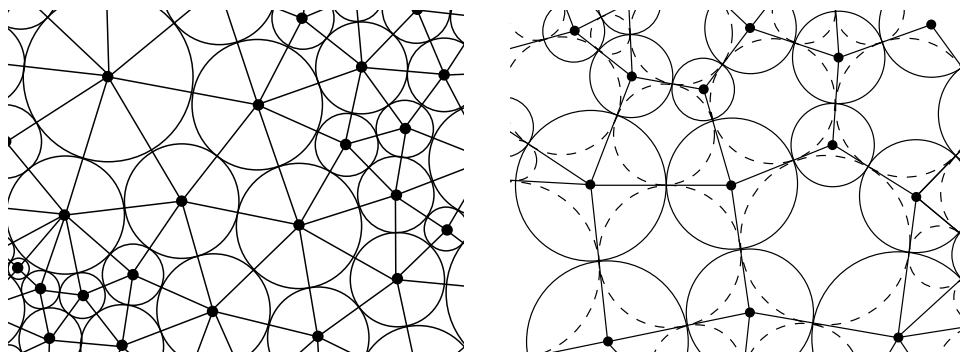*(i)*   Each edge is incident with two vertices. (There are no loops.)

FIGURE 1.1. *Left:* A circle packing corresponding to a triangulation. *Right:* A pair or orthogonally intersecting circle packings corresponding to a cell decomposition.

(ii) Each edge is incident with two faces. (There are no stalks.)

(iii) If a vertex v and a face f are incident, there are exactly two edges incident with both v and f.

The cell decomposition Σ is strongly regular if and only if, in addition, the following conditions hold.

(iv) No two edges are incident with the same two vertices.

(v) No two edges are incident with the same two faces.

(vi) If each of two faces is incident with each of two vertices, then there is an edge which is incident with both faces and both vertices.

The above characterization implies: The cell decomposition Σ is (strongly) regular if and only if its Poincaré-dual decomposition is (strongly) regular.

A cell decomposition of the sphere which arises from a circle packing is strongly regular. Conversely, Koebe's theorem implies that every strongly regular cell decomposition of the sphere comes from a circle packing. (Simply triangulate each face by adding an extra vertex inside and connecting it to the original vertices.) However, the corresponding packing is generally not unique up to Möbius transformations. The following theorem is a generalization of Koebe's theorem which retains uniqueness by requiring the existence of a second packing of orthogonally intersecting circles as in figure 1.1 *(right)*.

THEOREM 1.2. *For every strongly regular cell decomposition of the sphere, there exists a pair of circle packings with the following properties: The adjacency graph of the first packing is a geometric realization of the given cell decomposition. The adjacency graph of the second packing is a geometric realization of the Poincaré dual of the given cell decomposition. Therefore, to each edge there correspond four circles which touch in pairs. It is required that these pairs touch in the same point and intersect each other orthogonally.*

The pair of circle packings is unique up to Möbius transformations of the sphere.

In the case of a circle packing corresponding to a triangulation as in Koebe's theorem, the second orthogonal packing always exists. Thus, theorem 1.2 is indeed a generalization of Koebe's theorem. The first published proof is probably due to Brightwell and Scheinerman [**13**]. They do not claim to give the first proof. The works of Thurston [**45**] and Schramm [**40**] (see theorem 1.4 below) indicate that the theorem was well established at the time.

Associated with a polyhedron in $\mathbb{R}^3$ is a cell decomposition of the sphere representing its combinatorial type. We say that the polyhedron is a (geometric) realization of the cell decomposition. Steinitz' representation theorem for convex polyhedra in $\mathbb{R}^3$ says that a cell decomposition of the sphere represents the combinatorial type of a convex polyhedron if and only if it is strongly regular [**43**], [**44**]. Theorem 1.2 implies the following stronger representation theorem for convex polyhedra in $\mathbb{R}^3$ (see Ziegler [**47**], theorem 4.13 on p. 118).

THEOREM 1.3. *For every strongly regular cell decomposition of the sphere there is a convex polyhedron in $\mathbb{R}^3$ which realizes it, such that the edges of the polyhedron are tangent to the unit sphere. Such a geometric realization is unique up to projective transformations which fix the sphere.*

Simultaneously, there is a polyhedron with edges tangent to the sphere which realizes the Poincaré-dual cell decomposition such that corresponding edges of the two polyhedra intersect each other orthogonally and touch the sphere in their point of intersection.

Among the projectively equivalent polyhedral realizations, there is one and up to isometries only one with the property that the barycenter of the points where the
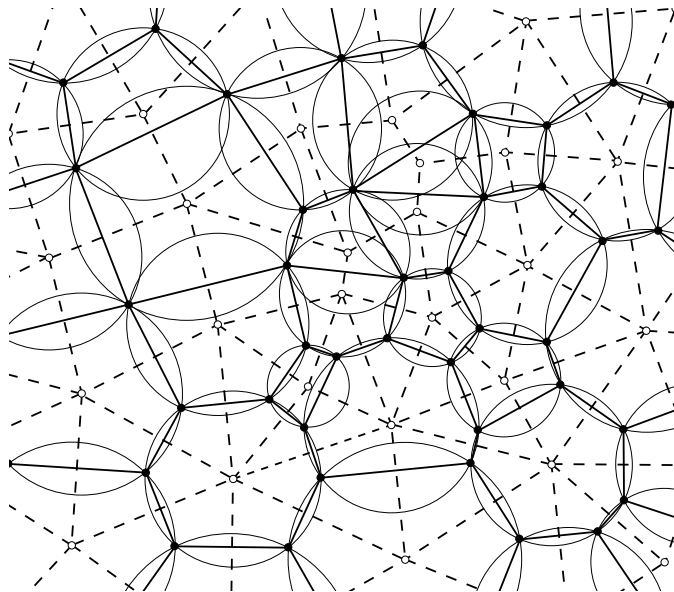
FIGURE 1.2. A Delaunay type circle pattern with Delaunay and Dirichlet cell decompositions.

edges touch the sphere is the center of the sphere. Every topological symmetry of the cell decomposition corresponds to an isometry of this polyhedral realization.

The following much more general theorem is due to Schramm [**40**]. The proof is based on topological methods which are beyond the scope of this thesis.

THEOREM 1.4 (Schramm). *Let P be a (3-dimensional) convex polyhedron, and let $K \subset \mathbb{R}^3$ be a smooth strictly convex body. Then there exists a convex polyhedron $Q \subset \mathbb{R}^3$ combinatorially equivalent to P whose edges are tangent to K.*

The two circle packings of theorem 1.2 form a pattern of orthogonally intersecting circles. By way of a further generalization, one may consider circle patterns with circles intersecting at arbitrary angles.

'DEFINITION'. A *circle pattern* is a configuration of circles in a constant curvature surface which corresponds in some way to a cell decomposition of the surface. According as the constant curvature is positive, zero, or negative, we speak of *spherical*, *euclidean*, or *hyperbolic circle patterns*.

To obtain a real definition, the correspondence between circle pattern and cell decomposition has to be specified. We will only be concerned with a special class of circle patterns which are connected to Delaunay cell decompositions. To be precise, we call them 'Delaunay type circle patterns', but we will usually refer to them simply as 'circle patterns'. Figure 1.2 shows an example.

DEFINITION. A *Delaunay decomposition* of a constant curvature surface is a cellular decomposition such that the boundary of each face is a geodesic polygon which is inscribed in a circular disc, and these discs have no vertices in their interior. The Poincaré-dual decomposition of a Delaunay decomposition with the centers of the circles as vertices and geodesic edges is a *Dirichlet decomposition* (or *Voronoi diagram*). A *Delaunay type circle pattern* is the circle pattern formed by the circles of a Delaunay decomposition. More generally, we allow the constant curvature surface to have cone-like singularities in the vertices and in the centers of the circles.
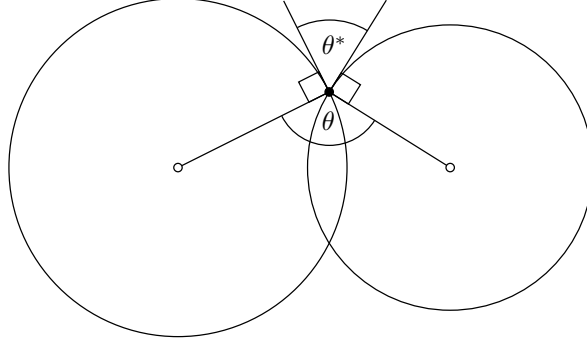
FIGURE 1.3. Interior intersection angle θ^* and exterior intersection angle θ of two circles. $\theta + \theta^* = \pi$.

Figure 1.2 shows a Delaunay decomposition (black vertices and solid lines), the dual Dirichlet decomposition (white vertices and dashed lines) and the corresponding circle pattern. The faces of the Delaunay decomposition correspond to circles. The vertices are intersection points of circles.

REMARK. In section 2.1, we will give an alternative and slightly more general definition for Delaunay type circle patterns.

A different class of circle patterns, *Thurston type circle patterns*, has been introduced by Thurston [**45**]. Here, the circles correspond to the faces of a cell decomposition, but the vertices do not correspond to intersection points. All vertices have degree 3. Two circles corresponding to faces which share a common edge intersect (or touch) with an interior intersection angle θ^* (see figure 1.3) satisfying $0 \leq \theta^* \leq \pi/2$.

Those Thurston type circle patterns in the sphere with the property that the sum of the three angles θ around each vertex is less or equal to 2π correspond to hyperbolic polyhedra of finite volume with dihedral angles at most $\pi/2$. Such polyhedra have been studied by Andreev [**1**], [**2**]. Delaunay type circle patterns in the sphere (without cone-like singularities) correspond to convex hyperbolic polyhedra with finite volume and all vertices on the infinite boundary of hyperbolic space.

From a Delaunay type circle pattern, one may obtain the following data. (For the definition of *interior* and *exterior intersection angle* of two circles see figure 1.3. We will always denote the exterior intersection angle by θ and the interior intersection angle by θ^*. Note that $\theta + \theta^* = \pi$.)

- A cell decomposition Σ of a 2-dimensional manifold.
- For each edge e of Σ the exterior (or interior) intersection angle θ_e (or θ_e^*). It satisfies $0 < \theta_e < \pi$.
- For each face f of Σ the cone angle $\Phi_f > 0$ of the cone-like singularity at the center of the circle corresponding to f. (If there is no cone-like singularity at the center, then $\Phi_f = 2\pi$.)

Note that the cone angle Θ_v at a vertex v of Σ is already determined by the intersection angles θ_e:

$$\Theta_v = \sum \theta_e, \tag{1.1}$$

where the sum is taken over all edges around v. (See figure 1.3.) If $\Theta_v = 2\pi$, there is no singularity at v. The curvature in a vertex v is

$$K_v = 2\pi - \Theta_v, \tag{1.2}$$

and the curvature in the center of a face f is

$$K_f = 2\pi - \Phi_f. \tag{1.3}$$

The following theorems assume that the surface is closed, and that there are no cone-like singularities. Only the last theorem 1.8 deals with the general case.

Consider the following problem: Given such data as listed above, is there a corresponding circle pattern? If so, is it unique? The following theorem of Rivin [**35**] gives an answer for circle patterns in the sphere without cone-like singularities.

THEOREM 1.5 (Rivin, circle pattern version). *Let Σ be a strongly regular cell decomposition of the sphere and let an angle θ_e with $0 < \theta_e < \pi$ be given for every edge e of Σ. Let Σ^* be the Poincaré dual decomposition of Σ, and for each edge e of Σ denote the dual edge of Σ^* by e^*.*

A Delaunay pattern corresponding to Σ with exterior intersection angles θ_e exists if and only if the conditions (i) and (ii) are satisfied.

(i) If some edges $e_1^*, \ldots, e_n^*$ form the boundary of a face of Σ^*, then

$$\sum \theta_{e_j} = 2\pi.$$

(ii) If some edges $e_1^*, \ldots, e_n^*$ form a closed path of Σ^* which is not the boundary of a face, then

$$\sum \theta_{e_j} > 2\pi.$$

If it exists, the circle pattern is unique up to Möbius transformations of the sphere.

The paper cited above deals with polyhedra in hyperbolic 3-space with vertices on the infinite boundary. The above theorem has the following, equivalent, form.

THEOREM 1.6 (Rivin, ideal hyperbolic polyhedra version). *Let Σ be a strongly regular cell decomposition of the sphere and let an angle θ_e with $0 < \theta_e < \pi$ be given for every edge e of Σ. Let Σ^* be the Poincaré dual decomposition of Σ, and for each edge e of Σ denote the dual edge of Σ^* by e^*.*

A polyhedron in hyperbolic 3-space with vertices on the infinite boundary which realizes Σ and has exterior dihedral angles θ_e exists if and only if the conditions (i) and (ii) are satisfied.

(i) If the edges $e_1^*, \ldots, e_n^*$ form the boundary of a face of Σ^*, then

$$\sum \theta_{e_j} = 2\pi.$$

(ii) If the edges $e_1^*, \ldots, e_n^*$ form a closed path of Σ^* which is not the boundary of a face, then

$$\sum \theta_{e_j} > 2\pi.$$

If it exists, the polyhedron is unique up to an isometry of hyperbolic space.

Theorem 1.7 below is a generalization of Rivin's theorem 1.5 to higher genus surfaces. Only the case of oriented surfaces has to be considered: Because of the uniqueness claim, non-orientable surfaces may be treated by applying the theorem to the orientable double cover.

In the higher genus case, it is too restrictive to allow only strongly regular cell decompositions. For example, figure 1.4 shows a cell decomposition of the torus which is not even regular and the corresponding circle pattern with orthogonally intersecting circles. With appropriate cone-like singularities in the vertices and centers of circles, even faces whose boundary is a loop and vertices of degree one are possible. As a consequence of this tolerance regarding which cell decompositions are acceptable, theorems 1.7 and 1.8 are really only true for Delaunay type circle patterns in the sense of the slightly more general definition in section 2.1.

The condition of theorem 1.7 does not involve cycles in the Poincaré dual decomposition like theorem 1.5. Instead, one has to consider cellular immersions of
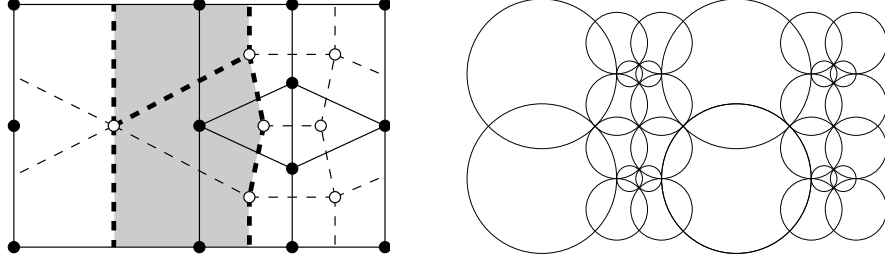
FIGURE 1.4. *Left:* A cell decomposition of a torus (solid lines and black dots) and its Poincaré dual (dashed lines and white dots). The top and bottom side, and the left and right side of the rectangle are identified. *Right:* The corresponding double periodic circle pattern with orthogonally intersecting circles.

discs, whose interior is embedded, into the Poincaré dual decomposition. The image of the boundary path of the disc is a closed path in which some edges might appear twice. For example, the shaded area in figure 1.4 *(left)* is the image of such a disc, where the heavy dashed lines are the image of its boundary. One edge appears twice in the image of the boundary path. The condition of theorem 1.7 is that the sum of θ over such a boundary, where the edges are counted with appropriate multiplicities, is at least 2π.

THEOREM 1.7. *Let Σ be a cell decomposition of a closed compact oriented surface of genus $g > 0$. Suppose exterior intersection angles are prescribed by a function $\theta \in (0, \pi)^E$ on the set E of edges. Then there exists a circle pattern corresponding to these data in a surface of constant curvature (equal to 0 if $g = 1$ and equal to -1 if $g > 1$), if and only if the following condition is satisfied.*

Suppose $\Delta \to \Sigma^*$ is any cellular immersion of a cell decomposition of the closed disc Δ into the Poincaré dual Σ^* of Σ which embeds the interior of Δ. Let $\hat{e}_1, \ldots, \hat{e}_k$ be the boundary edges of Δ, let be $e_1^*, \ldots, e_k^*$ their images in Σ^*, and let $e_1, \ldots, e_k$ be their dual edges in Σ. (An edge of Σ may appear twice among the e_j.) Then

$$\sum_{j=1}^{k} \theta_{e_j} \geq 2\pi, \tag{1.4}$$

where equality holds if and only if Δ has only one face.

In the case they exists, the constant mean curvature surface and the circle pattern are unique up to similarity, if $g = 1$, and unique up to isometry, if $g > 1$.

Schlenker [**39**] independently proves an existence and uniqueness result for hyperbolic manifolds with polyhedral boundary, all vertices at infinity, and prescribed dihedral angles. Theorem 1.7 follows as a special case. Interestingly, to obtain the general result, Schlenker needs to first prove this special case separately.

We deduce theorem 1.7 from the following more technical, but also more general theorem 1.8. It is not assumed that θ sums to 2π around each vertex. Hence there may be cone-like singularities in the vertices with cone angle θ given by equation (1.1). Also, cone-like singularities with prescribed cone angle Φ_f are allowed in the centers of circles. Furthermore, it applies also to surfaces with boundary. For a boundary face f, the angle Φ_f does not prescribe a cone angle, but the angle covered by the neighboring circles, as shown in figure 1.5 *(right)*. These angles on the boundary constitute *Neumann boundary conditions*. Alternatively, one might also prescribe the radii of the boundary circles. This would constitute *Dirichlet boundary conditions*. We consider only the Neumann problem.
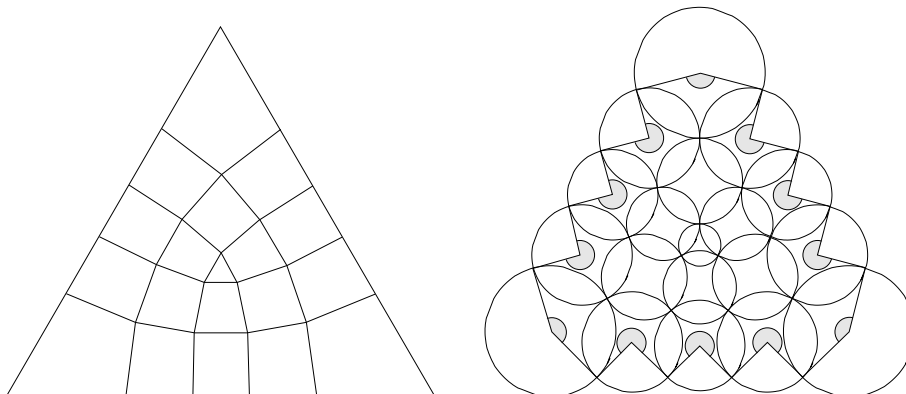
FIGURE 1.5. *Left:* A cell decomposition of the disc. *Right:* A corresponding circle pattern with orthogonally intersecting circles. The shaded angles are the angles Φ for boundary faces. Here, they are $5\pi/6$ for the three corner circles and $3\pi/2$ for the other boundary circles.

THEOREM 1.8. *Let Σ be a cell decomposition of a compact oriented surface, with or without boundary. Suppose (interior) intersection angles are prescribed by a function $\theta^* \in (0, \pi)^{E_0}$ on the set E_0 of interior edges. Let $\Phi \in (0, \infty)^F$ be a function on the set F of faces, which prescribes, for interior faces, the cone angle and, for boundary faces, the Neumann boundary conditions.*

(i) A euclidean circle pattern corresponding to these data exists if and only if the following condition is satisfied:

If $F' \subseteq F$ is any nonempty set of faces and $E' \subseteq E_0$ is the set of all interior edges which are incident with any face $f \in F'$, then

$$\sum_{f \in F'} \Phi_f \leq \sum_{e \in E'} 2\theta_e^*, \tag{1.5}$$

where equality holds if and only if $F' = F$.

If it exists, the circle pattern is unique up to similarity.

(ii) A hyperbolic circle pattern corresponding to these data exists, if and only if, in the above condition, strict inequality holds also in the case $F' = F$. If it exists, the circle pattern is unique up to hyperbolic isometry.

Similar results were obtained by Bowditch [9], Garrett [19], Rivin [36], and Leibon [28]. Bowditch treats the euclidean case for closed surfaces without cone-like singularities in the centers of the circles. His proof is topological in nature: It hinges on the fact that a certain function (essentially the gradient of our functional S_{euc}) is injective and proper. Rivin extends this result to surfaces with boundary. Also, he considers not only singular euclidean structures, but singular similarity structures. That is, he admits not only cone-like singularities (with rotational holonomy) but singularities with dilatational and rotational holonomy. The proof uses his variational principle [34]. Leibon treats the hyperbolic case for closed surfaces and without cone-like singularities. The proof uses his variational principle (see section 3.6). Garrett [19] obtains a similar theorem for euclidean and hyperbolic circle *packings* with prescribed cone-like singularities. He considers the Dirichlet boundary value problem (prescribed radii at the boundary). His proof uses the relaxation method developed by Thurston [45].

1.2. The method of proof

Chapter 2 contains our proofs of the theorems 1.2, 1.3, 1.5, 1.6, 1.7, and 1.8. Here, we give a brief outline of the proofs of theorems 1.8, 1.7, and 1.5, which are the most involved. Most of the effort goes into proving the fundamental theorem 1.8, from which the others are deduced. We extend methods introduced by Colin de Verdière for circle packings [16].

First, the geometric problem of constructing a circle pattern is transformed into the analytic problem of finding the (euclidean or hyperbolic) radii of the circles, which have to satisfy some non-linear equations (closure conditions). These non-linear closure conditions turn out to be variational: The functionals S_{euc} and S_{hyp} (defined in sections 2.3 and 2.4) are functions of the radii, and their critical points are the solutions of the closure conditions. The functionals S_{euc}, S_{hyp} are convex (except for scale-invariance in the euclidean case). This implies the uniqueness claims of theorem 1.8 (section 2.5). The existence claim is more difficult. We have to show that the functionals tend to infinity if some radii go to zero or infinity. In section 2.7, we show that this is the case if a 'coherent angle system' exists. This is a function on the oriented edges, which satisfies a system of linear equations and inequalities. The existence problem for circle patterns is thus reduced to the feasibility problem of a linear program. In section 2.8, we prove the existence of a coherent angle system if the conditions of theorem 1.8 are satisfied. This is done by interpreting a coherent angle system as a feasible flow in a network (with capacity bounds on the branches) and invoking the feasible flow theorem.

In section 2.9, theorem 1.7 for circle patterns in hyperbolic surfaces is deduced from theorem 1.8 using methods of combinatorial topology. The basis of this deduction is lemma 2.14. We present a self-contained proof of it in appendix D.

In section 2.10 the analogous theorem 1.5 for circle patterns in the sphere is deduced from theorem 1.7. First, the problem is transferred to the plane by stereographic projection. Then the proof proceeds in a similar way as in the hyperbolic case.

1.3. Variational principles

In chapter 2, we define the functionals S_{euc}, S_{hyp}, and S_{sph} for euclidean, hyperbolic, and spherical circle patterns. The functional S_{sph} is not convex. Thus, we cannot use it to prove existence and uniqueness theorems. The variables are (up to a coordinate transformation) the (euclidean, hyperbolic, or spherical) radii of the circles. A Legendre transformation of these functionals (section 3.1) leads to a new variational principle involving *one* new functional $\widehat{S}$ for all geometries (euclidean, hyperbolic, and spherical). The variables of $\widehat{S}$ are certain angles; and the variation is constrained to coherent angle systems. Depending on whether the constraint involves euclidean, hyperbolic, or spherical coherent angle systems (section 2.7), the critical points correspond to euclidean, hyperbolic, or spherical circle patterns.

Colin de Verdière first used a variational principle to prove existence and uniqueness for circle packings [16]. He constructs two functionals, one for the euclidean case, one for the hyperbolic case. The variables are the radii of the circles. Critical points correspond to circle packings. Explicit formulas are given only for the derivatives of the functionals, not for the functionals themselves. In section 3.2, we derive Colin de Verdière's functionals from our functionals S_{euc} and S_{hyp}. In particular, this effects the integration of Colin de Verdière's differential formulas.

Apparently, Brägger [12] had already tried to integrate Colin de Verdière's formulas. He derives a new variational principle for euclidean circle packings. The

variables of his functional are certain angles, and the variation is constrained to coherent angle systems. This functional turns out to be related to Colin de Verdière's functional by a Legendre transformation. In section 3.4, we derive it from our functional $\widehat{S}$.

Rivin's functional for euclidean circle patterns [**34**] is also derived from $\widehat{S}$ (section 3.5). It is less general, because the cell decomposition is assumed to be a triangulation, and there can be no curvature in the centers of circles.

Leibon [**27**], [**28**] derived a functional for hyperbolic circle patterns which can be seen as a hyperbolic version of Rivin's functional (section 3.6). It is therefore natural to expect that Leibon's functional can be derived from $\widehat{S}$ as well. However, this is not the case. The Legendre dual of Leibon's functional (section 3.7) is not S_{hyp}, but a new functional. Unfortunately, we cannot present an explicit formula for this functional. In section 4.7, we derive yet another functional, from which both $\widehat{S}$ and Leibon's functional can be derived.

At least since Brägger [**12**], there was an awareness of the fact that the circle packing functionals have something to do with the volume of hyperbolic 3-simplices. Chapter 4 deals with the connection between the circle pattern functionals and the volumes of hyperbolic polyhedra. Schläfli's differential volume formula turns out to be the unifying principle behind all circle pattern functionals. This geometric approach is essential for the construction of the common ancestor of $\widehat{S}$ and Leibon's functional.

Thurston's method to construct circle patterns [**45**] (implemented in Stephenson's program `CirclePack` [**17**]) involves iteratively adjusting the radius of each circle so that the neighboring circles fit around. This is equivalent to minimizing our functionals (S_{euc}, S_{hyp}) iteratively in each coordinate direction.

1.4. Open questions

There is a functional for Thurston type circle patterns (at least in the euclidean case), its variables being the radii of the circles. In fact, Chow and Luo [**14**] show that the corresponding closure conditions are variational. Can an explicit formula be derived? (For Thurston type circle patterns with "holes", we derive a functional in section 3.3.)

One may also consider Thurston type circle patterns with non-intersecting circles. Instead of the intersection angle, one prescribes the inversive distance (an imaginary intersection angle) between neighboring circles (see Bowers and Hurdal [**10**]). Is there a functional for such circle patterns, and can one write an explicit formula? Can this approach be used to prove existence and uniqueness theorems? These questions are interesting, because inversive-distance circle patterns may be the key to 'conformally parametrized' polyhedral surfaces in $\mathbb{R}^3$.

Even though the spherical functional is not convex, may it be used to prove existence and (Möbius-)uniqueness theorems for branched circle patterns in the sphere? (See also Bowers and Stephenson [**11**].) Can the representation theorem 1.3 be generalized for star-polyhedra? This question is interesting because branched circle patterns in the sphere can be used to construct 'discrete minimal surfaces' [**6**].

Rodin and Sullivan showed that circle packings approximate conformal mappings [**37**]. Schramm proved a similar result for 'circle patterns with the combinatorics of the square grid' [**41**]. There have been numerous refinements (for example, the proof of 'C^∞-convergence' by He and Schramm [**21**]), but all convergence results deal with circle patterns with the topology of the disc and regular combinatorics (square grid or hexagonal). Can the variational approach help in proving convergence results for circle patterns with non-trivial topology and irregular combinatorics?

1.5. Acknowledgments

I would like to thank my academic advisor, Alexander I. Bobenko, for being a great teacher, for his judicious guidance, and for letting me work at my own pace. I also thank Ulrich Pinkall, not only but in particular for help with the proof of the strong Steinitz theorem. I thank Günter M. Ziegler for his kind and active interest in my work. His expert advice on discrete and combinatorial matters has been extremely helpful.

I am also indebted to my parents, but that is beyond the scope of this thesis.

The functionals. Proof of the existence and uniqueness theorems

2.1. Quad graphs and an alternative definition for Delaunay circle patterns

A 'quad graph' (the term was coined by Bobenko and Suris [**8**]) is a cell decomposition of a surface such that the faces are quadrilaterals. We also demand that the vertices are bicolored. On the other hand, we allow identifications on the boundary of a face. For example, figure 2.1 *(left)* shows a quad graph decomposition of the sphere with only one 'quadrilateral'. To put is more precisely:

DEFINITION. A *quad graph* is a cell decomposition of a surface, such that each closed face is the image of a quadrilateral under a cellular map which immerses the open cells, and the vertices are colored black and white so that each edge is incident with one white and one black vertex.

From any cell decomposition Σ of a surface one obtains a quad graph $\mathcal{Q}$ such that the correspondence between elements of Σ and elements of $\mathcal{Q}$ is as follows:

Σ	$\mathcal{Q}$
vertices	black vertices
faces	white vertices
interior edges	quadrilaterals

Figure 2.1 *(right)* shows an example which should make the construction clear. This construction may be reversed, such that from every quad graph one obtains a cell decomposition. (The reverse construction is not quite unique in the case of
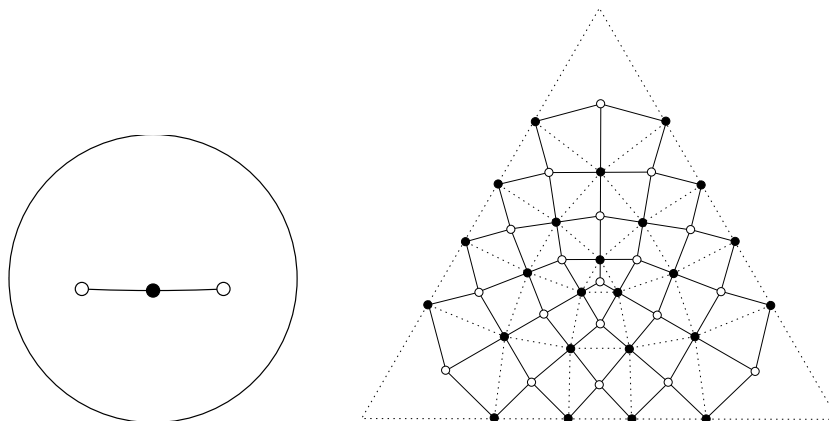

FIGURE 2.1. *Left:* The smallest quad graph decomposition of the sphere. *Right:* The quad graph corresponding to the cell decomposition of figure 1.5 (dotted). Note that boundary edges do not correspond to quadrilaterals.
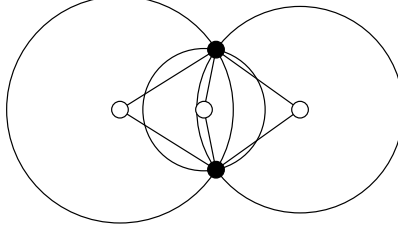
FIGURE 2.2. Not a Delaunay type circle pattern by the definition of section 1.1.

surfaces with boundary, because one is free to insert any number boundary edges. Fortunately, boundary edges play no role in our treatment of circle patterns.)

The following simple definition of Delaunay type circle patterns in terms of quad graphs is a bit more general than the one in section 1.1.

DEFINITION. A *(generalized) Delaunay type circle pattern* is a quad graph in a constant curvature surface, possibly with cone-like singularities in the vertices, such that the edges are geodesic and all edges incident with the same white vertex have the same length.

This definitions allows for configurations as shown in figure 2.2. The corresponding cell decomposition has a digon corresponding to the white vertex in the middle.

2.2. Analytic formulation of the circle pattern problem; euclidean case

Consider the following euclidean circle pattern problem: For a given finite cell decomposition Σ of a compact surface with or without boundary, a given angle θ_e with $0 < \theta_e < \pi$ for each interior edge e, and a given angle Φ_f for each face f, construct a euclidean Delaunay type circle pattern (as defined in section 1.1) with cell decomposition Σ, intersection angles given by θ, and cone angles and Neumann boundary conditions given by Φ.

We will reduce this problem to solving a set of nonlinear equations for the radii of the circles. The following lemma is the basis for this.

LEMMA 2.1. *Let Σ be a cell decomposition of a compact surface, possibly with boundary. Let $\theta : E_{int} \to (0, \pi)$ be a function on the set E_{int} of interior edges, and $r : F \to (0, \infty)$ be a function on the set F of faces. Then there exists a unique euclidean circle pattern with cone-like singularities in the vertices and in the centers of circles such that the corresponding cell decomposition is Σ, the intersection angles are given by θ and the radii are given by r.*

The cone angle Θ_v in a vertex v is given by $\Theta_v = \sum \theta_e$, where the sum is taken over all edges e around v. The cone angle in the center of an interior face f_j (or the boundary angle for a boundary face) is

$$\Phi_{f_j} = 2 \sum_{f_j \circ \mspace{-10mu} \rule[-1ex]{0.4pt}{3ex} \mspace{2mu} \circ f_k} \frac{1}{2i} \log \frac{r_{f_j} - r_{f_k} e^{-i\theta_e}}{r_{f_j} - r_{f_k} e^{i\theta_e}} \, , \tag{2.1}$$

where the sum is taken over all interior edges e between the face f_j and its neighbors f_k.

PROOF. Given the cell decomposition, intersection angles, and radii, one constructs the corresponding circle pattern as follows. For each interior edge e with faces f_j and f_k on either side, construct a euclidean kite shaped quadrilateral with
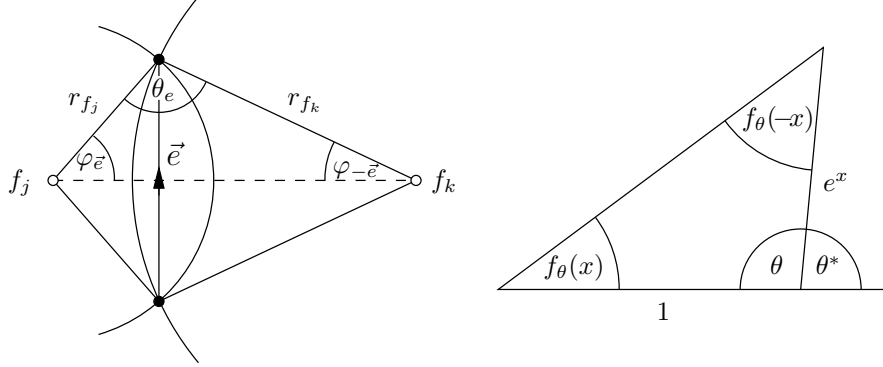
FIGURE 2.3. *Left:* A kite shaped quadrilateral of the quad graph. The oriented edge $\vec{e}$ has the face f_j on its left side and the face f_k on its right side. *Right:* The function $f_\theta(x)$.

side lengths r_{f_j} and r_{f_k} and angle θ_e as in figure 2.3 *(left)*. Glue these quadrilaterals together to obtain a flat surface with cone-like singularities, and, in fact, the desired circle pattern. The uniqueness claim is obvious, as is the claim about Θ_v. For each oriented edge $\vec{e}$, let $\varphi_{\vec{e}}$ be half the angle covered by $\vec{e}$ as seen from the center of the circle on the left side of $\vec{e}$. See figure 2.3 *(left)*. Now,

$$\Phi_f = 2\sum \varphi_{\vec{e}},$$

where the sum is taken over all oriented edges in oriented the boundary of f, and

$$\varphi_{\vec{e}} = \frac{1}{2i} \log \frac{r_{f_j} - r_{f_k} e^{-i\theta_e}}{r_{f_j} - r_{f_k} e^{i\theta_e}}. \tag{2.2}$$

(The argument of a non-zero complex number z is $\arg z = \frac{1}{2i} \log \frac{z}{\bar{z}}$.) Equation (2.1) follows. ∎

It is convenient to introduce the logarithmic radii

$$\rho = \log r \tag{2.3}$$

as variables. Then, equation (2.2) may be rewritten as

$$\varphi_{\vec{e}} = f_{\theta_e}(\rho_{f_k} - \rho_{f_j}), \tag{2.4}$$

where, for $0 < \theta < \pi$, the function $f_\theta : \mathbb{R} \to \mathbb{R}$ is defined by

$$f_\theta(x) := \frac{1}{2i} \log \frac{1 - e^{x-i\theta}}{1 - e^{x+i\theta}}, \tag{2.5}$$

and the branch of the logarithm is chosen such that

$$0 < f_\theta(x) < \pi.$$

In the following lemma, we list a few properties of the function $f_\theta(x)$ for reference.

LEMMA 2.2.

(i) The remaining angles of a triangle with sides 1 and e^x and with enclosed angle θ are $f_\theta(x)$ and $f_\theta(-x)$, as shown in figure 2.3 (right).

(ii) The derivative of $f_\theta(x)$ is

$$f'_\theta(x) = \frac{\sin \theta}{2(\cosh x - \cosh \theta)} > 0, \tag{2.6}$$

so $f_\theta(x)$ is strictly increasing.

(iii) The function $f_\theta(x)$ satisfies the functional equation

$$f_\theta(x) + f_\theta(-x) = \pi - \theta. \tag{2.7}$$

(iv) The limiting values of $f_\theta(x)$ are

$$\lim_{x \to -\infty} f_\theta(x) = 0 \quad and \quad \lim_{x \to \infty} f_\theta(x) = \pi - \theta, \tag{2.8}$$

(v) For $0 < y < \pi - \theta$, the inverse function is

$$f_\theta^{-1}(y) = \log \frac{\sin y}{\sin(y + \theta)}. \tag{2.9}$$

(vi) The integral of $f_\theta(x)$ is

$$F_\theta(x) := \int_{-\infty}^x f_\theta(\xi) \, d\xi = \operatorname{Im} \operatorname{Li}_2(e^{x+i\theta}), \tag{2.10}$$

where $\operatorname{Li}_2(z)$ is the dilogarithm function; see appendix B.

By lemma 2.1, the euclidean circle pattern problem is equivalent to the nonlinear equations (2.11) below.

LEMMA 2.3. *Given a cell decomposition Σ of a compact surface with or without boundary, an angle θ_e with $0 < \theta_e < \pi$ for each interior edge e, and an angle Φ_f for each face f. Suppose $r \in \mathbb{R}_+^F$ and $\rho \in \mathbb{R}^F$ are related by equation (2.3). Then the following statements (i) and (ii) are equivalent:*

(i) There is a euclidean circle pattern with radii r_f, intersection angles θ_e and cone/boundary angles Φ_f.

(ii) For each face $f \in F$,

$$\Phi_f - 2 \sum_{f \circ \overset{e}{\underset{\bullet}{\rule{0pt}{0pt}}} \circ f_k} f_{\theta_e}(\rho_{f_k} - \rho_f) = 0, \tag{2.11}$$

where the sum is taken over all interior edges e between the face f and its neighbors f_k.

2.3. The euclidean circle pattern functional

The euclidean circle pattern functional defined below is a function of the logarithmic radii ρ_f. Equations (2.11) are the conditions for a critical point.

DEFINITION. The *euclidean circle pattern functional* is the function

$$S_{\mathrm{euc}} : \mathbb{R}^F \longrightarrow \mathbb{R}$$

$$S_{\mathrm{euc}}(\rho) =$$
$$\sum_{f_j \circ \overset{e}{\underset{\bullet}{\rule{0pt}{0pt}}} \circ f_k} \left(\operatorname{Im} \operatorname{Li}_2\left(e^{\rho_{f_k} - \rho_{f_j} + i\theta_e}\right) + \operatorname{Im} \operatorname{Li}_2\left(e^{\rho_{f_j} - \rho_{f_k} + i\theta_e}\right) - (\pi - \theta_e)\left(\rho_{f_j} + \rho_{f_k}\right) \right)$$

$$+ \sum_{\circ f} \Phi_f \rho_f. \tag{2.12}$$

The first sum is taken over all interior edges e, and f_j and f_k are the faces on either side of e. (The terms are symmetric in f_j and f_k, so it does not matter which face is considered as f_j and which as f_k.) The second sum is taken over all faces f.

LEMMA 2.4. *A function $\rho \in \mathbb{R}^F$ is a critical point of the euclidean circle pattern functional S_{euc}, if and only if it satisfies equations (2.11). The critical points of S_{euc} are therefore in one-to-one correspondence with the solutions of the euclidean circle pattern problem.*
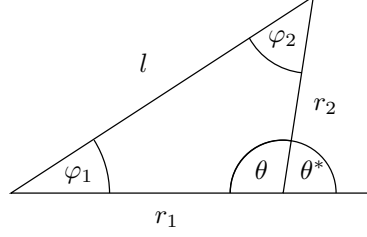
FIGURE 2.4.

PROOF. Using equations (2.10) and (2.7), one obtains

$$\frac{\partial S_{\text{euc}}}{\partial \rho_f} = \Phi_f - 2 \sum_{f \circ \underset{\bullet}{|} \circ f_k} f_{\theta_e}(\rho_{f_k} - \rho_f),$$

where the sum is taken over all edges e between the face f and its neighbors f_k. ∎

2.4. The hyperbolic circle pattern functional

This case is treated in the same fashion as the euclidean case. Of course, the trigonometric relations are different:

LEMMA 2.5. *Suppose r_1 and r_2 are two sides of a hyperbolic triangle, the enclosed angle between them is θ, and the remaining angles are φ_1 and φ_2, as shown in figure 2.4. Then*

$$\varphi_1 = f_\theta(\rho_2 - \rho_1) - f_\theta(\rho_2 + \rho_1), \tag{2.13}$$

where $f_\theta(x)$ is defined by equation (2.5), and

$$\rho = \log \tanh \frac{r}{2}. \tag{2.14}$$

The inverse relation is

$$\rho_1 = \frac{1}{2} \log \frac{\sin\left(\frac{\theta^* - \varphi_1 - \varphi_2}{2}\right) \sin\left(\frac{\theta^* - \varphi_1 + \varphi_2}{2}\right)}{\sin\left(\frac{\theta^* + \varphi_1 + \varphi_2}{2}\right) \sin\left(\frac{\theta^* + \varphi_1 - \varphi_2}{2}\right)}, \tag{2.15}$$

where $\theta^* = \pi - \theta$, $\varphi_{1,2} > 0$, and $\varphi_1 + \varphi_2 < \theta^*$.

Equation (2.13) is derived in appendix A. Equation (2.15) follows from (2.13) (and the corresponding equation for φ_2) by a straightforward calculation using equations (2.9) and (2.7). Note that positive radii r correspond to negative ρ.

In the hyperbolic case, the new variables ρ are given by equation (2.14). Instead of equation (2.4), one has

$$\varphi_{\vec{e}} = f_{\theta_e}(\rho_{f_k} - \rho_{f_j}) - f_{\theta_e}(\rho_{f_k} + \rho_{f_j}). \tag{2.16}$$

and the nonlinear equations for the variables ρ_f are

$$\Phi_f - 2 \sum_{f \circ \underset{\bullet}{|} \circ f_k} \left(f_{\theta_e}(\rho_{f_k} - \rho_f) - f_{\theta_e}(\rho_{f_k} + \rho_f) \right) = 0, \tag{2.17}$$

where the sum is taken over all interior edges e between the face f and its neighbors f_k.

LEMMA 2.6. *If $\rho \in \mathbb{R}^F$ is a solution of the equations (2.17), then $\rho_f < 0$ for all $f \in F$. The solutions of the equations (2.17) are therefore in one-to-one correspondence with the solutions of the hyperbolic circle pattern problem.*

PROOF. Since, by equation (2.6), the function $f_\theta(x)$ is strictly increasing for $0 < \theta < \pi$,

$$f_{\theta_e}(\rho_{f_k} + \rho_f) - f_{\theta_e}(\rho_{f_k} - \rho_f) \geq 0, \quad \text{if} \quad \rho_f \geq 0.$$

Since $\Phi_f > 0$ by assumption, the left hand side of equation (2.17) is positive if $\rho_f \geq 0$. ∎

DEFINITION. The *hyperbolic circle pattern functional* is the function

$$S_{\text{hyp}} : \mathbb{R}^F \longrightarrow \mathbb{R}$$

$$S_{\text{hyp}}(\rho) = \sum_{f_j \circ\!\!\stackrel{\bullet}{\big|}\!\!\circ f_k} \Big(\operatorname{Im} \operatorname{Li}_2 \left(e^{\rho_{f_k} - \rho_{f_j} + i\theta_e}\right) + \operatorname{Im} \operatorname{Li}_2 \left(e^{\rho_{f_j} - \rho_{f_k} + i\theta_e}\right)$$

$$+ \operatorname{Im} \operatorname{Li}_2 \left(e^{\rho_{f_j} + \rho_{f_k} + i\theta_e}\right) + \operatorname{Im} \operatorname{Li}_2 \left(e^{-\rho_{f_j} - \rho_{f_k} + i\theta_e}\right) \Big) \quad (2.18)$$

$$+ \sum_{\circ f} \Phi_f \rho_f.$$

The first sum is taken over all interior edges e, and f_j and f_k are the faces on either side of e. (The terms are symmetric in f_j and f_k, so it does not matter which face is considered as f_j and which as f_k.) The second sum is taken over all faces f.

LEMMA 2.7. *A function $\rho \in \mathbb{R}^F$ is a critical point of the hyperbolic circle pattern functional S_{hyp}, if and only if ρ satisfies equations (2.17). In that case, ρ is negative. The critical points of S_{hyp} are therefore in one-to-one correspondence with the solutions of the hyperbolic circle pattern problem.*

PROOF. Similarly as in the euclidean case, one finds that

$$\frac{\partial S_{\text{hyp}}}{\partial \rho_f} = \Phi_f - 2 \sum_{f \circ\!\!\stackrel{\bullet}{\big|}\!\!\circ f_k} \left(f_{\theta_e}(\rho_{f_k} - \rho_f) - f_{\theta_e}(\rho_k + \rho_f) \right), \quad (2.19)$$

such that $dS_{\text{hyp}} = 0$, if and only if equations (2.17) are satisfied. By lemma 2.6, $\rho < 0$ follows. ∎

For future reference, we note that equation (2.19) and the proof of lemma 2.6 imply

$$\frac{\partial S_{\text{hyp}}}{\partial \rho_f} > 0, \quad \text{if} \quad \rho_f \geq 0. \quad (2.20)$$

2.5. Convexity of the euclidean and hyperbolic functionals. Proof of the uniqueness claims of theorem 1.8

LEMMA 2.8. *If a euclidean circle pattern with data Σ, θ, Φ exists, then the euclidean functional is* scale-invariant: *Multiplying all radii r with the same positive factor (equivalently, adding the same constant to all ρ) does not change its value.*

PROOF. Let $1_F \in \mathbb{R}^F$ be the function which is 1 on every face $f \in F$. Equation (2.12) implies

$$S_{\text{euc}}(\rho + h\, 1_F) = S_{\text{euc}}(\rho) + h \Big(\sum_{f \in F} \Phi_f - 2 \sum_{e \in E_{int}} (\pi - \theta_e) \Big),$$

where E_{int} is the set of interior edges. Clearly, the functional can have a critical point only if the coefficient of h vanishes. In this case, the functional is scale invariant. ∎

If the euclidean functional is scale invariant, one may restrict the search for critical points to the subspace

$$U = \{\rho \in \mathbb{R}^F | \sum_{f \in F} \rho_f = 0\}. \tag{2.21}$$

LEMMA 2.9. *The euclidean functional S_{euc} is strictly convex on the subspace U. The hyperbolic functional S_{hyp} is strictly convex on $\mathbb{R}^F$.*

PROOF. By a straightforward calculation, one finds that the second derivative of the euclidean functional is the quadratic form

$$S''_{euc} = \sum_{f_j \circ \mkern-3mu \mid \circ f_k} \frac{\sin \theta_e}{\cosh(\rho_{f_k} - \rho_{f_j}) - \cos \theta_e} (d\rho_{f_k} - d\rho_{f_j})^2,$$

where the sum is taken over all interior edges e, and f_j and f_k are the faces on either side. Since it is (quietly) assumed that the surface is connected, the second derivative is positive unless $d\rho_{f_j} = d\rho_{f_k}$ for all $f_j, f_k \in F$. Hence it is positive definite on U.

For the hyperbolic functional, one obtains

$$S''_{hyp} = \sum_{f_j \circ \mkern-3mu \mid \circ f_k} \left(\frac{\sin \theta_e}{\cosh(\rho_{f_k} - \rho_{f_j}) - \cos \theta_e} (d\rho_{f_j} - d\rho_{f_k})^2 + \right.$$

$$\left. \frac{\sin \theta_e}{\cosh(\rho_{f_j} + \rho_{f_k}) - \cos \theta_e} (d\rho_{f_j} + d\rho_{f_k})^2 \right),$$

which is positive definite on $\mathbb{R}^F$. ∎

This proves the uniqueness claims of theorem 1.8.

2.6. The spherical circle pattern functional

Like in the euclidean and hyperbolic cases, there is a functional for spherical circle patterns whose critical points correspond to solutions of the circle pattern problem.

LEMMA 2.10. *Suppose r_1 and r_2 are two sides of a spherical triangle (with $0 < r_{1,2} < \pi$), the included angle between them is θ, and the remaining angles are φ_1 and φ_2, as shown in figure 2.4. Then*

$$\varphi_1 = f_\theta(\rho_2 - \rho_1) + f_{\pi-\theta}(\rho_2 + \rho_1), \tag{2.22}$$

where $f_\theta(x)$ is defined by equation (2.5), and

$$\rho = \log \tan \frac{r}{2}. \tag{2.23}$$

The inverse relation is

$$\rho_1 = \frac{1}{2} \log \frac{\sin\left(\frac{-\theta^* + \varphi_1 + \varphi_2}{2}\right) \sin\left(\frac{\theta^* - \varphi_1 + \varphi_2}{2}\right)}{\sin\left(\frac{\theta^* + \varphi_1 + \varphi_2}{2}\right) \sin\left(\frac{\theta^* + \varphi_1 - \varphi_2}{2}\right)}, \tag{2.24}$$

where $\theta^* = \pi - \theta$, $\varphi_{1,2} > 0$, and $\theta^* < \varphi_1 + \varphi_2 < 2\pi - \theta^*$.

Equation (2.22) is derived in appendix A. Equation (2.24) follows from (2.22) (and the corresponding equation for φ_2) by a straightforward calculation using equations (2.9) and (2.7).

To construct the spherical circle pattern functional, one proceeds like in the euclidean and hyperbolic cases (sections 2.2–2.4). In this case, the new variables ρ_f

are given by equation (2.23). There is a one-to-one correspondence between radii r with $0 < r < \pi$, and $\rho \in \mathbb{R}$. Instead of equations (2.4) or (2.16), one has

$$\varphi_{\vec{e}} = f_{\theta_e}(\rho_{f_k} - \rho_{f_j}) + f_{\theta_e^*}(\rho_{f_k} + \rho_{f_j}), \tag{2.25}$$

where $\theta^* = \pi - \theta$. Consequently, the nonlinear equations for the variables ρ_f are

$$\Phi_f - 2 \sum_{f \circ \bullet \circ f_k} \left(f_{\theta_e}(\rho_{f_k} - \rho_f) + f_{\theta_e^*}(\rho_{f_k} + \rho_f) \right) = 0, \tag{2.26}$$

where the sum is taken over all interior edges e around f, and f_k is the face on the other side of e.

DEFINITION. The *spherical circle pattern functional* is the function

$$S_{\mathrm{sph}} : \mathbb{R}^F \longrightarrow \mathbb{R}$$

$$S_{\mathrm{sph}}(\rho) = \sum_{f_j \circ \bullet \circ f_k} \left(\operatorname{Im} \operatorname{Li}_2 \left(e^{\rho_{f_k} - \rho_{f_j} + i\theta_e} \right) + \operatorname{Im} \operatorname{Li}_2 \left(e^{\rho_{f_j} - \rho_{f_k} + i\theta_e} \right) \right.$$

$$- \operatorname{Im} \operatorname{Li}_2 \left(e^{\rho_{f_j} + \rho_{f_k} + i(\pi - \theta_e)} \right) - \operatorname{Im} \operatorname{Li}_2 \left(e^{-\rho_{f_j} - \rho_{f_k} + i(\pi - \theta_e)} \right)$$

$$\left. - \pi(\rho_{f_j} + \rho_{f_k}) \right)$$

$$+ \sum_{\circ f} \Phi_f \rho_f. \tag{2.27}$$

The first sum is taken over all interior edges e, and f_j and f_k are the faces on either side of e. (The terms are symmetric in f_j and f_k, so it does not matter which face is considered as f_j and which as f_k.) The second sum is taken over all faces f.

LEMMA 2.11. *A function $\rho \in \mathbb{R}^F$ is a critical point of the spherical circle pattern functional S_{sph}, if and only if ρ satisfies equations (2.26). The critical points of S_{sph} are therefore in one-to-one correspondence with the solutions of the spherical circle pattern problem.*

This proposition is proved in the same way as the lemmas 2.4 and 2.7.

The spherical circle pattern functional is not convex. By a straightforward calculation, one finds that

$$S_{\mathrm{sph}}'' = \sum_{f_j \circ \bullet \circ f_k} \left(\frac{\sin \theta_e}{\cosh(\rho_{f_k} - \rho_{f_j}) - \cos \theta_e} (d\rho_{f_j} - d\rho_{f_k})^2 \right.$$

$$\left. - \frac{\sin \theta_e}{\cosh(\rho_{f_j} + \rho_{f_k}) + \cos \theta_e} (d\rho_{f_j} + d\rho_{f_k})^2 \right). \tag{2.28}$$

This quadratic form is negative for the tangent vector $1_F \in \mathbb{R}^F$, which has a 1 in every component. Hence, the negative index is at least one.

REMARK. This has a geometric explanation. Consider a circle pattern in the sphere. Focus on one flower: a central circle with its neighbors. The neighbors nicely fit around the central circle. Now decrease the radii of all circles by the same factor. The effect is the same as increasing the radius of the sphere by that factor. This makes the sphere flatter. The neighbors will not fit around the central circle anymore, but there will be a gap. To adjust the radius of the central circle so that the neighbors fit around, one would make it even smaller.

Nevertheless, in numerical experiments, the spherical functional has been used with amazing success to construct circle patterns in the sphere. This following method was used. Consider the reduced functional

$$\widetilde{S}_{\text{sph}}(\rho) = \max_{t \in \mathbb{R}} S_{\text{sph}}(\rho + t\, 1_F). \tag{2.29}$$

Clearly, $\widetilde{S}_{\text{sph}}(\rho)$ is invariant under a shift $\rho \mapsto \rho + t1_F$. To solve a spherical circle pattern problem, minimize $\widetilde{S}_{\text{sph}}(\rho)$ on the set U defined by equation (2.21). Equivalently, minimize $\widetilde{S}_{\text{sph}}(\rho)$ under the constraint $\rho_f = 0$ for some fixed $f \in F$.

The numerical evidence suggests that this method works whenever the circle pattern in question exists. In particular, this method can be used to construct branched circle patterns in the sphere. In general, such patterns cannot be constructed using the euclidean functional after a stereographic projection.

We return to the definition of the reduced functional $\widetilde{S}_{\text{sph}}(\rho)$, equation (2.29). The following proposition provides a geometric interpretation for the condition

$$\frac{d}{dt}\, dS_{\text{sph}}(\rho + t\, 1_F)\Big|_{t=0} = 0.$$

Consider the spherical circle pattern problem with data Σ, $\theta \in (0, \pi)^E$, and $\Phi \in (0, \infty)^F$. For the sake of simplicity, assume that Σ is a decomposition of a surface without boundary. Suppose there exists a corresponding circle pattern in a surface M with constant curvature 1 and cone-like singularities. Then, due to the Gauss-Bonnet theorem, the total area A of M is determined by the formula:

$$A + K_v + K_f = 2\pi(|F| - |E| + |V|), \tag{2.30}$$

where K_v and K_f are as in equations (1.2) and (1.3), and $|F|$, $|E|$, and $|V|$ are the numbers of faces, edges and vertices of Σ, respectively.

PROPOSITION. *Let $\rho \in \mathbb{R}^F$ be arbitrary. Given a cell decomposition Σ of a closed compact surface, the intersection angles θ, and radii $r = 2\arctan e^\rho$, construct the surface $M^{(\rho)}$ with constant curvature 1 and cone-like singularities by gluing together spherical kite-shaped quadrilaterals, as was described (for the euclidean case) in the proof of lemma 2.1. Let $A^{(\rho)}$ be the total area of $M^{(\rho)}$. Then*

$$\frac{d}{dt}\, dS_{sph}(\rho + t\, 1_F)\Big|_{t=0} = A - A^{(\rho)} \tag{2.31}$$

where A is determined by equation (2.30).

PROOF. Let $A_e^{(\rho)}$ be the area of the quadrilateral corresponding to an edge e as in figure 2.3 *(left)*. Then

$$\begin{aligned}
A_e^{(\rho)} &= 2\varphi + 2\varphi' + 2\theta_e - 2\pi \\
&\overset{(2.25)}{=} 2f_{\theta_e}(\rho_k - \rho_j) + 2f_{\theta_e}(\rho_j - \rho_k) + 4f_{(\pi - \theta_e)}(\rho_j + \rho_k) + 2\theta_e - 2\pi \\
&\overset{(2.7)}{=} 4f_{(\pi - \theta_e)}(\rho_j + \rho_k).
\end{aligned}$$

Also,

$$\sum_{e \in E} 2\theta_e = 2\pi|V| - \sum_{v \in V} K_v$$

and

$$\sum_{f \in F} \Phi_f = 2\pi|F| - \sum_{f \in F} K_f.$$

Finally,

$$\frac{d}{dt}\, dS_{\mathrm{sph}}(\rho + t\mathbf{1}_F) = \Big(\sum_{f \in F} \frac{d}{d\rho_f}\Big) S_{\mathrm{sph}}(\rho)$$

$$\overset{\substack{(2.27)\\(2.10)}}{=} \sum_{f_j \circ \!\overset{\bullet}{\big[} \circ f_k} \big(-2f_{(\pi-\theta_e)}(\rho_j + \rho_k) + 2f_{(\pi-\theta_e)}(-\rho_j - \rho_k) - 2\pi\big) + \sum_{\circ f} \Phi_f$$

$$\overset{(2.7)}{=} \sum_{f_j \circ \!\overset{\bullet}{\big[} \circ f_k} \big(-4f_{(\pi-\theta_e)}(\rho_j + \rho_k) + 2\theta_e - 2\pi\big) + \sum_{\circ f} \Phi_f$$

Equation (2.30) follows. ∎

2.7. Coherent angle systems. The existence of circle patterns

In section 2.5, the uniqueness of a circle pattern was deduced from the convexity of the euclidean and hyperbolic functionals. This section and the next one are devoted to the existence part of theorem 1.8. To establish that the euclidean functional attains a minimum, we will show that

$$S_{\mathrm{euc}}(\rho) \longrightarrow \infty \quad \text{if} \quad \|\rho\| \longrightarrow \infty \text{ in } U,$$

where $U \in \mathbb{R}^F$ is the subspace defined by equation (2.21). To establish that the hyperbolic functional attains a minimum, we will to show that

$$S_{\mathrm{hyp}}(\rho) \longrightarrow \infty \quad \text{if} \quad \|\rho\| \longrightarrow \infty \text{ with } \rho < 0.$$

Because of the inequality (2.20), this suffices.

To estimate the functionals from below, one has to compare the sum over interior edges with the sum over faces in equations (2.12) and (2.18). This is achieved with the help of a so called 'coherent angle system'. In this section, we prove that the functionals have minima if and only if coherent angle systems exist. In section 2.8, we will show that the conditions of theorem 1.8 are necessary and sufficient for the existence of a coherent angle system.

Coherent angle systems also play an important role in chapter 3, when we derive other variational principles by Legendre transformations. Spherical coherent angle systems are defined below, but not used until chapter 3.

Let $\vec{E}$ be the set of oriented edges. For an oriented edge $\vec{e} \in \vec{E}$, denote by $-\vec{e} \in \vec{E}$ the edge with the opposite orientation, and by e the corresponding non-oriented edge.

DEFINITION. A *euclidean coherent angle system* is a function $\varphi \in \mathbb{R}^{\vec{E}_{int}}$ on the set $\vec{E}_{int}$ of interior oriented edges which satisfies the following two conditions.
(i) For all oriented edges $\vec{e} \in \vec{E}_{int}$,

$$\varphi_{\vec{e}} > 0 \quad \text{and} \quad \varphi_{\vec{e}} + \varphi_{-\vec{e}} = \pi - \theta_e.$$

(ii) For all faces $f \in F$,

$$\sum 2\varphi_{\vec{e}} = \Phi_f,$$

where the sum is taken over all oriented interior edges $\vec{e}$ in the oriented boundary of f.

A *hyperbolic coherent angle system* satisfies
(i′) For all oriented edges $e \in \vec{E}$,

$$\varphi_{\vec{e}} > 0 \quad \text{and} \quad \varphi_{\vec{e}} + \varphi_{-\vec{e}} < \pi - \theta_e.$$

and condition *(ii)* above.

A *spherical coherent angle system* satisfies

(i″) For all oriented edges $e \in \vec{E}$,

$$0 < \varphi_{\vec{e}} < \pi, \quad \pi - \theta_e < \varphi_{\vec{e}} + \varphi_{-\vec{e}} < \pi + \theta_e, \quad \text{and} \quad \left| \varphi_{\vec{e}} - \varphi_{-\vec{e}} \right| < \pi - \theta_e,$$

and condition *(ii)* above.

(Note that the exterior angles of a spherical triangle satisfy the triangle inequalities.) The following lemma reduces the question of existence of a (euclidean or hyperbolic) circle pattern to the question of existence of a coherent angle system.

LEMMA 2.12. *The functional S_{euc} (S_{hyp}) has a critical point, if and only if a euclidean (hyperbolic) coherent angle system exists.*

PROOF. If the functional S_{euc} (S_{hyp}) has a critical point ρ, then equation (2.4) (equation (2.16)) yields a coherent angle system. It is left to show that, conversely, the existence of a coherent angle system implies the existence of a critical point.

Consider the euclidean case. Suppose a euclidean coherent angle system φ exists. This implies

$$\sum_{f \in F} \Phi_f = 2 \sum_{e \in E_{int}} (\pi - \theta_e).$$

Hence, the functional S_{euc} is scale invariant. (See the proof of lemma 2.8.) We will show that $S_{\text{euc}}(\rho) \to \infty$ if $\rho \to \infty$ in the subspace U defined in equation 2.21. More precisely, we will show that for $\rho \in U$,

$$S_{\text{euc}}(\rho) > 2 \min_{\vec{e} \in \vec{E}_{int}} \varphi_{\vec{e}} \max_{f \in F} |\rho_f|. \tag{2.32}$$

The functional S_{euc} must therefore attain a minimum, which is a critical point.

For $x \in \mathbb{R}$ and $0 < \theta < \pi$,

$$\operatorname{Im} \operatorname{Li}_2(e^{x+i\theta}) + \operatorname{Im} \operatorname{Li}_2(e^{-x+i\theta}) > (\pi - \theta)\,|x|,$$

and hence, by equation (2.12),

$$S_{\text{euc}}(\rho) > -2 \sum_{e \in E} (\pi - \theta_e) \min\left(\rho_{f_k}, \rho_{f_j}\right) + \sum_{f \in F} \Phi_f \rho_f,$$

where the sum is taken over the unoriented interior edges e, and f_j and f_k are the faces on either side of e. Now, we use the coherent angle system φ to merge the two sums. Because

$$\sum_{f \in F} \Phi_f \rho_f = 2 \sum_{e \in E_{int}} \left(\varphi_{\vec{e}} \rho_{f_j} + \varphi_{-\vec{e}} \rho_{f_k} \right),$$

one obtains

$$S_{\text{euc}}(\rho) > 2 \sum_{e \in E_{int}} \min\left(\varphi_{\vec{e}}, \varphi_{-\vec{e}} \right) \left| \rho_{f_k} - \rho_{f_j} \right|.$$

Since we assume the cellular surface to be connected, we get

$$S_{\text{euc}}(\rho) > 2 \min_{\vec{e} \in \vec{E}_{int}} \varphi_{\vec{e}} \left(\max_{f \in F} \rho_f - \min_{f \in F} \rho_f \right),$$

and from this the estimate (2.32).

The hyperbolic case is similar. One shows that, if all $\rho_f < 0$,

$$S_{\text{hyp}}(\rho) > 2 \min_{e \in E_{int}} \left| \varphi_{\vec{e}} + \varphi_{-\vec{e}} - (\pi - \theta_e) \right| \max_{f \in F} \left| \rho_f \right|.$$

∎
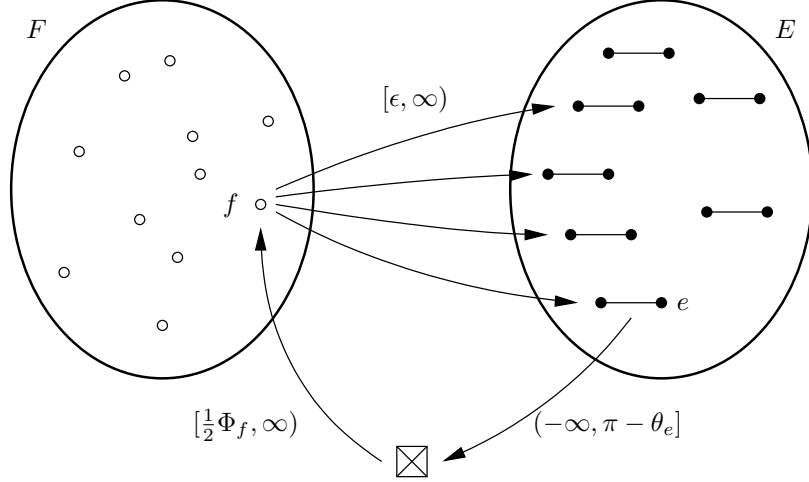
FIGURE 2.5. The network (N, X). Only a few of the branches and capacity intervals are shown.

2.8. Conclusion of the proof of theorem 1.8

With this section we complete the proof of theorem 1.8. In section 2.5, we have shown the uniqueness claim. By lemma 2.12, the circle patterns exist, if and only if a coherent angle system exists. All that is left to show is the following lemma.

LEMMA 2.13. *A euclidean/hyperbolic coherent angle system exists if and only if the conditions of theorem 1.8 hold.*

The rest of this section is devoted to the proof of lemma 2.13. It is easy to see that these conditions are necessary. To prove that they are sufficient, we apply the feasible flow theorem of network theory. Let (N, X) be a network (i.e. a directed graph), where N is the set of nodes and X is the set of branches. For any subset $N' \subset N$ let $ex(N')$ be the set of branches having their initial node in N' but not their terminal node. Let $in(N')$ be the set of branches having their terminal node in N' but not their initial node. Assume that there is a lower capacity bound a_x and an upper capacity bound b_x associated with each branch x, with $-\infty \leq a_x \leq b_x \leq \infty$.

DEFINITION. A *feasible flow* is a function $\varphi \in \mathbb{R}^X$, such that Kirchoff's current law is satisfied, that is, for each $n \in N$,

$$\sum_{x \in ex(\{n\})} \varphi_x = \sum_{x \in in(\{n\})} \varphi_x,$$

and $a_x \leq \varphi_x \leq b_x$ for all branches $x \in X$.

FEASIBLE FLOW THEOREM. *A feasible flow exists if and only if for every nonempty subset $N' \subset N$ of nodes with $N' \neq N$,*

$$\sum_{x \in ex(N')} b_x \geq \sum_{x \in in(N')} a_x.$$

A proof is given by Ford and Fulkerson [**18**, ch. II, §3]. (Ford and Fulkerson assume the capacity bounds to be non-negative, but this is not essential.)

To prove lemma 2.13 in the euclidean case, consider the following network; see figure 2.5. The nodes are all faces and non-oriented interior edges of the cellular surface, and one further node that we denote by $\boxtimes$: $N = F \cup E \cup \{\boxtimes\}$. There is a branch in X going from $\boxtimes$ to each face $f \in F$ with capacity interval $[\frac{1}{2}\Phi_f, \infty)$.

From each face f there is a branch in X going to the non-oriented interior edges of the boundary of f with capacity interval $[\epsilon, \infty)$, where $\epsilon > 0$ will be determined later. Finally there is a branch in X going from each non-oriented edge $e \in E$ to $\boxtimes$ with capacity $(-\infty, \pi - \theta_e]$.

Assume the conditions of theorem 1.8 are fulfilled. A feasible flow in the network yields a coherent angle system. Indeed, since we have equality in (1.5) if $F' = F$, Kirchoff's current law at $\boxtimes$ implies that the flow into each face f is $\frac{1}{2}\Phi_f$ and the flow out of each edge e is $\pi - \theta_e$. It follows that the flow in the branches from F to E constitutes a coherent angle system.

We need to show that the condition of the feasible flow theorem is satisfied. Suppose N' is a nonempty proper subset of N. Let $F' = N' \cap F$ and $E' = N' \cap E_{int}$.

Consider first the case that $\boxtimes \in N'$, which is the easy one. Since N' is a proper subset of N there is a face $f \in F$ or an edge $e \in E$ which is not in N'. In the first case there is a branch out of N' with infinite upper capacity bound. In the second case there is a branch into N' with negative infinite lower capacity bound. Either way, the condition of the feasible flow theorem is trivially fulfilled.

Now consider the case that $\boxtimes \notin N'$. We may assume that for each face $f \in F'$, the interior edges in the boundary of E are contained in E'. Otherwise, there would be branches out of N' with infinite upper capacity bound. For subsets $A, B \subset N$ denote by $A \to B$ the set of branches in X having initial node in A and terminal node in B. Then the condition of the feasible flow theorem is equivalent to

$$\sum_{f \in F'} \frac{1}{2}\Phi_f + \epsilon \, |F \setminus F' \to E'| \le \sum_{e \in E'} \theta_e^*.$$

It is fulfilled if we choose

$$\epsilon < \frac{1}{2|E|} \min_{F'} \left(\sum_{e \in E'(F')} (\pi - \theta_e) - \sum_{f \in F'} \frac{1}{2}\Phi_f \right), \tag{2.33}$$

where the minimum is taken over all proper nonempty subsets F' of F and $E'(F')$ is the set of all non-oriented edges incident with a face in F'. The minimum is greater than zero because strict inequality holds in (1.5) if F' is a proper subset of F.

In the hyperbolic case, the proof is only a little bit more complicated. In the network, the flow in the branches going from $\boxtimes$ to a face f must constrained to be exactly $\frac{1}{2}\Phi_f$; and the capacity interval of branches going from an edge e to $\boxtimes$ has to be changed to $(-\infty, \theta_e^* - \epsilon]$.

2.9. Proof of theorem 1.7

The necessity of the condition of theorem 1.7 can be seen from the following geometrical argument. Figure 2.6 shows a closed path in the Poincaré dual cell decomposition Σ^*, which cuts out a disc. By the Gauss-Bonnet theorem,

$$\sum_j (\pi - \alpha_j - \beta_j - \gamma_j) = 2\pi - \epsilon A,$$

where $\epsilon \in \{0, -1\}$ is the curvature of the surface and A is the area enclosed by the path. But

$$\pi - \alpha_j - \beta_j = \theta_j - \epsilon A_j,$$

where A_j is the are of triangle j. Hence,

$$\sum_j \theta_j = 2\pi + \sum_j \gamma_j - \epsilon(A - \sum_j A_j). \tag{2.34}$$
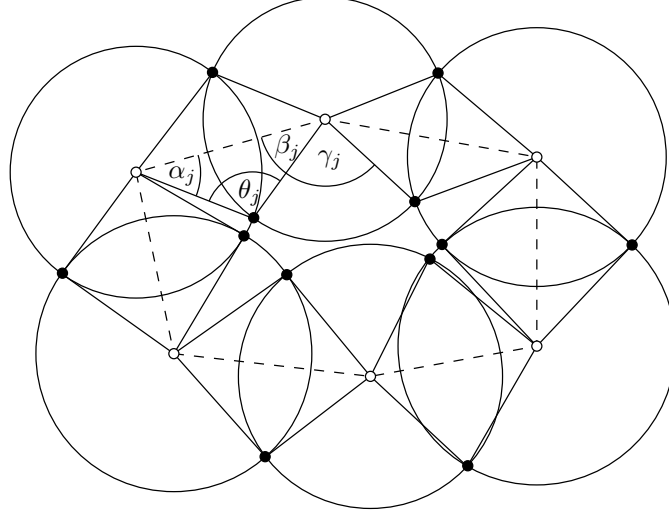
FIGURE 2.6. The circles and quadrilaterals corresponding to a closed path in the Poincaré dual *(dashed)*, which cuts out a disc.

Inequality (1.4) follows, with equality holding if and only if all γ_j are zero and $\epsilon(A - \sum A_j) = 0$. This is the case if and only if the path contains only a single vertex of Σ in its interior.

We will now prove the sufficiency of the condition. The principle tool in the proof is the following lemma.

LEMMA 2.14. *Suppose a nonempty 1-dimensional cell complex (a graph) $\Gamma = (V_1, E_1)$ is cellularly embedded in a cell decomposition $\Sigma = (V, E, F)$ of a closed compact surface. Suppose Γ separates Σ into r contiguous regions. Then*

$$r - |E_1| + |V_1| = |F| - |E| + |V| + \sum_{j=1}^{r} h_j, \qquad (2.35)$$

where h_j is the dimension of the first $\mathbb{Z}_2$-homology group of the jth region.

If all regions are simply connected, then all $h_j = 0$, and equation (2.35) states that the Euler characteristic is invariant under subdivisions. A multiply connected region can be turned into a simply connected one by adding h_j cuts to Γ which do not separate the region. Each cut reduces the left hand side of equation (2.35) by one. For a more formal proof of lemma 2.14, see Giblin [**20**, ch. 9] or appendix D.

Suppose the condition of theorem 1.7 holds. We will deduce the condition of theorem 1.8. Thus, let $F' \subseteq F$ be a nonempty subset of the set F of faces, and let $E' \subseteq E$ be the set of edges, which are incident with any face in F'. We have to show inequality (1.5) where all $\Phi_f = 2\pi$. That is, we have to show

$$\sum_{e \in E'} 2\theta_e^* \geq 2\pi |F'|, \qquad (2.36)$$

where equality holds if and only if the genus $g = 1$ and $F' = F$.

Let

$$F'' = F \setminus F' \quad \text{and} \quad E'' = E \setminus E'$$

be the complements of F' and E'. Identify the faces, edges, and vertices of the cell decomposition Σ with the corresponding vertices, edges, and faces of its Poincaré dual Σ^*. Consider the 1-dimensional subcomplex $\Gamma = (F'', E'')$ of Σ^* which consists of the vertex set F'' and edge set E''. (It is easy to see that it is indeed a

subcomplex.) First, suppose that $F' \neq F$. Then the graph Γ is not empty. By lemma 2.14, applied to Γ in Σ^*,

$$r - |E''| + |F''| = |V| - |E| + |F| + \sum_{j=1}^{r} h_j,$$

or, equivalently,

$$|F'| - |E'| + |V| = \sum_{j=1}^{r}(1 - h_j). \tag{2.37}$$

Now,

$$\sum_{e \in E'} 2\theta_e^* = 2\pi |E'| - \sum_{e \in E'} 2\theta_e.$$

$$= 2\pi |E'| - \sum_{e \in E} 2\theta_e + \sum_{e \in E''} 2\theta_e.$$

Because, by the condition of theorem 1.7, θ sums to 2π around each vertex,

$$\sum_{e \in E} 2\theta_e = 2\pi |V|,$$

and hence

$$\sum_{e \in E'} 2\theta_e^* = 2\pi \big(|E'| - |V|\big) + \sum_{e \in E''} 2\theta_e. \tag{2.38}$$

With equation (2.37), we get

$$\sum_{e \in E'} 2\theta_e^* - 2\pi |F'| = \sum_{e \in E''} 2\theta_e - 2\pi \sum_{j=1}^{r}(1 - h_j). \tag{2.39}$$

Let $e_1^j, \ldots, e_{b_j}^j$ be the boundary path of the jth region into which Σ^* decomposes if cut along the edges in E''. (The same edge may appear twice in one boundary path.) Each edge of E'' appears exactly twice in any of the boundary paths. Therefore,

$$\sum_{e \in E''} 2\theta_e = \sum_{j=1}^{r} \sum_{i=1}^{b_j} \theta_{e_i^j},$$

and, with equation (2.39),

$$\sum_{e \in E'} 2\theta_e^* - 2\pi |F'| = \sum_{j=1}^{r} \Big(\sum_{i=1}^{b_j} \theta_{e_i^j} - 2\pi(1 - h_j) \Big).$$

In any case,

$$\sum_{i=1}^{b_j} \theta_{e_i^j} - 2\pi(1 - h_j) > 0. \tag{2.40}$$

For if the jth region is not a disc, then $h_j \geq 1$, and (2.40) follows because $\theta > 0$. If the jth region is a disc, then $h_j = 0$ and (2.40) follows by the condition of theorem 1.7. We have shown that inequality (2.36) holds strictly, if $F' \neq F$.

Now assume $F' = F$, and hence $E' = E$. Like equation (2.38), we get

$$\sum_{e \in E} 2\theta_e^* = 2\pi \big(|E| - |V|\big).$$

Therefore, since $2 - 2g = |F| - |E| + |V|$,

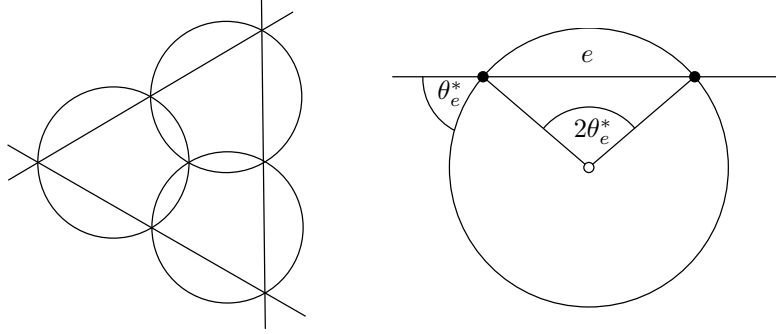$$\sum_{e \in E} 2\theta_e^* = 2\pi(|F| - 2 + 2g).$$

FIGURE 2.7. *Left:* The regular cubic pattern after stereographic projection to the plane. *Right:* The Neumann boundary condition Φ_f for the new boundary circles.

Thus, inequality (2.36) holds strictly, except if $|F'| = |F|$ and $g = 1$. This completes the proof of theorem 1.7.

2.10. Proof of theorem 1.5

A circle pattern in the sphere may be projected stereographically to the plane, choosing some vertex, v_∞, as the center of projection. (For example, figure 2.7 *(left)* shows the circle pattern combinatorially equivalent to the cube and with intersection angles $\pi/3$ after stereographic projection.) One obtains a circle pattern in the plane, in which some circles (those corresponding to faces incident with v_∞) have degenerated to straight lines. Since stereographic projection is conformal, the intersection angles are the same as in the spherical pattern. Furthermore, Möbius-equivalent circle patterns in the sphere correspond to patterns in the plane which differ by a similarity transformation; that is, provided the same vertex is chosen as the center of projection.

To prove that the condition of theorem 1.5 is necessary for a circle pattern to exist, project the pattern to the plane as described above and proceed as in section 2.9. Some circles may have degenerated to straight lines, but equation (2.34) holds nonetheless, with $\epsilon = 0$. All γ_j are zero if the dual path has one finite vertex in its interior, or if all circles have degenerated to straight lines. In that case the dual path on the sphere encircles the vertex which is the center of projection.

It is left to show that the condition of theorem 1.5 is sufficient. So assume the condition holds. The idea is to show that corresponding planar pattern exists using theorem 1.8, and then project it stereographically to the sphere.

To show the existence of the planar pattern, first choose a vertex v_∞ of the cell decomposition Σ of the sphere. Let F be the set of faces of Σ, and let $F_\infty \subset F$ be the set of faces which are incident with v_∞. Then remove from Σ the vertex v_∞, all the faces in F_∞, and the edges between them, to obtain a cell complex Σ_0 with face set $F_0 = F \setminus F_\infty$. Because Σ is a strongly regular cell decomposition of the sphere, Σ_0 is a cell decomposition of the closed disc. Hence, theorem 1.8 may be applied to prove the existence and uniqueness of the planar pattern. (Except in the trivial case when Σ_0 has only one face.) The Neumann boundary conditions need to be specified. For a boundary face f of Σ_0, set

$$\Phi_f = 2\pi - \sum 2\theta_e^*, \tag{2.41}$$

where the sum is taken over all boundary edges e of Σ_0 which are incident with f. See figure 2.7 *(right)*. For all interior faces f, set

$$\Phi_f = 2\pi. \tag{2.42}$$

If the conditions of theorem 1.8 are satisfied, one may construct the corresponding planar pattern, add the lines corresponding to the removed faces, and project to the sphere. Hence, we need to show the statements *(i)* and *(ii)*:

(i) For a boundary face f of Σ_0, Φ_f as defined in equation (2.41) is positive.

(ii) If $F_0' \in F_0$ is a nonempty set of faces of Σ_0, and E_0' is the set of of all interior edges of Σ_0 which are incident with any face in F_0', then

$$\sum_{f \in F_0'} \Phi_f \leq \sum_{e \in E_0'} 2\theta_e^*, \tag{2.43}$$

where equality holds if and only if $F_0' = F_0$.

LEMMA 2.15. *The statements (i) and (ii) above follow from the statement (iii) below.*

(iii) If F' is a nonempty subset of $F \setminus F_\infty$, and E' is the set of all edges of Σ which are incident with any face in F', then

$$2\pi |F'| \leq \sum_{e \in E'} 2\theta^*(e), \tag{2.44}$$

where equality holds if and only if $F' = F \setminus F_\infty$.

PROOF. We deduce statement *(i)*. First let $F' = F \setminus F_\infty$ to obtain

$$2\pi |F'| = \sum_{\substack{\text{edges} \\ \text{of } \Sigma_0}} 2\theta_e^*. \tag{2.45}$$

Then let $F' = F \setminus (F_\infty \cup \{f\})$, where f is a boundary face of Σ_0. Subtract the corresponding strict inequality from equation (2.45) to obtain

$$2\pi > \sum 2\theta_e^*,$$

where the sum is taken over all boundary edges of Σ_0 which are incident with f. Hence, assertion *(i)* is true.

We deduce statement *(ii)*. If $F_0' = F'$ then

$$E_0' = E' \setminus \{\text{boundary edges of } \Sigma_0\}.$$

By the definition of Φ_f, inequality (2.44) is equivalent to inequality (2.43). ∎

It is left to prove assertion *(iii)* under the assumption of the condition of theorem 1.5. We proceed in a similar way as in section 2.9.

Suppose that F' is a subset of $F \setminus F_\infty$, and E' is the set of all edges of Σ which are incident with any face in F'. Consider $F'' = F \setminus F'$, the complement of F', and $E'' = E \setminus E'$, the complement of E'. Consider the Poincaré-dual cell decomposition Σ^* and, in it, the 1-dimensional subcomplex (or graph) $\Gamma = (F'', E'')$ with vertex set F'' and edge set E''. As for any graph, we have

$$|E''| - |F''| = c - n,$$

where n is the number of connected components of Γ and c is the dimension of the cycle space. Since the graph is embedded in Σ^*, a cellular decomposition of the sphere, we have

$$c = r - 1,$$

where r is the number of regions into which Γ separates Σ^*. Since E'' contains the edges of Σ incident with v_∞, or, dually, the edges of Σ^* in the boundary of v_∞, the number of regions is at least two. Hence, the boundary of each region is nonempty.

By the condition of theorem 1.5, the sum of θ over the boundary of each region is at least 2π. Sum over all regions to obtain

$$2\pi r \leq \sum_{e \in E''} 2\theta_e.$$

Indeed, each edge in E'' appears in 0 or 2 boundaries. Equality holds if and only if every edge of E'' is in the boundary of a region and each boundary is the boundary of a single face of Σ^*. Thus, equality holds if and only if $E'' = E$ or E'' is the boundary of a single face of Σ^*. This is the case, if and only if $F' = \emptyset$ (this is ruled out by assumption) or $F' = F \setminus F_\infty$.

Thus, we have shown that

$$2\pi(|E''| - |F''|) \leq \sum_{e \in E''} 2\theta_e - 2\pi(n+1), \tag{2.46}$$

with equality if and only if $F' = F \setminus F_\infty$.

Equation (2.38) from section 2.9 also holds here. Thus, inequality (2.46) is equivalent to

$$-2\pi(|F| - |E| + |V|) + |F'| \leq \sum_{e \in E'} 2\theta_e^* - 2\pi(n+1),$$

and, using Euler's formula,

$$|F| - |E| + |V| = 2,$$

equivalent to

$$2\pi|F'| \leq \sum_{e \in E'} 2\theta_e^* - 2\pi(n-1).$$

Since $n \geq 1$, and $n = 1$ if $F' = F \setminus F_\infty$, we have deduced the assertion *(iii)* above. This completes the proof of theorem 1.5.

2.11. Proof of theorem 1.6

There is a one-to-one correspondence between Delaunay type circle patterns in the sphere and polyhedra in hyperbolic 3-space with vertices in the infinite boundary. In the Poincaré ball model, hyperbolic space corresponds to the interior of the unit ball. The unit sphere corresponds to its infinite boundary. Hyperbolic planes are represented by spheres that intersect the unit sphere orthogonally. Hence, there is a correspondence between circles in the unit sphere and hyperbolic planes. Furthermore, the intersection angle of two circles equals the dihedral angle of the corresponding planes. The isometries of hyperbolic space correspond to the Möbius transformations of the sphere at infinity.

2.12. Proof of theorem 1.2

Theorem 1.5 has the following corollary.

COROLLARY. *Let Σ be a strongly regular cell decomposition of the sphere, and suppose every vertex has n edges. (Because Σ is strongly regular, $n \geq 3$.) In other words, in the Poincaré dual decomposition Σ^*, every boundary of a face has n edges. Suppose that every simple closed path in Σ^* which is not the boundary of single face is more than n edges long. Then there exists, uniquely up to Möbius transformations, a corresponding circle pattern in the sphere with exterior intersection angles $2\pi/n$.*
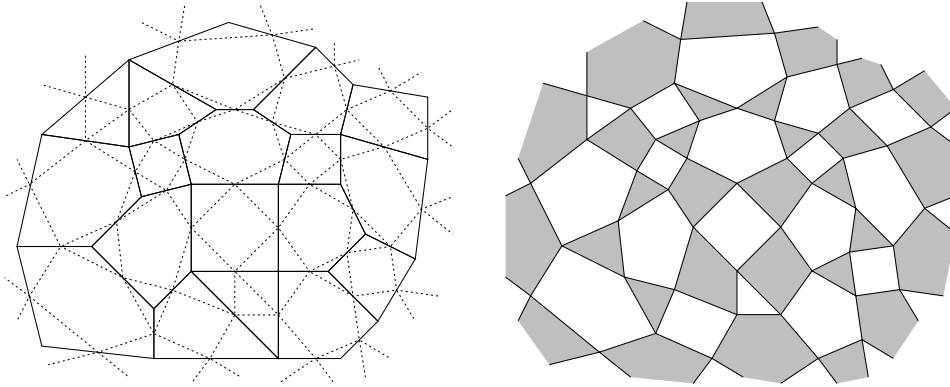
FIGURE 2.8. A cellular decomposition *(left)* and its medial decomposition *(right)*.

The case $n = 4$ implies theorem 1.2. Indeed, suppose Σ is a strongly regular cell decomposition of the sphere. In theorem 1.2, circles correspond to faces and vertices. To apply the corollary, consider the *medial* cell decomposition Σ_m of Σ. The faces of Σ_m correspond to the faces and vertices of Σ and the vertices of Σ_m correspond to edges of Σ. Figure 2.8 shows part of a cell decomposition of the sphere *(left)* and its medial decomposition *(right)*. The dotted lines in the left figure represent the edges of the medial decomposition. On the right, the faces of the medial decomposition which correspond to vertices in the original decomposition are shaded.

The vertices of the medial decomposition Σ_m are 4-valent. The assumption that Σ is strongly regular implies that Σ_m is also strongly regular. It also implies that every simple closed path in the Poincaré dual Σ_m^* which is not the boundary of single face is more than 4 edges long. See the remark on page 1, point *(vi)*. Hence, the corollary implies theorem 1.2.

2.13. Proof of theorem 1.3

The main part of theorem 1.3 follows directly from theorem 1.2. Given the cell decomposition Σ, by theorem 1.2, there is a Möbius-unique circle pattern with orthogonally intersecting circles corresponding to the faces and vertices of Σ. The circles which correspond to the faces lie in planes which form the sides of the polyhedron in question. Indeed, the circles corresponding to neighboring faces of Σ touch, and hence the corresponding planes intersect in a line which touches the sphere. Consider the faces of Σ which are incident with one vertex v of Σ. The corresponding planes go through one point, namely, the apex of the cone touching the sphere in the circle corresponding to the vertex v. Thus, one obtains a convex polyhedron—provided, that is, that all vertex-circles are smaller than a great circle. But one can always achieve this by a suitable Möbius transformation. We will show below that, by applying a suitable Möbius transformation, one can always get the center of gravity of the intersection points of the orthogonal pattern into the center of the sphere. In that position, all circles must be smaller than a great circle, because otherwise all intersection points would lie in one hemisphere.

The construction above is reversible. Given a polyhedron with edges tangent to the sphere, one obtains a circle pattern as in theorem 1.2.

The dual polyhedron is obtained by interchanging the role of face-circles and vertex-circles.

Any Möbius transformation of the sphere is the restriction of a projective transformation of the ambient space which maps the sphere onto itself. Conversely, a
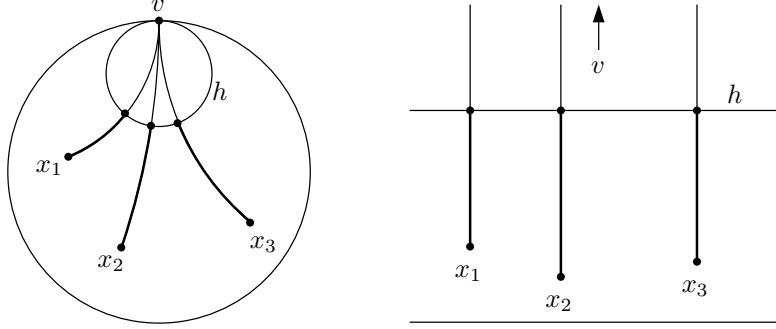
FIGURE 2.9. The 'distance' to an infinite point v is measured by cutting off at some horosphere through v. *Left:* Poincaré ball model. *Right:* half-space model.

projective transformation of the ambient space which maps the unit sphere onto itself induces a Möbius transformation of the sphere. Thus, the uniqueness claim of theorem 1.3 follows form the uniqueness claim of theorem 1.2.

It is left to show that, by applying a suitable Möbius transformation to the orthogonal circle pattern, one can get the center of gravity of the intersection points into the center of the sphere. This follows from the following lemma. The remainder of this section is devoted to proving it.

LEMMA 2.16. *Let $v_1, \ldots, v_n$ be $n \geq 3$ distinct points in the d-dimensional unit sphere $S^d \subset \mathbb{R}^{d+1}$. There exits a Möbius transformation T of S^d, such that*

$$\sum_{j=1}^{n} T v_j = 0.$$

If $\widetilde{T}$ is another such Möbius transformation, then $\widetilde{T} = RT$, where R is an isometry of S^d.

The proof relies on the close connection between the Möbius geometry of S^d and the geometry of $(d+1)$-dimensional hyperbolic space H^{d+1}. In the Poincaré ball model of hyperbolic space, H^{d+1} is identified with the unit ball in $\mathbb{R}^{d+1}$, its infinite boundary is S^d. The isometries of H^{d+1} extend to Möbius transformations of S^d. Conversely, every Möbius transformation of S^d is the extension of a unique isometry of H^{d+1}.

Given $n \geq 3$ points $v_1, \ldots, v_n \in S^d$, we are going show that there is a unique point $x \in H^{d+1}$ such that the sum of the 'distances' to $v_1, \ldots, v_n$ is minimal. Of course, the distance to an infinite point is infinite. The quantity to use is the distance to a horosphere through the infinite point. See figure 2.9

DEFINITION. For a horosphere h in H^{d+1}, define

$$\delta_h : H^{d+1} \to \mathbb{R},$$

$$\delta_h(x) = \begin{cases} -\operatorname{dist}(x, h) & \text{if } x \text{ is inside } h, \\ 0 & \text{if } x \in h, \\ \operatorname{dist}(x, h) & \text{if } x \text{ is outside } h, \end{cases}$$

where $\operatorname{dist}(x, h)$ is the distance from the point x to the horosphere h.

Suppose v is the infinite point of the horosphere h. Then the shortest path from x to h lies on the geodesic connecting x and v. If h' is another horosphere through v, then $\delta_h - \delta_{h'}$ is constant. If $g : \mathbb{R} \to H^{d+1}$ is an arc-length parametrized geodesic, then $\delta_h \circ g$ is a strictly convex function if v is not an infinite point of the

geodesic g. Otherwise, $\delta_h \circ g(s) = \pm(s - s_0)$. These claims are straightforward to prove using the Poincaré half-space model where v is the infinite point of the boundary plane. Also, one finds that

$$\lim_{x \to \infty} \sum_{j=1}^{n} \delta_{h_j}(x) = \infty,$$

where h_j are horospheres through different infinite points and $n \geq 3$. Thus, the following definition is proper.

DEFINITION (AND LEMMA). Let $v_1, \ldots, v_n$ be n points in the infinite boundary of H^{d+1}, where $n \geq 3$. Choose horospheres $h_1, \ldots, h_n$ through $v_1, \ldots, v_n$, respectively. There is a unique point $x \in H^{d+1}$ for which $\sum_{j=1}^{n} \delta_{h_j}(x)$ is minimal. This point x does not depend on the choice of horospheres. It is the *point of minimal distance sum* from the infinite points $v_1, \ldots, v_n$.

There seems to be no simpler characterization for the point of minimal distance sum. However, it is easy to check whether it is the origin in the Poincaré ball model.

LEMMA 2.17. *Let $v_1, \ldots, v_n$ be $n \geq 3$ different points in the infinite boundary of H^{d+1}. In the Poincaré ball model, $v_j \in S^d \subset \mathbb{R}^{d+1}$. The origin is the point of minimal distance sum, if and only if $\sum v_j = 0$.*

PROOF. If h_j is a horosphere through v_j, then the gradient of δ_{h_j} at the origin is the unit vector $-\frac{1}{2} v_j$. (The metric is $ds^2 = \left(\frac{2}{1 - \sum x_j^2} \right)^2 \sum dx_j^2$.) ∎

Lemma 2.16 is now almost immediate. Let x be the point of minimal distance sum from the $v_1, \ldots, v_n$ in the Poincaré ball model. There is a hyperbolic isometry T which moves x into the origin. If $\widetilde{T}$ is another hyperbolic isometry which moves x into the origin, then $\widetilde{T} = RT$, with R is an orthogonal transformation of $\mathbb{R}^{d+1}$. Lemma 2.16 follows.

This concludes the proof of theorem 1.3.

Other variational principles

3.1. Legendre transformations

In this section, we derive different variational principles for circle patterns by Legendre transformations of the functionals S_{euc}, S_{hyp}, and S_{sph}. We obtain the functional $\widehat{S}$, defined below, which depends not on the (transformed) radii $\rho \in \mathbb{R}^F$ but on the angles $\varphi \in \mathbb{R}^{\vec{E}_{int}}$. According to whether the variation is constrained to the space of euclidean, hyperbolic, or spherical coherent angle systems, the critical points correspond to circle patterns of the respective geometry. On the euclidean and hyperbolic coherent angle systems, the functional $\widehat{S}$ is strictly convex upwards, so that there can be only one critical point, which is a maximum. (A function f on a convex domain D is called *strictly convex upwards (downwards)*, if

$$f\big((1-t)x_1 + tx_2\big) \underset{(<)}{>} (1-t)f(x_1) + tf(x_2)$$

for all $x_1, x_2 \in D$ and $0 < t < 1$.) The function $\widehat{S}(\varphi)$ is defined in terms of Clausen's integral $\text{Cl}_2(x)$, see appendix B.

THEOREM 3.1. *Let $\vec{E}_{int}$ be the set of oriented interior edges and define*

$$\widehat{S} : \mathbb{R}^{\vec{E}_{int}} \to \mathbb{R}$$

$$\widehat{S}(\varphi) = \sum_{e:\, \vec{e}\, \uparrow\downarrow\, -\vec{e}} \Big(\text{Cl}_2(\theta_e^* + \varphi_{\vec{e}} - \varphi_{-\vec{e}}) + \text{Cl}_2(\theta_e^* - \varphi_{\vec{e}} + \varphi_{-\vec{e}})$$

$$+ \text{Cl}_2(\theta_e^* + \varphi_{\vec{e}} + \varphi_{-\vec{e}}) + \text{Cl}_2(\theta_e^* - \varphi_{\vec{e}} - \varphi_{-\vec{e}}) - 2\,\text{Cl}_2(2\theta_e^*) \Big),$$

$$(3.1)$$

where the sum is taken over all non-oriented interior edges e, and $\vec{e}$, $-\vec{e}$ are the two oppositely oriented edges corresponding to it.

(i) The function $\widehat{S}$ is strictly convex upwards on the set of all euclidean coherent angle systems.

If the function S_{euc} attains its minimum at $\rho \in \mathbb{R}^F$, then the restriction of $\widehat{S}$ to the space of euclidean coherent angle systems attains its maximum at $\varphi \in \mathbb{R}^{\vec{E}_{int}}$ defined by equations (2.4).

Conversely, suppose the restriction of $\widehat{S}$ to the space of euclidean coherent angle systems attains its maximum at $\varphi \in \mathbb{R}^{\vec{E}}$. Then the equations

$$\rho_{f_k} - \rho_{f_j} = \log \frac{\sin \varphi_{\vec{e}}}{\sin(\varphi_{\vec{e}} + \theta_e)} \quad for \quad f_j \,\underset{\vec{e}}{\overset{\bullet}{\uparrow}}\, f_k \qquad (3.2)$$

are compatible. (There is one equation for each oriented interior edge $\vec{e}$ and f_j, f_k are the faces to its left and right, respectively.) Therefore, they define $\rho \in \mathbb{R}^F$ uniquely up to an additive constant. The function S_{euc} attains its minimum at this ρ.

If they exist, the extremal values are equal:

$$\min_{\rho \in \mathbb{R}^F} S_{euc}(\rho) = \max_{\varphi\, euc.\ coherent} \widehat{S}(\varphi)$$

(ii) The function $\widehat{S}$ is strictly convex upwards on the set of hyperbolic coherent angle systems.

If the function S_{hyp} attains its minimum at $\rho \in \mathbb{R}^F$, then the restriction of $\widehat{S}$ to the space of hyperbolic coherent angle systems attains its maximum at the $\varphi \in \mathbb{R}^{\vec{E}_{int}}$ defined by equation (2.16).

Conversely, suppose the restriction of $\widehat{S}$ to the space of hyperbolic coherent angle systems attains its maximum at $\varphi \in \mathbb{R}^{\vec{E}_{int}}$. Then the equations

$$\rho_f = \frac{1}{2} \log \frac{\sin\left(\frac{\theta^* - \varphi_{\vec{e}} - \varphi_{-\vec{e}}}{2}\right) \sin\left(\frac{\theta^* - \varphi_{\vec{e}} + \varphi_{-\vec{e}}}{2}\right)}{\sin\left(\frac{\theta^* + \varphi_{\vec{e}} + \varphi_{-\vec{e}}}{2}\right) \sin\left(\frac{\theta^* + \varphi_{\vec{e}} - \varphi_{-\vec{e}}}{2}\right)} \tag{3.3}$$

are compatible and define, therefore, a unique $\rho \in \mathbb{R}^F$. (There is one equation for each oriented interior edge $\vec{e}$, and f is the face on its left side.) The function S_{hyp} attains its minimum at this ρ.

If they exist, the extremal values are equal:

$$\min_{\rho \in \mathbb{R}^F} S_{hyp}(\rho) = \max_{\substack{\varphi \in \vec{E}, \, hyp. \\ coherent}} \widehat{S}(\varphi)$$

(iii) If $\rho \in \mathbb{R}^F$ is a critical point of the function S_{sph}, then $\varphi \in \mathbb{R}^{\vec{E}_{int}}$ defined by equations (2.25) is a critical point of the restriction of $\widehat{S}$ to the space of spherical coherent angle systems.

Conversely, suppose the restriction of $\widehat{S}$ to the space of spherical coherent angle systems is critical at $\varphi \in \mathbb{R}^{\vec{E}}$. Then the equations

$$\rho_f = \frac{1}{2} \log \frac{\sin\left(\frac{-\theta^* + \varphi_{\vec{e}} + \varphi_{-\vec{e}}}{2}\right) \sin\left(\frac{\theta^* - \varphi_{\vec{e}} + \varphi_{-\vec{e}}}{2}\right)}{\sin\left(\frac{\theta^* + \varphi_{\vec{e}} + \varphi_{-\vec{e}}}{2}\right) \sin\left(\frac{\theta^* + \varphi_{\vec{e}} - \varphi_{-\vec{e}}}{2}\right)} \tag{3.4}$$

are compatible and define, therefore, a unique $\rho \in \mathbb{R}^F$. (There is one equation for each oriented interior edge $\vec{e}$, and f is the face on its left side.) The function S_{sph} is critical at this ρ.

The values at corresponding critical points are equal:

$$S_{sph}(\rho_{critical}) = \widehat{S}(\varphi_{critical}).$$

REMARK. 1. If φ is a euclidean coherent angle system, then equation (3.1) simplifies to

$$\widehat{S}(\varphi) = \sum \left(\operatorname{Cl}_2(2\varphi_{\vec{e}}) + \operatorname{Cl}_2(2\varphi_{-\vec{e}}) - \operatorname{Cl}_2(2\theta_e^*) \right), \tag{3.5}$$

where the sum is taken over all interior non-oriented edges e, and $\vec{e}$, $-\vec{e}$ are the corresponding oriented edges.

2. Equations (3.3) and (3.4) may be subsumed under the equation

$$\rho_f = \frac{1}{2} \log \left| \frac{\sin\left(\frac{\theta^* - \varphi_{\vec{e}} - \varphi_{-\vec{e}}}{2}\right) \sin\left(\frac{\theta^* - \varphi_{\vec{e}} + \varphi_{-\vec{e}}}{2}\right)}{\sin\left(\frac{\theta^* + \varphi_{\vec{e}} + \varphi_{-\vec{e}}}{2}\right) \sin\left(\frac{\theta^* + \varphi_{\vec{e}} - \varphi_{-\vec{e}}}{2}\right)} \right|.$$

The rest of this section is devoted to the derivation of the functional $\widehat{S}(\varphi)$ and the proof of theorem 3.1.

In classical mechanics, the Legendre transformation translates between the Lagrangian and Hamiltonian descriptions of a mechanical system. (For a thorough treatment, see, for example, Arnold's textbook [**3**].) The motion of such a system is typically described by functions $q(t)$ which are critical for the functional $\int L(\dot{q}, q)\, dt$, where $L(v, q)$ is the Lagrangian of the system. The Hamiltonian $H(p, q)$ is obtained

by a Legendre transformation with respect to v: $H(p,q) = pv - L(v,q)$, where $p = \partial L(v,q)/\partial v$. It turns out that the motion of the system is described by functions $p(t)$, $q(t)$ which are critical for the functional $\int (pq - H(p,q))\, dt$. Here, p and q vary independently.

The construction of $\widehat{S}$ proceeds in a similar way. The role of the position variables q is played by the variables ρ. Whereas q depends continuously on the time t, ρ is a function on the finite set of faces. Instead of integrals, the functionals are finite sums. For each functional, euclidean, hyperbolic, and spherical, we will define a Lagrangian form first. From it, we will obtain a Hamiltonian form by a Legendre transformation. A reduction leads to the functional $\widehat{S}$ in every case.

First, we recapitulate the definition and basic properties of the Legendre transformation of a smooth function of one variable. Then we deal with the euclidean, hyperbolic, and spherical functionals separately.

3.1.1. The Legendre transformation of a smooth function of one variable. The Legendre transformation is defined for convex functions. In general, they need not be smooth and may depend on many variables. For the following sections, it is sufficient to consider only the simplest case. The generalization to many variables, which is needed in section 3.7, is straightforward.

DEFINITION. Suppose F is a smooth real valued function on some interval in $\mathbb{R}$, and $F'' > 0$ (or $F'' < 0$). Then

$$y = F'(x) \tag{3.6}$$

defines a smooth coordinate transformation. The *Legendre transform* of F is

$$\widehat{F}(y) = xy - F(x), \tag{3.7}$$

where x is related to y by (3.6).

The Legendre transformation is an involution: If $\widehat{F}$ is the Legendre transform of F and, say, $F'' > 0$, then $\widehat{F}'' > 0$ and F is the Legendre transform of $\widehat{F}$. Indeed,

$$\widehat{F}'(y) \stackrel{(3.7)}{=} \frac{dx}{dy} y + x - \frac{dx}{dy} F'(x) \stackrel{(3.6)}{=} x$$

and

$$\widehat{F}''(y) = \frac{dx}{dy} = \frac{1}{F''(x)}.$$

3.1.2. The euclidean functional. Equation (2.12), defining the functional S_{euc}, may be rewritten as

$$S_{\mathrm{euc}}(\rho) = \sum_{f_j \circ \!\!\uparrow\!\! \circ f_k} \left(F_{\theta_e}(\rho_{f_k} - \rho_{f_j}) - (\pi - \theta_e)\rho_{f_k} \right) + \sum_{\circ f} \Phi_f \rho_f.$$

Here, the first sum is taken over all interior *oriented* edges $\vec{e}$, and f_j and f_k are the faces on the left and right of $\vec{e}$, and e is the corresponding non-oriented edge. The second sum is taken over all faces f. The function $F_\theta(x)$ is defined in equation (2.10). Define the Lagrangian form of the functional by

$$S_{\mathrm{euc}}^L : \mathbb{R}^{\vec{E}_{int}} \times \mathbb{R}^F \to \mathbb{R},$$

$$S_{\mathrm{euc}}^L(v, \rho) = \sum_{f_j \circ \!\!\uparrow\!\! \circ f_k} \left(F_{\theta_e}(v_{\vec{e}}) - (\pi - \theta_e)\rho_{f_k} \right) + \sum_{\circ f} \Phi_f \rho_f.$$

If, for all oriented interior edges $\vec{e} \in \vec{E}$,

$$v_{\vec{e}} = \rho_{f_k} - \rho_{f_j},$$

where f_j and f_k to are the faces to the the left and to the right of $\vec{e}$, respectively, then

$$S_{\mathrm{euc}}^{L}(v, \rho) = S_{\mathrm{euc}}(\rho).$$

In general, however, we do not assume that v comes from a ρ in this way, or even that $v_{\vec{e}} = -v_{-\vec{e}}$.

By equations (2.6) and (2.10), $F_\theta''(x) > 0$. The Legendre transform of $F_\theta(x)$ is

$$\widehat{F}_\theta(y) = -\frac{1}{2}\,\mathrm{Cl}_2(2y) + \frac{1}{2}\,\mathrm{Cl}_2(2y + 2\theta) - \frac{1}{2}\,\mathrm{Cl}_2(2\theta)\,,$$

where

$$y = F_\theta'(x) = f_\theta(x).$$

This follows from equation (B.7) of appendix B. By equation (2.8), the domain of $\widehat{F}_\theta(y)$ is

$$0 < y < \pi - \theta.$$

Define the 'Hamiltonian' form of the functional by

$$S_{\mathrm{euc}}^{H} : D \times \mathbb{R}^{F} \longrightarrow \mathbb{R},$$

$$S_{\mathrm{euc}}^{H}(\varphi, \rho) = \sum_{f_j \circ \overset{\bullet}{\underset{}{\uparrow}} \circ f_k} \left(\varphi_{\vec{e}}(\rho_{f_k} - \rho_{f_j}) - \widehat{F}_{\theta_e}(\varphi_{\vec{e}}) - (\pi - \theta_e)\rho_{f_k} \right) + \sum_{\circ j} \Phi_f \rho_f,$$

where the φ-domain D is

$$D = \left\{ \varphi \in \mathbb{R}^{\vec{E}_{int}} \,\middle|\, 0 < \varphi_{\vec{e}} < \pi - \theta_e \ \text{for all} \ \vec{e} \in \vec{E}_{int} \right\}. \tag{3.8}$$

(This is a superset of the space of euclidean coherent angle systems.) Writing it all out, one has

$$S_{\mathrm{euc}}^{H}(\varphi, \rho) = \sum_{f_j \circ \overset{\bullet}{\underset{}{\uparrow}} \circ f_k} \left(\varphi_{\vec{e}}\,(\rho_{f_k} - \rho_{f_j}) + \frac{1}{2}\big(\mathrm{Cl}_2(2\varphi_{\vec{e}}) - \mathrm{Cl}_2(2\varphi_{\vec{e}} + 2\theta_e) + \mathrm{Cl}_2(2\theta_e) \big) \right.$$

$$\left. - (\pi - \theta_e)\rho_{f_k} \right) + \sum_{\circ f} \Phi_f \rho_f.$$

If φ and ρ are related by equations (2.4), then

$$S_{\mathrm{euc}}^{H}(\varphi, \rho) = S_{\mathrm{euc}}(\rho).$$

Now, $\widehat{F}_\theta'' > 0$. This follows from $F_\theta'' > 0$ and the properties of the Legendre transformation. (It can also be verified by a direct calculation.) Therefore, $S_{\mathrm{euc}}^{H}(\varphi, \rho)$ is strictly convex upwards with respect to φ.

The motivation for this construction of S_{euc}^{H} is, that the critical points of S_{euc} correspond to critical points of S_{euc}^{H} where ρ and φ may vary independently:

LEMMA 3.1. *If (φ, ρ) is a critical point of S_{euc}^{H}, then ρ is a critical point of S_{euc}. Conversely, suppose ρ is a critical point of S_{euc}. Define φ by equations (2.4). Then (φ, ρ) is a critical point of S_{euc}^{H}. At a critical point, $S_{euc}(\rho) = S_{euc}^{H}(\varphi, \rho)$.*

PROOF. For any interior oriented edge $\vec{e} \in \vec{E}$,

$$\frac{\partial S_{\mathrm{euc}}^{H}}{\partial \varphi_{\vec{e}}}(\varphi, \rho) = \rho_{f_k} - \rho_{f_j} - \widehat{F}_{\theta_e}'(\varphi_{\vec{e}}),$$

Hence, all partial derivatives with respect to the variables $\varphi_{\vec{e}}$ vanish, if and only if φ and ρ are related by $\rho_{f_k} - \rho_{f_j} = \widehat{F}_{\theta_e}'(\varphi_{\vec{e}})$, or, equivalently, by $\varphi_{\vec{e}} = F_{\theta_e}'(\rho_{f_k} - \rho_{f_k}) = f_{\theta_e}(\rho_{f_k} - \rho_{f_j})$. In this case, $S_{\mathrm{euc}}^{H}(\varphi, \rho) = S_{\mathrm{euc}}(\rho)$. ∎

Note that $S_{\text{euc}}^H(\varphi, \rho)$ depends linearly on ρ. Collecting the coefficients of each ρ_f, one finds that, if φ is a euclidean coherent angle system, then $S_{\text{euc}}^H(\varphi, \rho)$ does not depend on ρ at all. In fact, in that case,

$$S_{\text{euc}}^H(\varphi, \rho) = \widehat{S}(\varphi).$$

To see this, note that if φ is a coherent angle system, then $\varphi_{\vec{e}} + \theta_e = \pi - \varphi_{-\vec{e}}$. Hence $\text{Cl}_2(2\varphi_{\vec{e}} + 2\theta_e) = -\text{Cl}_2(2\varphi_{-\vec{e}})$. Also, $\text{Cl}_2(2\theta) = -\text{Cl}_2(2\theta^*)$.

The convexity claim of theorem 3.1(i) follows from the convexity of $S_{\text{euc}}^H(\varphi, \rho)$ with respect to φ. Equations (3.2) are the inverse relations to equations (2.4). It is left to prove that they are compatible if φ is a critical point of $\widehat{S}$ under variations in the space of coherent angle systems. The rest follows from lemma 3.1. Suppose φ is a critical point of $\widehat{S}$ under variations in the space of coherent angle systems. Since we are only interested in the restriction of $\widehat{S}$ to the space of euclidean coherent angle systems, we may use equation (3.5) for $\widehat{S}$. The partial derivatives are then

$$\frac{\partial \widehat{S}}{\partial \varphi_{\vec{e}}} = -2\log(2\sin\varphi_{\vec{e}}).$$

The tangent space to the space of euclidean coherent angle systems is spanned by vectors of the form

$$\sum_{\vec{e} \in \gamma} \Big(\frac{\partial}{\partial \varphi_{\vec{e}}} - \frac{\partial}{\partial \varphi_{-\vec{e}}} \Big),$$

where γ is some oriented closed path in the Poincaré dual cell decomposition. (If we add to $\varphi_{\vec{e}}$ we have to subtract the same amount from $\varphi_{-\vec{e}}$. But the sum of φ around each face has to remain constant, so we step from one face to the next, adding and subtracting along some closed path of the Poincaré dual.) Since φ is a critical point under variations in the space of coherent angle systems,

$$\sum_{\vec{e} \in \gamma} \log \frac{\sin\varphi_{\vec{e}}}{\sin(\varphi_{\vec{e}} + \theta_e)} = 0$$

for all closed paths γ in the Poincaré dual. Hence, equations (3.2) are compatible. This completes the proof of part *(i)* of theorem 3.1.

3.1.3. The hyperbolic functional. The construction in this case is similar to the euclidean case, but a bit more involved. This is due to the fact that the nonlinear terms in equation (2.18) (the definition of $S_{\text{hyp}}(\rho)$) depend not only on the differences $\rho_k - \rho_j$, but also on the sums $\rho_k + \rho_j$. In fact, equation (2.18) may be written as

$$S_{\text{hyp}}(\rho) = \sum_{f_j \circ \lvert \circ f_k} \big(G_{\theta_e}(\rho_{f_k} - \rho_{f_j}) + G_{\theta_e}(\rho_{f_j} + \rho_{f_k}) \big) + \sum_{\circ f} \Phi_f \rho_f,$$

where

$$G_\theta(x) = F_\theta(x) + F_\theta(-x) = \text{Im}\,\text{Li}_2\big(e^{x+i\theta}\big) + \text{Im}\,\text{Li}_2\big(e^{-x+i\theta}\big).$$

The first sum is taken over all non-oriented edges e, and f_j and f_k are the faces on either side of e. The function $G_\theta(x)$ is even, so that it does not matter which face is taken to be f_j and which f_k. The second sum is taken over all faces f.

We introduce some notation before we define the Lagrangian form of the functional. The space $\mathbb{R}^{\vec{E}_{int}}$ of functions on the oriented interior edges splits into the direct sum of antisymmetric and symmetric functions:

$$\mathbb{R}^{\vec{E}_{int}} = \text{Alt}(\vec{E}_{int}) \oplus \text{Sym}(\vec{E}_{int}),$$

where

$$\text{Alt}(\vec{E}_{int}) = \big\{ v \in \mathbb{R}^{\vec{E}_{int}} \,\big|\, v_{-\vec{e}} = -v_{\vec{e}} \big\} \tag{3.9}$$

and
$$\mathrm{Sym}(\vec{E}_{int}) = \left\{ w \in \mathbb{R}^{\vec{E}_{int}} \,\middle|\, w_{-\vec{e}} = w_{\vec{e}} \right\}.$$

Define the function
$$S^L_{\mathrm{hyp}} : \mathrm{Alt}(\vec{E}_{int}) \times \mathrm{Sym}(\vec{E}_{int}) \times \mathbb{R}^F \to \mathbb{R},$$
$$S^L_{\mathrm{hyp}}(v, w, \rho) = \sum_{f_j \circ \!\!\!\!\overset{\bullet}{\underset{}{\rule{0pt}{6pt}}}\!\! \circ f_k} \left(G_{\theta_e}(v_{\vec{e}}) + G_{\theta_e}(w_{\vec{e}}) \right) + \sum_{\circ f} \Phi_f \rho_f.$$

The first sum is taken over all non-oriented interior edges e, and $\vec{e}$ is one of the oriented representatives e. The second sum is taken over all faces f.

If, for all oriented edges $\vec{e} \in \vec{E}$,
$$v_{\vec{e}} = \rho_{f_k} - \rho_{f_j} \quad \text{and} \quad w_{\vec{e}} = \rho_{f_k} + \rho_{f_j},$$
where f_j and f_k are the faces to the the left and to the right of $\vec{e}$, respectively, then
$$S^L_{\mathrm{hyp}}(v, w, \rho) = S_{\mathrm{hyp}}(\rho).$$

By a straightforward calculation,
$$G'_\theta(x) = f_\theta(x) - f_\theta(-x) = 2\arctan\left(\tan\left(\frac{\theta^*_e}{2}\right) \tanh\left(\frac{y}{2}\right) \right),$$
and
$$G''_\theta(x) = f'_\theta(x) + f'_\theta(-x) = 2f'_\theta(x) > 0.$$

The Legendre transform of $G_\theta(x)$ is
$$\widehat{G}_\theta(y) = -\mathrm{Cl}_2(\theta^* + y) - \mathrm{Cl}_2(\theta^* - y) + \mathrm{Cl}_2(2\theta^*),$$
where $y = G'_\theta(x)$. This follows from equation (B.8) of appendix B. The domain of $\widehat{G}_\theta(y)$ is $-\theta^* < y < \theta^*$.

The 'Hamiltonian' form of the functional is
$$\left\{ p \in \mathrm{Alt}(\vec{E}_{int}) \,\middle|\, |p_{\vec{e}}| < \theta^*_e \right\} \times \left\{ s \in \mathrm{Sym}(\vec{E}_{int}) \,\middle|\, |s_{\vec{e}}| < \theta^*_e \right\} \times \mathbb{R}^F \longrightarrow \mathbb{R},$$
$$S^H_{\mathrm{hyp}}(p, s, \rho) = \sum_{f_j \circ \!\!\!\!\overset{\bullet}{\underset{}{\rule{0pt}{6pt}}}\!\! \circ f_k} \left(p_{\vec{e}}(\rho_{f_k} - \rho_{f_j}) - \widehat{G}_{\theta_e}(p_{\vec{e}}) + s_{\vec{e}}(\rho_{f_k} + \rho_{f_j}) - \widehat{G}_{\theta_e}(s_{\vec{e}}) \right.$$
$$\left. + \sum_{\circ f} \Phi_f \rho_f, \right.$$

where the first sum is taken over all non-oriented interior edges e, and $\vec{e}$ is one of the oriented representatives e. The second sum is taken over all faces f. Writing it all out, we have
$$S^H_{\mathrm{hyp}}(p, s, \rho) = \sum_{f_j \circ \!\!\!\!\overset{\bullet}{\underset{}{\rule{0pt}{6pt}}}\!\! \circ f_k} \left(p_{\vec{e}}(\rho_{f_k} - \rho_{f_j}) + \mathrm{Cl}_2\left(\theta^*_e + p_{\vec{e}}\right) + \mathrm{Cl}_2\left(\theta^*_e - p_{\vec{e}}\right) \right.$$
$$\left. + s_{\vec{e}}(\rho_{f_j} + \rho_{f_k}) + \mathrm{Cl}_2\left(\theta^*_e + s_{\vec{e}}\right) + \mathrm{Cl}_2\left(\theta^*_e - s_{\vec{e}}\right) \qquad (3.10) \right.$$
$$\left. - 2\,\mathrm{Cl}_2\left(2\theta^*_e\right) \right) + \sum_{\circ f} \Phi_f \rho_f.$$

The functional $S^H_{\mathrm{hyp}}(p, s, \rho)$ is convex upwards in the variables p, s. If p and s are related to ρ by
$$p_{\vec{e}} = G'_{\theta_e}(\rho_k - \rho_j) = 2\arctan\left(\tan\left(\frac{\theta^*_e}{2}\right) \tanh\left(\frac{\rho_k - \rho_j}{2}\right) \right) \qquad (3.11)$$
and
$$s_{\vec{e}} = G'_{\theta_e}(\rho_k + \rho_j) = 2\arctan\left(\tan\left(\frac{\theta^*_e}{2}\right) \tanh\left(\frac{\rho_k + \rho_j}{2}\right) \right) \qquad (3.12)$$

where f_j and f_k are the faces to the left and right of $\vec{e}$, respectively, then

$$S_{\mathrm{hyp}}^H(p, s, \rho) = S(\rho).$$

Again, the critical points of $S_{\mathrm{hyp}}(\rho)$ correspond to the critical points of $S_{\mathrm{hyp}}^H(p, s, \rho)$ where p, s, and ρ may vary independently. (However, the domain of $S_{\mathrm{hyp}}^H(p, s, \rho)$ has to be respected, of course. In particular, the constraints $p \in \mathrm{Alt}(\vec{E}_{int})$ and $s \in \mathrm{Sym}(\vec{E}_{int})$ apply.) The following lemma is proved in the same way as lemma 3.1.

LEMMA 3.2. *If (p, s, ρ) is a critical point of S_{hyp}^H, then ρ is a critical point of S_{hyp}. Conversely, suppose ρ is a critical point of S_{hyp}. Define p and s by equations (3.11) and (3.12). Then (p, s, ρ) is a critical point of S_{hyp}^H. At a critical point, $S_{hyp}(\rho) = S_{hyp}^H(p, s, \rho)$.*

Now, we introduce the variables $\varphi \in \mathbb{R}^{\vec{E}_{int}}$,

$$\varphi_{\vec{e}} = \tfrac{1}{2}(p_{\vec{e}} - s_{\vec{e}})$$

instead of (p, s):

$$S_{\mathrm{hyp}}^H(\varphi, \rho) = S_{\mathrm{hyp}}^H(p, s, \rho).$$

Since

$$\varphi_{-\vec{e}} = \tfrac{1}{2}(-p_{\vec{e}} - s_{\vec{e}}),$$

we have

$$p_{\vec{e}} = \varphi_{\vec{e}} - \varphi_{-\vec{e}},$$
$$s_{\vec{e}} = -\varphi_{\vec{e}} - \varphi_{-\vec{e}},$$

and therefore

$$S_{\mathrm{hyp}}^H(\varphi, \rho) =$$

$$\sum_{f_j \circ \Big[\circ f_k} \Big(-2\big(\varphi_{\vec{e}}\rho_{f_j} + \varphi_{-\vec{e}}\rho_{f_k}\big) + \mathrm{Cl}_2\left(\theta_e^* + \varphi_{\vec{e}} - \varphi_{-\vec{e}}\right) + \mathrm{Cl}_2\left(\theta_e^* - \varphi_{\vec{e}} + \varphi_{-\vec{e}}\right)$$

$$+ \mathrm{Cl}_2\left(\theta_e^* - \varphi_{\vec{e}} - \varphi_{-\vec{e}}\right) + \mathrm{Cl}_2\left(\theta_e^* + \varphi_{\vec{e}} + \varphi_{-\vec{e}}\right) - 2\,\mathrm{Cl}_2\left(2\theta_e^*\right)\Big)$$

$$+ \sum_{\circ f} \Phi_f \rho_f.$$

The domain of $S_{\mathrm{hyp}}^H(\varphi, \rho)$ is the set of all $(\varphi, \rho) \in \mathbb{R}^{\vec{E}_{int}} \times \mathbb{R}^F$ such that φ satisfies the inequalities

$$|\varphi_{\vec{e}} + \varphi_{-\vec{e}}| < \theta_e^* \quad \text{and} \quad |\varphi_{\vec{e}} - \varphi_{-\vec{e}}| < \theta_e^*.$$

This is a superset of the space of hyperbolic coherent angle systems. The relations (3.11) and (3.12) between p, s and ρ are equivalent to the relation (2.16) between φ and ρ. Hence, if φ and ρ are related by equation (2.16), then $S_{\mathrm{hyp}}^H(\varphi, \rho) = S_{\mathrm{hyp}}(\rho)$. The functional $S_{\mathrm{hyp}}^H(\varphi, \rho)$ is linear in ρ. As in the euclidean case, collecting the coefficients of each ρ_f, one observes that if φ is a hyperbolic coherent angle system, then S_{hyp}^H does not depend on ρ. In fact, in that case, $S_{\mathrm{hyp}}^H(\varphi, \rho) = \widehat{S}(\varphi)$.

The convexity claim of theorem 3.1 *(ii)* follows from the convexity of $S_{\mathrm{hyp}}^H(\varphi, \rho)$ with respect to φ. Equations (3.3) are the inverse relations to equations (2.16); see lemma 2.5. It is left to prove that they are compatible if φ is a critical point of $\widehat{S}$ under variations in the space of hyperbolic coherent angle systems. The rest follows from lemma 3.2. Suppose the oriented edges $\vec{e}_1$ and $\vec{e}_2$ are both in the oriented boundary of a face f. We need to show that the value for ρ_f obtained from the equation (3.3) involving $\varphi_{\pm\vec{e}_1}$ is the same as the value obtained from the

equation involving $\varphi_{\pm\vec{e}_2}$. The tangent space to the space of coherent angle systems is spanned by vectors of the form

$$\frac{\partial}{\partial\varphi_{\vec{e}_2}} - \frac{\partial}{\partial\varphi_{\vec{e}_1}}$$

where $\vec{e}_1$ and $\vec{e}_2$ are two oriented edges in the boundary of a face. But $\partial\widehat{S}/\partial\varphi_{\vec{e}}$ is twice the right hand side of equation (3.3). Thus, they are consistent if φ is a critical point of S_{hyp} under variations in the space of coherent angle systems. This completes the proof of part *(ii)* of theorem 3.1.

3.1.4. The spherical functional. This case is similar to the hyperbolic case. Define the 'Lagrangian' form of the spherical circle pattern functional S_{sph} (defined in equation (2.27)) to be

$$S^L_{\text{sph}} : \text{Alt}(\vec{E}_{int}) \times \text{Sym}(\vec{E}_{int}) \times \mathbb{R}^F \to \mathbb{R},$$

$$S^L_{\text{sph}}(v,w,\rho) = \sum_{f_j \circ \underset{}{\overset{}{\vert}} \circ f_k} \big(G_{\theta_e}(v_{\vec{e}}) - G_{\pi-\theta_e}(w_{\vec{e}}) - \pi(\rho_{f_j}+\rho_{f_k})\big) + \sum_{\circ f} \Phi_f \rho_f.$$

If, for all oriented edges $\vec{e} \in \vec{E}$,

$$v_{\vec{e}} = \rho_{f_k} - \rho_{f_j} \quad \text{and} \quad w_{\vec{e}} = \rho_{f_k} + \rho_{f_j},$$

where f_j and f_k to are the faces to the the left and to the right of $\vec{e}$, respectively, then

$$S^L_{\text{sph}}(v,w,\rho) = S_{\text{sph}}(\rho).$$

The 'Hamiltonian' form is defined as

$$\big\{p \in \text{Alt}(\vec{E}_{int}) \,\big|\, |p_{\vec{e}}| < \theta^*_e\big\} \times \big\{s \in \text{Sym}(\vec{E}_{int}) \,\big|\, |s_{\vec{e}}| < \theta_e\big\} \times \mathbb{R}^F \longrightarrow \mathbb{R},$$

$$S^H_{\text{sph}}(p,s,\rho) = \sum_{f_j \circ \underset{}{\overset{}{\vert}} \circ f_k} \big(p_{\vec{e}}(\rho_{f_k}-\rho_{f_j}) - \widehat{G}_{\theta_e}(p_{\vec{e}}) - s_{\vec{e}}(\rho_{f_k}+\rho_{f_j}) + \widehat{G}_{\pi-\theta_e}(s_{\vec{e}})$$

$$- \pi(\rho_{f_j}+\rho_{f_k})\big) + \sum_{\circ f}\Phi_f\rho_f.$$

Writing it all out, we have

$$S^H_{\text{sph}}(p,s,\rho) = \sum_{f_j \circ \underset{}{\overset{}{\vert}} \circ f_k}\Big(p_{\vec{e}}\big(\rho_{f_k}-\rho_{f_j}\big) + \text{Cl}_2\big(\theta^*_e+p_{\vec{e}}\big) + \text{Cl}_2\big(\theta^*_e-p_{\vec{e}}\big)$$

$$- s_{\vec{e}}\big(\rho_{f_j}+\rho_{f_k}\big) - \text{Cl}_2\big(\theta_e+s_{\vec{e}}\big) - \text{Cl}_2\big(\theta_e-s_{\vec{e}}\big)$$

$$- 2\,\text{Cl}_2\big(2\theta^*_e\big) - \pi\big(\rho_{f_j}+\rho_{f_k}\big)\Big) \qquad (3.13)$$

$$+ \sum_{\circ f}\Phi_f\rho_f.$$

(We have used that $\text{Cl}_2(2\theta) = -\text{Cl}_2(2\theta^*)$.) The functional $S^H_{\text{sph}}(p,s,\rho)$ is convex upwards in the variables p and convex downwards in the variables s. If p and s are related to ρ by

$$p_{\vec{e}} = G'_{\theta_e}(\rho_k-\rho_j) = 2\arctan\left(\tan\left(\frac{\theta^*_e}{2}\right)\tanh\left(\frac{\rho_k-\rho_j}{2}\right)\right) \qquad (3.14)$$

and

$$s_{\vec{e}} = G'_{\theta^*_e}(\rho_k+\rho_j) = 2\arctan\left(\tan\left(\frac{\theta_e}{2}\right)\tanh\left(\frac{\rho_k+\rho_j}{2}\right)\right) \qquad (3.15)$$

where f_j and f_k are the faces to the left and right of $\vec{e}$, respectively, then

$$S^H_{\text{sph}}(p,s,\rho) = S(\rho).$$

Again, the critical points of $S_{\mathrm{sph}}(\rho)$ correspond to the critical points of $S_{\mathrm{sph}}^H(p, s, \rho)$ where p, s, and ρ may vary independently. The following lemma is proved in the same way as lemmas 3.1 and 3.2.

LEMMA 3.3. *If (p, s, ρ) is a critical point of S_{sph}^H, then ρ is a critical point of S_{sph}. Conversely, suppose ρ is a critical point of S_{sph}. Define p and s by equations (3.14) and (3.15). Then (p, s, ρ) is a critical point of S_{sph}^H. At a critical point, $S_{sph}(\rho) = S_{sph}^H(p, s, \rho)$.*

Now we introduce the variables $\varphi \in \mathbb{R}^{\vec{E}}$,

$$\varphi_{\vec{e}} = \tfrac{1}{2}(p_{\vec{e}} + s_{\vec{e}} + \pi)$$

instead of (p, s):

$$S_{\mathrm{sph}}^H(\varphi, \rho) = S_{\mathrm{sph}}^H(p, s, \rho).$$

We have

$$p_{\vec{e}} = \varphi_{\vec{e}} - \varphi_{-\vec{e}},$$
$$s_{\vec{e}} = \varphi_{\vec{e}} + \varphi_{-\vec{e}} - \pi,$$

and hence

$$S_{\mathrm{sph}}^H(\varphi, \rho) =$$
$$\sum_{f_j \circ \,\vert\, \circ f_k} \Big(-2\big(\varphi_{\vec{e}}\rho_{f_j} + \varphi_{-\vec{e}}\rho_{f_k}\big) + \mathrm{Cl}_2\left(\theta_e^* + \varphi_{\vec{e}} - \varphi_{-\vec{e}}\right) + \mathrm{Cl}_2\left(\theta_e^* - \varphi_{\vec{e}} + \varphi_{-\vec{e}}\right)$$
$$+ \mathrm{Cl}_2\left(\theta_e^* - \varphi_{\vec{e}} - \varphi_{-\vec{e}}\right) + \mathrm{Cl}_2\left(\theta_e^* + \varphi_{\vec{e}} + \varphi_{-\vec{e}}\right) - 2\,\mathrm{Cl}_2\left(2\theta_e^*\right)\Big)$$
$$+ \sum_{\circ f} \Phi_f \rho_f \,.$$

(We have used that $\mathrm{Cl}_2(x)$ is odd and 2π-periodic.) The domain of $S_{\mathrm{sph}}^H(\varphi, \rho)$ is the set of all $(\varphi, \rho) \in \mathbb{R}^{\vec{E}_{int}} \times \mathbb{R}^F$ such that φ satisfies the inequalities

$$|\varphi_{\vec{e}} + \varphi_{-\vec{e}} - \pi| < \theta_e \quad \text{and} \quad |\varphi_{\vec{e}} - \varphi_{-\vec{e}}| < \theta_e^*.$$

If φ and ρ are related by equation (2.25), then $S_{\mathrm{sph}}^H(\varphi, \rho) = S_{\mathrm{sph}}(\rho)$. The functional $S_{\mathrm{sph}}^H(\varphi, \rho)$ is linear in ρ. Collecting the coefficients of each ρ_f, one observes that if φ is a spherical coherent angle system, then S_{sph}^H does not depend on ρ. In fact, in that case, $S_{\mathrm{sph}}^H(\varphi, \rho) = \widehat{S}(\varphi)$.

Equations (3.4) are the inverse relations to equations (2.25); see lemma 2.10. It is left to prove that they are compatible if φ is a critical point of $\widehat{S}$ under variations in the space of spherical coherent angle systems. This follows in exactly the same way as in the hyperbolic case. The rest follows from lemma 3.3. This completes the proof of part *(iii)* of theorem 3.1.

3.2. Colin de Verdière's functionals

Colin de Verdière [16] considers circle packings in which the circles correspond to the vertices of a triangulation. He considers the 1-form

$$\omega = \alpha \, du + \beta \, dv + \gamma \, dw$$

on the space of euclidean triangles, where

$$u = \log x, \quad v = \log y, \quad \text{and} \quad w = \log z$$

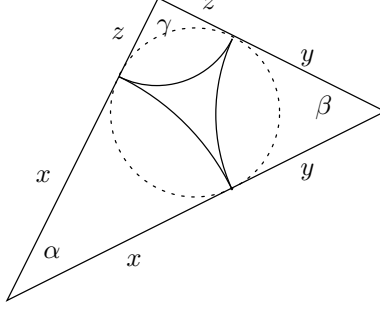and x, y, z and α, β, γ are as shown in figure 3.1.

FIGURE 3.1. A euclidean triangle

It turns out that $d\omega = 0$, hence one may integrate. Define the function $f_{\alpha_0,\beta_0,\gamma_0}$ on $\mathbb{R}^3$ by

$$f_{\alpha_0,\beta_0,\gamma_0}(u,v,w) = \int^{(u,v,w)} (\alpha_0 - \alpha)\,du + (\beta_0 - \beta)\,dv + (\gamma_0 - \gamma)\,dw.$$

The initial point of the integration does not matter.

Suppose we are given a triangulation and a coherent angle system for it. Here, a coherent angle system is a positive function on the set of angles of the triangles, such that the sum in each triangle is π, and the sum around each vertex is 2π. For a function ρ on the vertices of the triangulation, Colin de Verdière's functional for euclidean circle packings is

$$S_{CdV}(\rho) = \sum f_{\alpha_0,\beta_0,\gamma_0}(u,v,w),$$

where the sum is taken over all triangles, u, v, and w are the values of ρ on the vertices of each triangle, and α_0, β_0 and γ_0 are the corresponding angles of the coherent angle system.

The critical points of this functional correspond to the logarithmic radii of a circle packing.

The hyperbolic case is treated in the same way, except that now

$$u = \log\tanh(x/2), \quad v = \log\tanh(y/2), \quad \text{and} \quad w = \log\tanh(z/2),$$

and in the definition of a coherent angle system, it is required that the sum of the angles in a triangle is less than π.

To treat circle packings with our functionals, we consider circle patterns with orthogonally intersecting circles on the medial decomposition of the triangulation (see figure 2.8).

Suppose Σ_0 is a triangulation. Let Σ be the medial decomposition. Set $\theta_e = \pi/2$ for all edges e. For simplicity, we will consider only the case of closed surfaces, so let $\Phi_f = 2\pi$ for all faces f. The faces of Σ are of two types: those that correspond to faces of Σ_0 and those that correspond to vertices of Σ_0. Let $F = F_1 \cup F_2$, where F_1 contains the faces of the first type and F_2 contains the faces of the second type.

Consider S_{euc} as function on $\mathbb{R}^{F_1} \times \mathbb{R}^{F_2}$ and define $S_2 : \mathbb{R}^{F_2} \to \mathbb{R}$,

$$S_2(\rho_2) = \min_{\rho_1 \in \mathbb{R}^{F_1}} S_{\text{euc}}(\rho_1, \rho_2).$$

Hence, $S_2(\rho_2) = S_{\text{euc}}(\rho_1, \rho_2)$, where $\rho_1 \in \mathbb{R}^{F_1}$ is determined as follows. Suppose $f \in F_1$ and $f_a, f_b, f_c \in F_2$ are the neighboring faces of f. Construct the euclidean triangle whose sides are

$$e^{\rho_2 f_a} + e^{\rho_2 f_b}, \quad e^{\rho_2 f_b} + e^{\rho_2 f_c}, \quad \text{and} \quad e^{\rho_2 f_c} + e^{\rho_2 f_a}.$$

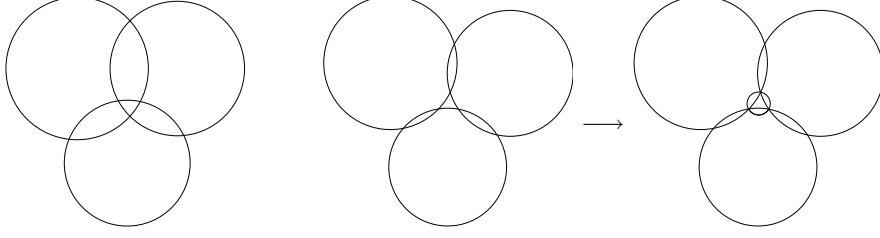Let $\rho_1(f)$ be the logarithmic radius of the inscribed circle.

FIGURE 3.2. *Left:* Thurston type circle pattern with overlap. *Middle:* Thurston type circle pattern with hole. *Right:* Add a circle to fill the hole.

For $\rho_2 \in \mathbb{R}^{F_2}$, and ρ_1 the corresponding point in $\mathbb{R}^{F_1}$,

$$\frac{\partial S_{\mathrm{euc}}}{\partial \rho_1}(\rho_1, \rho_2) = 0, \quad \frac{\partial S_{\mathrm{euc}}}{\partial \rho_2}(\rho_1, \rho_2) = \frac{\partial S_2}{\partial \rho_2}(\rho_2).$$

Consider S_{CdV} as function on $\mathbb{R}^{F_2}$. It is not hard to see that $dS_2 = dS_{CdV}$. This implies that Colin de Verdière's euclidean functional is, up to an additive constant, equal to S_2.

Colin de Verdière's functional for hyperbolic circle packings can be derived from S_{hyp} in the same way.

3.3. Digression: Thurston type circle patterns with "holes"

A similar reduction leads to functionals for Thurston type circle patterns with "holes" [**42**]. Thurston type circle patterns were mentioned in the introduction, section 1.1. Here, the vertices do not correspond to intersection points. All vertices have three edges, but the intersection angles θ do not have to sum to 2π. If the sum is less than 2π, the circles will overlap as in figure 3.2 *(left)*. If the sum is greater than 2π, there will be a hole as in figure 3.2 *(middle)*. If the sum is greater than 2π around *all* vertices, one obtains a Delaunay type circle pattern by adding circles as shown in figure 3.2 *(right)*. Combinatorially, this corresponds to "truncating" all vertices. The intersection angles for the new edges (see figure 3.3) are determined by the equations

$$\theta_{12} + \theta_{20} + \theta_{01} = 2\pi$$
$$\theta_{23} + \theta_{30} + \theta_{02} = 2\pi$$
$$\theta_{31} + \theta_{10} + \theta_{03} = 2\pi,$$

so that

$$\theta_{01} = \pi - \frac{1}{2}(\theta_{12} - \theta_{23} + \theta_{31}), \quad \text{etc.}$$

3.4. Brägger's functional

Like Colin de Verdière, Brägger [**12**] considers circle packings in which the circles correspond to the vertices of a triangulation. A coherent angle system in the sense of section 3.2 is clearly equivalent to a coherent angle system in the sense of this article. Thus, Brägger's functional is seen to be equal to $\widehat{S}/2$ up to an additive constant.

3.5. Rivin's functional

Rivin [**34**] considers euclidean circle patterns with arbitrary prescribed intersection angles. The pattern of intersection is determined by a triangulation. Circles correspond to faces of the triangulation. However, since Rivin allows intersection
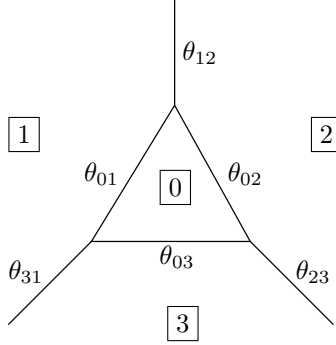
FIGURE 3.3. A "truncated vertex". The old faces are labeled 1, 2, 3; the new face is labeled 0.

angles $\theta = 0$, adjacent triangles may in effect belong to the same circle. Thus, cellular decompositions with non-triangular cases may be treated by first dissecting all faces into triangles. Rivin treats cone-like singularities in the vertices but not in the centers of the circles. His functional is up to an additive constant equal to $\widehat{S}/2$ with $\widehat{S}$ as in equation (3.5).

3.6. Leibon's functional

Like Rivin, Leibon [**27**], [**28**] considers circle patterns with arbitrary prescribed intersection angles. The circles correspond to the faces of a triangulation and the variables are the angles of the inscribed triangles. Whereas Rivin treats the euclidean case, Leibon treats the hyperbolic case. Leibon's functional cannot be derived directly from our functionals. In section 4.7, we will construct yet another functional, from which both Leibon's functional and $\widehat{S}(\varphi)$ can be derived. This section is an exposition of Leibon's variational principle.

Let Σ be a triangulation of a compact surface without boundary and let intersection angles be prescribed by a function $\theta : E \to (0, \pi)$ on the non-oriented edges. Assume that θ sums to 2π around each vertex. (This assumption is made only to simplify the exposition. It means that we consider only the case without cone-like singularities. If the assumption is violated, one obtains prescribed cone-like singularities in the vertices. Cone-like singularities in the centers of the circles cannot be treated by this method.) The variables of Leibon's functional are the angles of the triangles of the triangulation. We associate each angle of a triangle with the opposite directed edge in the oriented boundary of that triangle. Thus, for a geodesic triangulation of a hyperbolic surface, the angles of the triangles define a function on the oriented edges. (In the figures, however, we label the angles in the usual way.)

For a function $\alpha \in \mathbb{R}^{\vec{E}}$ on the oriented edges, Leibon's functional is

$$H(\alpha) = \sum_{t \in F} V(\alpha_1^t, \alpha_2^t, \alpha_3^t),$$

where the sum is taken over all triangles t; $\alpha_1^t, \alpha_2^t, \alpha_3^t$ are the three angles of a triangle t, and

$$
\begin{aligned}
V(\alpha_1, \alpha_2, \alpha_3) = \frac{1}{2} \Big(& \text{Cl}_2(2\alpha_1) + \text{Cl}_2(2\alpha_2) + \text{Cl}_2(2\alpha_3) \\
& + \text{Cl}_2(\pi + \alpha_1 - \alpha_2 - \alpha_3) + \text{Cl}_2(\pi - \alpha_1 + \alpha_2 - \alpha_3) \qquad (3.16) \\
& + \text{Cl}_2(\pi - \alpha_1 - \alpha_2 + \alpha_3) + \text{Cl}_2(\pi - \alpha_1 - \alpha_2 - \alpha_3) \Big).
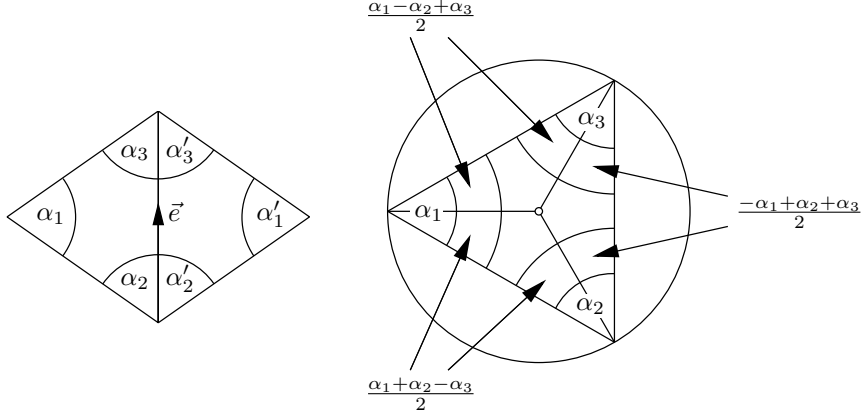\end{aligned}
$$

FIGURE 3.4. *Left:* Adjacent triangles. *Right:* Triangle with circumscribed circle. (For simplicity, euclidean triangles are drawn in the figure.)

A *coherent angle system* in this setting is a function $\alpha \in \mathbb{R}^{\vec{E}}$ on the oriented edges, which satisfies the following conditions:

(i) For all $\vec{e} \in \vec{E}$, $\alpha_{\vec{e}} > 0$.

(ii) For all triangles $t \in F$, $\alpha_1^t + \alpha_2^t + \alpha_3^t < \pi$.

(iii) The angles of two adjacent triangles with common edge $e \in E$, as shown in figure 3.4 *(left)*, satisfy

$$\frac{-\alpha_1 + \alpha_2 + \alpha_3}{2} + \frac{-\alpha_1' + \alpha_2' + \alpha_3'}{2} = \theta_e.$$

Note that condition *(iii)* implies that the angles α sum to 2π around each vertex (since the angles θ do). For a Delaunay triangulation with circles intersecting at angles given by θ, the angles of the triangles form a coherent angle system. Figure 3.4 *(right)* shows that condition *(iii)* is satisfied.

LEMMA 3.4 (Leibon [**28**]). *The hyperbolic triangles with angles prescribed by $\alpha \in \mathbb{R}^{\vec{E}}$ fit together to form a Delaunay triangulation of a hyperbolic surface with circles intersecting at angles given by θ if and only if $\alpha \in \mathbb{R}^{\vec{E}}$ is a critical point of the functional $H(\alpha)$ under variations in the space of coherent angle systems.*

Leibon also shows that the functional is strictly convex upwards and uses his variational principle to prove an existence and uniqueness theorem for hyperbolic circle patterns, which is a special case of theorem 1.8 [**28**].

PROOF OF LEMMA 3.4. It is clear that, if the triangles may be glued together, one obtains a Delaunay triangulation of a hyperbolic surface with circles intersecting at angles given by θ. The triangles fit together if sides along which two triangles are supposed to be glued have the same length. Hence, the lemma follows from the following facts:

(a) For each oriented edge $\vec{e} \in \vec{E}$, let

$$w_{\vec{e}} = \frac{\partial}{\partial\alpha_2} + \frac{\partial}{\partial\alpha_3} - \frac{\partial}{\partial\alpha_2'} - \frac{\partial}{\partial\alpha_3'},$$

where $\alpha_2, \alpha_3, \alpha_2', \alpha_3'$ are as in figure 3.4 *(left)*. The tangent space to the space of coherent angle systems is spanned by the vectors $w_{\vec{e}}$, $\vec{e} \in \vec{E}$.

(b) For positive α_1, α_2, α_3 with $\alpha_1 + \alpha_2 + \alpha_3 < \pi$,

$$\left(\frac{\partial}{\partial\alpha_2} + \frac{\partial}{\partial\alpha_3}\right) V(\alpha_1, \alpha_2, \alpha_3) = 2\log\sinh\frac{a_1}{2}, \tag{3.17}$$
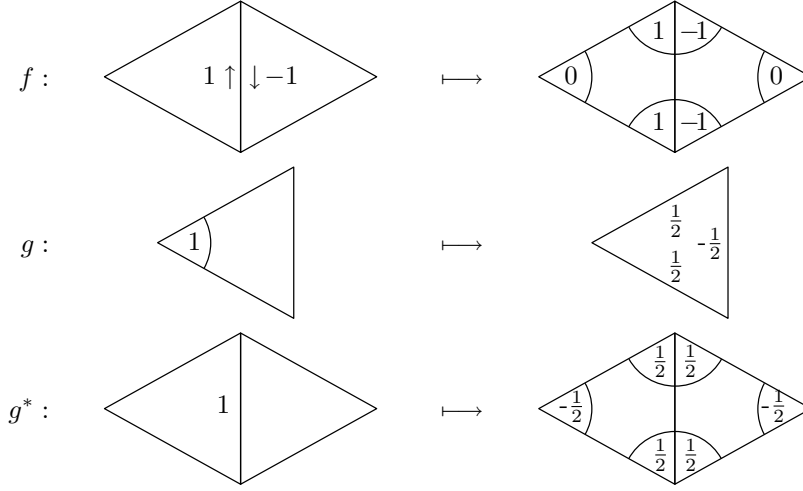
FIGURE 3.5. The linear functions f, g, and g^*.

where a_1 is the length of the side opposite α_1 in a hyperbolic triangle with angles α_1, α_2, α_3.

   Proof of *(a)*. Consider the linear functions

$$
\begin{aligned}
f: &\quad \mathrm{Alt}(\vec{E}) \longrightarrow \mathbb{R}^{\vec{E}}, \\
g: &\quad \mathbb{R}^{\vec{E}} \longrightarrow \mathbb{R}^{E}, \\
g^*: &\quad \mathbb{R}^{E} \longrightarrow \mathbb{R}^{\vec{E}}
\end{aligned}
$$

defined by figure 3.5. ($\mathrm{Alt}(\vec{E})$ denotes the space of antisymmetric functions on the oriented edges; see equation (3.9).) Suppose the vector spaces $\mathbb{R}^{\vec{E}}$, and $\mathbb{R}^{E}$ are equipped with the canonical scalar product. Then g and g^* are adjoint linear operators. The tangent space to the space of coherent angle systems is

$$
(\mathrm{Im}\, g^*)^{\perp} = \mathrm{Ker}\, g.
$$

Hence we need to show that

$$
\mathrm{Im}\, f = \mathrm{Ker}\, g. \tag{3.18}
$$

In fact, we will show that

$$
0 \longrightarrow \mathrm{Alt}(\vec{E}) \xrightarrow{\ f\ } \mathbb{R}^{\vec{E}} \xrightarrow{\ g\ } \mathbb{R}^{E} \longrightarrow 0
$$

is an exact sequence. It is easy to see that

$$
\mathrm{Ker}\, f = 0
$$

and

$$
\mathrm{Im}\, f \subseteq \mathrm{Ker}\, g
$$

It is also easy to see that

$$
\mathrm{Ker}\, g^* = 0
$$

and hence

$$
\mathrm{Im}\, g = (\mathrm{Ker}\, g^*)^{\perp} = \mathbb{R}^{E}.
$$

Since

$$
\dim \mathrm{Ker}\, g = |\vec{E}| - |E| = |E| = \dim \mathrm{Im}\, f,
$$

equation (3.18) follows. This proves *(a)*.

Proof of *(b)*. By equation (B.4),

$$\left(\frac{\partial}{\partial\alpha_2} + \frac{\partial}{\partial\alpha_3}\right) V(\alpha_1, \alpha_2, \alpha_3) = \log \frac{\cos\frac{\alpha_1+\alpha_2+\alpha_3}{2} \cos\frac{-\alpha_1+\alpha_2+\alpha_3}{2}}{\sin\alpha_2 \sin\alpha_3}.$$

From the hyperbolic angle cosine theorem (see, for example, Beardon [**5**])

$$\cosh a_1 = \frac{\cos\alpha_2 \cos\alpha_3 + \cos\alpha_1}{\sin\alpha_2 \sin\alpha_3}$$

one derives the half-angle formula

$$\sinh^2 \frac{a_1}{2} = \frac{\cos\frac{\alpha_1+\alpha_2+\alpha_3}{2} \cos\frac{-\alpha_1+\alpha_2+\alpha_3}{2}}{\sin\alpha_2 \sin\alpha_3}.$$

This proves *(b)*. ∎

3.7. The Legendre dual of Leibon's functional

In this section, we construct the circle pattern functional $\widehat{H}$, which is Legendre dual to Leibon's functional. The variables are (essentially) the edge lengths of the triangles. Unfortunately, we cannot give an explicit formula for $\widehat{H}$ in terms of the dilogarithm or related functions. Whether a manageable formula exists, seems to be an interesting question.

Introduce new variables $\beta \in \mathbb{R}^{\vec{E}}$ instead of $\alpha \in \mathbb{R}^{\vec{E}}$: For each triangle, the angles β_1, β_2, β_3 are related to α_1, α_2, α_3 by

$$\begin{aligned}
\beta_1 &= \frac{-\alpha_1 + \alpha_2 + \alpha_3}{2} \\
\beta_2 &= \frac{\alpha_1 - \alpha_2 + \alpha_3}{2} \\
\beta_3 &= \frac{\alpha_1 + \alpha_2 - \alpha_3}{2}.
\end{aligned} \tag{3.19}$$

Note that

$$\frac{\partial}{\partial\beta_1} = \frac{\partial}{\partial\alpha_2} + \frac{\partial}{\partial\alpha_3}, \quad \text{etc.,}$$

such that equation (3.17) is equivalent to

$$\frac{\partial V}{\partial\beta_j} = 2\log\sinh a_j.$$

Let $\widehat{V}$ be the Legendre transform of V, considered as a function of β_1, β_2, β_3. (See section 3.1.1.) That is, let

$$\widehat{V}(2\log\sinh a_1, 2\log\sinh a_2, 2\log\sinh a_3) =$$
$$2\beta_1\log\sinh a_1 + 2\beta_2\log\sinh a_2 + 2\beta_3\log\sinh a_3 - V(\alpha_1, \alpha_2, \alpha_3),$$

where α_1, α_2, α_3 and a_1, a_2, a_3 are the angles and side lengths of a hyperbolic triangle. Then

$$\frac{\partial\widehat{V}}{\partial(2\log\sin a_j)} = \beta_j.$$

For a function $a \in \mathbb{R}^E$ on the non-oriented edges which satisfies the triangle inequalities, define the functional

$$\widehat{H}(2\log\sinh a) = \sum_{t\in F} \widehat{V}(2\log\sinh a_1^t, 2\log\sinh a_2^t, 2\log\sinh a_3^t) - \sum_{e\in E} 2\theta_e \log\sinh a_e.$$

The first sum is taken over all triangles t, and a_1^t, a_2^t, a_3^t are the sides of triangle t. The second sum is taken over all non-oriented edges e. The functional $\widehat{H}$ is the Legendre dual of Leibon's functional H:

PROPOSITION. *Suppose* $a \in \mathbb{R}^E$ *satisfies the triangle inequalities. Then the hyperbolic triangles with edge lengths given by* a *form a Delaunay triangulation of a hyperbolic surface with circles intersecting at angles given by* θ *if and only if* $2 \log \sinh a$ *is a critical point of the functional* $\widehat{H}$.

PROOF. Suppose $\vec{e}$ and $-\vec{e}$ are the two orientations of the unoriented edge $e \in E$. Then the partial derivative of $\widehat{H}$ with respect to $2 \log \sinh a_e$ is

$$\frac{\partial \widehat{H}(2 \log \sinh a)}{\partial (2 \log \sinh a_e)} = \beta_{\vec{e}} + \beta_{-\vec{e}} - \theta_e.$$

This partial derivative vanishes if and only if the circumscribed circles of the two triangles incident with e intersect at the angle θ_e; see figure 3.4 *(right)*.   ∎

CHAPTER 4

Circle patterns and the volumes of hyperbolic polyhedra

In chapter 2, we constructed circle patterns by tiling (euclidean, hyperbolic or spherical) 2-space with kite-shaped quadrilaterals. In this chapter, we extend these tilings to 'tilings' of hyperbolic 3-space with 3-dimensional polyhedral tiles. This provides a geometric interpretation of the functional $\widehat{S}$ of section 3.1. It turns out to be the sum of the volumes of the polyhedral tiles. The functional attains its maximum (under variation constrained to coherent angle systems) if the tiles fit together to form a 3-dimensional polyhedron. The maximal value is therefore the volume of this polyhedron.

4.1. Schläfli's differential volume formula

In 1852, Schläfli discovered the remarkable formula (4.1) for the differential of the volume of a spherical simplex of arbitrary dimension [**38**]. In 1936, Kneser gave an elegant proof (in a nasty journal) [**25**]. It works also for hyperbolic simplices.

THEOREM 4.1 (Schläfli's differential volume formula). *For an n-dimensional simplex S in spherical or hyperbolic space, let $V(S)$ be its n-dimensional volume. Denote the $(n-1)$-faces by S_i, $0 \leq i \leq n$. Let a_{jk} be the $(n-2)$-dimensional volume of the $(n-2)$-face $S_j \cap S_k$, and let α_{jk} be the the dihedral angle between S_j and S_k. Then the differential of the volume function V is*

$$dV = \frac{\varepsilon}{n-1} \sum_{0 \leq j < k \leq n} a_{jk} \, d\alpha_{jk}, \qquad (4.1)$$

where $\varepsilon = 1$ in the spherical and $\varepsilon = -1$ in the hyperbolic case.

For 3-dimensional hyperbolic simplices (tetrahedra), formula (4.1) may be written

$$dV = -\frac{1}{2} \sum_{\text{edges } j} a_j \, d\alpha_j, \qquad (4.2)$$

where the sum is taken over the edges j, and a_j, α_j are the length and dihedral angle of edge j. In fact, this formula holds for arbitrary polyhedral shapes:

COROLLARY. *Formula (4.2) holds for arbitrary compact hyperbolic 3-manifolds with polyhedral boundary (in particular, for 3-dimensional hyperbolic polyhedra), when they are deformed without changing the combinatorial type of the polyhedral boundary.*

This follows by triangulating the 3-manifold with polyhedral boundary. At all edges of the triangulation, except those which are contained in edges of the polyhedral boundary, the sum of dihedral angles is constant.

Now consider hyperbolic polyhedra (or manifolds with polyhedral boundary) with some vertices in the infinite boundary of H^3. Even though they are not compact, their volume is finite. However, formula (4.2) does not apply directly,

because some edges have infinite length. The following lemma is ascribed to Milnor [**34**, p. 576].[1]

LEMMA 4.1 (Milnor). *Suppose P is a 3-dimensional hyperbolic polyhedron with some vertices on the infinite boundary. For each infinite vertex of P, choose an arbitrary horosphere centered at this vertex. For a finite edge j of P, let a_j be its length. For an edge j with one (or two) vertices at infinity, let a_j be its length up to the cut-off point(s) at the corresponding horosphere(s). (This may be negative if the horospheres are not small enough.) With this agreement, the following holds: If P is deformed in such a way that its combinatorial type does not change and the infinite vertices stay infinite, then the volume differential is given by formula (4.2).*

PROOF. Because the sum of dihedral angles at an infinite vertex with n edges is constantly $(n-2)\pi$ during the deformation, the right hand side of equation (4.2) is independent of the choice of horospheres. We may thus assume that the horospheres are small enough, so that each intersects only the planes incident with the vertex at which it is centered and no other planes or horospheres. By triangulating the polyhedron appropriately, one finds that it suffices to consider a triply orthogonal tetrahedron with one vertex at infinity, see figure C.1 *(left)*. The volume of such a tetrahedron can be found by a straightforward integration without using Schläfli's formula, as shown in appendix C. Differentiate equation (C.1) to obtain, after a straightforward calculation,

$$\frac{\partial V}{\partial \alpha} = -\frac{1}{2}\log\sqrt{1 - \frac{\cos^2\beta}{\cos^2\alpha}}.$$

Truncate the tetrahedron by the horosphere centered at the infinite vertex which touches the opposite face. Then the truncated sides with dihedral angles α and $\frac{\pi}{2} - \alpha$ have length $a = 0$ and $\tilde{a} = -\log\sqrt{1 - \frac{\cos^2\beta}{\cos^2\alpha}}$, respectively. Hence,

$$dV\big|_{\beta=const.} = -\frac{1}{2}\big(a\,d\alpha + \tilde{a}\,d(\pi - \alpha)\big).$$

This proves the theorem. ∎

4.2. A prototypical variational principle and its Legendre dual

In this section, we take a little detour to illustrate the fundamental ideas which are applied in the next sections. It may be skipped, or read after the following sections. We derive a pair of Legendre dual variational principles connected with triangulations of hyperbolic 3-manifolds with polyhedral boundary. The arguments below may be adapted to deal with the case where all vertices of the triangulation are at infinity [**39**]. In that case, one does obtain convex functionals.

Let $\mathcal{T}$ be a finite triangulation of a compact topological 3-manifold M with boundary, and let $\mathcal{T}_0, \ldots, \mathcal{T}_3$ be the sets of vertices, edges, triangles, and tetrahedra. Let $\mathcal{S}$ be the manifold of shapes of hyperbolic tetrahedra. This is diffeomorphic to a connected open subset of $\mathbb{R}^6$. Global coordinates are the six dihedral angles (or, alternatively, the six edge lengths), which satisfy certain inequalities.

For a function $\sigma : \mathcal{T}_3 \to \mathcal{S}$, which assigns a shape to each combinatorial tetrahedron of $\mathcal{T}$ independently, let

$$\widehat{S}_{\mathrm{proto}}(\sigma) = 2\sum_{t\in\mathcal{T}_3} V(\sigma(t)), \tag{4.3}$$

where V is the volume function on $\mathcal{S}$. This defines a differentiable functional $\widehat{S}_{\mathrm{proto}} : \mathcal{S}^{\mathcal{T}_3} \to \mathbb{R}$.

---

[1]However, the proof given by Rivin does not seem to be valid, because, in the "slicing a carrot" argument, Schläfli's formula is applied to shapes bounded by planes and horospheres.

Let $\Phi : \mathcal{T}_1 \cap \partial M \to \mathbb{R}_+$ be a function that assigns a positive angle to each boundary edge. A shape assignment $\sigma : \mathcal{T}_3 \to \mathcal{S}$ is *coherent*, if the dihedral angles sum to 2π around each interior edge and to $\Phi(e)$ around each boundary edge e.

PROPOSITION. *A coherent shape assignment $\sigma \in \mathcal{S}^{\mathcal{T}_3}$ is a critical point of the functional $\widehat{S}_{proto}$ under variations in the space of coherent shape assignments if and only if the hyperbolic tetrahedra $\sigma(\mathcal{T}_3)$ fit together to form a hyperbolic manifold with polyhedral boundary, where the boundary angles are prescribed by Φ.*

PROOF. Let σ be a coherent shape assignment. Suppose $t_1, t_2 \in \mathcal{T}_3$ share an edge $e \in \mathcal{T}_1$. Let α_1, α_2 be the dihedral angles of $\sigma(t_1), \sigma(t_2)$ at e, and let a_1, a_2 be the side lengths of e in $\sigma(t_1), \sigma(t_2)$. There is a variation v in the space of coherent shape assignments with $1 = d\alpha_1(v) = -d\alpha_2(v)$ which keeps all other dihedral angles constant. By Schläfli's formula (4.2),

$$d\widehat{S}_{\text{proto}}(v) = -a_1 + a_2.$$

Hence, if σ is a critical point of $\widehat{S}_{\text{proto}}$ under variations in the space of coherent shape assignments, then σ assigns a unique length to all edges $e \in \mathcal{T}_1$. Therefore, the tetrahedra fit together.

The converse statement follows, because variations like v span the tangent space to the space of coherent shape assignments. ∎

To define the Legendre dual functional, consider a different subset of shape assignments: the space $\mathcal{R} \subset \mathcal{S}^{\mathcal{T}_3}$ of those $\sigma \in \mathcal{S}^{\mathcal{T}_3}$ which assign a unique length to each edge $e \in \mathcal{T}_1$. This means, if $t_1, t_2 \in \mathcal{T}_3$ are both incident with e, then the length of e in $\sigma(t_1)$ equals the length of e in $\sigma(t_2)$. For each such shape assignment $\sigma \in \mathcal{R}$ and each edge $e \in \mathcal{T}_1$, let $a_e(\sigma)$ be the length assigned to e by σ. The functions $a_e : \mathcal{R} \to \mathbb{R}_+$ (which satisfy certain inequalities) form a system of coordinates of $\mathcal{R}$. Hence, $\mathcal{R}$ is diffeomorphic to an open subset of $\mathbb{R}^{\mathcal{T}_1}$. For a tetrahedron $t \in \mathcal{T}_3$ with edge $e \in t \cap \mathcal{T}_1$, let $\alpha_{t,e}(\sigma)$ be the dihedral angle at e in $\sigma(t)$. Extend the function Φ, which was defined on the boundary edges, to a function on all edges by setting $\Phi(e) = 2\pi$ if e is an interior edge.

Define the functional $S_{\text{proto}} : \mathcal{R} \to \mathbb{R}$,

$$S_{\text{proto}}(\sigma) = -\sum_{t \in \mathcal{T}_3} \Big(\sum_{e \in t \cap \mathcal{T}_1} a_e(\sigma) \alpha_{t,e}(\sigma) + 2V(\sigma(t)) \Big) + \sum_{e \in \mathcal{T}_1} \Phi(e) a_e(\sigma).$$

PROPOSITION. *A shape assignment $\sigma \in \mathcal{R}$ is a critical point of the functional S_{proto} (under variations in $\mathcal{R}$) if and only if the tetrahedra $\sigma(\mathcal{T}_3)$ fit together to form a hyperbolic manifold with polyhedral boundary, where the boundary angles are prescribed by Φ.*

PROOF. By Schläfli's differential volume formula (4.2),

$$dS_{\text{proto}} = \sum_{e \in \mathcal{T}_1} \Big(\Phi(e) - \sum_{\substack{t \in \mathcal{T}_3: \\ t \ni e}} \alpha_{t,e} \Big) \, da_e.$$

Thus, at a critical point, the sum of all dihedral angles at an edge e is $\Phi(e)$. ∎

4.3. The euclidean functional

Suppose that $0 < \theta < \pi$ and $\varphi_1 > 0$, $\varphi_2 > 0$. If

$$\varphi_1 + \varphi_2 = \pi - \theta,$$

we define a hyperbolic polyhedron $P_\theta(\varphi_1, \varphi_2)$ as follows.

If φ_1 and φ_2 are not greater than $\frac{\pi}{2}$, let $P_\theta(\varphi_1, \varphi_2)$ be the hyperbolic polyhedron shown in figure 4.1 in the Poincaré half-space model of hyperbolic 3-space: $H^3 =$
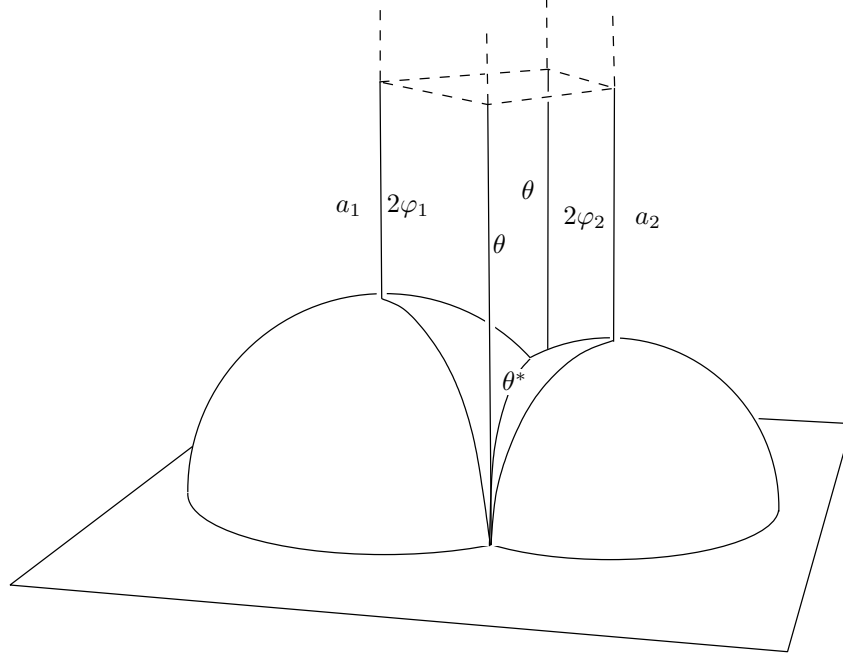
FIGURE 4.1. The hyperbolic polyhedron $P_\theta(\varphi_1, \varphi_2)$ for $\varphi_1 + \varphi_2 = \theta^*$ (where $\theta^* = \pi - \theta$) shown in the Poincaré half-space model. The dihedral angle at the four unmarked edges is $\frac{\pi}{2}$.
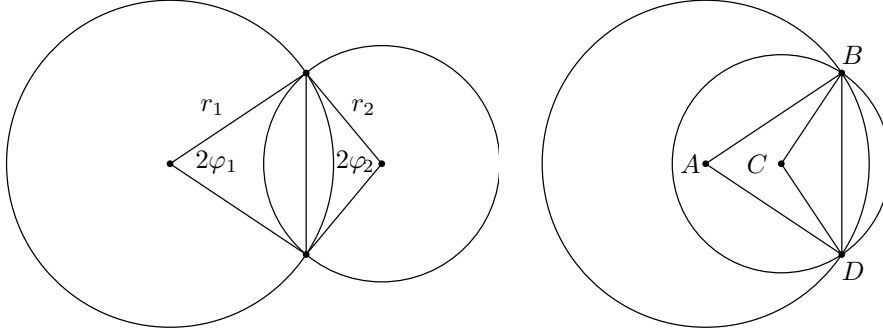

FIGURE 4.2. *Left:* The polyhedron of figure 4.1, projected orthogonally into the z-plane. *Right:* The corresponding picture for the case $\varphi_2 > \frac{\pi}{2}$.

$\{(x, y, z) \in \mathbb{R}^3 \mid z > 0\}$ with metric $|ds| = \frac{1}{z}\sqrt{x^2 + y^2 + z^2}$. It has three infinite vertices: two lie in the plane $z = 0$ and third is the infinite point compactifying the closed half-space. The dihedral angles are as indicated. The unmarked edges have dihedral angle $\frac{\pi}{2}$.

If either φ_1 or φ_2 are greater than $\frac{\pi}{2}$, we define $P_\theta(\varphi_1, \varphi_2)$ as an algebraic sum. Figure 4.2 *(left)* shows the orthogonal projection of figure 4.1 into the z-plane. The corresponding figure for the case $\varphi_2 > \frac{\pi}{2}$ is shown on the right. In this case, let P_1 be the polyhedron bounded by the planes corresponding to the circle around A and the line segments AB, BD, and DA; and let P_2 be the polyhedron bounded by the planes corresponding to the circle around C and the line segments CB, BD, and DC. Define $P_\theta(\varphi_1, \varphi_2)$ as the algebraic sum $P_\theta(\varphi_1, \varphi_2) = P_1 - P_2$. Extend the volume function linearly to such algebraic sums: $V(P_1 - P_2) = V(P_1) - V(P_2)$.

PROPOSITION. *Suppose $\varphi \in \mathbb{R}^{\vec{E}_{int}}$ is a euclidean coherent angle system (see section 2.7). Then the functional $\widehat{S}(\varphi)$ of theorem 3.1 satisfies*

$$\widehat{S}(\varphi) = \sum_{e \in E_{int}} \Big(2V\big(P_{\theta_e}(\varphi_{\vec{e}}, \varphi_{-\vec{e}})\big) - \operatorname{Cl}_2(2\theta_e^*) \Big),$$

where V is the volume function, the sum is taken over all non-oriented interior edges e, and $\vec{e}$, $-\vec{e}$ are the two corresponding oriented edges.

PROOF. Because of equation (3.5) for $\widehat{S}(\varphi)$, where φ is a euclidean coherent angle system, the proposition follows directly from the following lemma. ∎

LEMMA 4.2. *The volume of $P_\theta(\varphi_1, \varphi_2)$ is*

$$V\big(P_\theta(\varphi_1, \varphi_2)\big) = \frac{1}{2} \operatorname{Cl}_2(2\varphi_1) + \frac{1}{2} \operatorname{Cl}_2(2\varphi_2). \tag{4.4}$$

PROOF. The polyhedron $P_\theta(\varphi_1, \varphi_2)$ may be decomposed into four triply orthogonal tetrahedra (see appendix C), each having two vertices at infinity. The characteristic angle is φ_1 for two of the tetrahedra and φ_2 for the other two. Equation (4.4) follows from equation (C.2). (This argument works also in the case where φ_1 or φ_2 are greater than $\frac{\pi}{2}$.) ∎

COROLLARY. *If $\varphi \in \mathbb{R}^{\vec{E}_{int}}$ is a critical point of $\widehat{S}$ under variations in the space of euclidean coherent angle systems, then the polyhedra $P_{\theta_e}(\varphi_{\vec{e}}, \varphi_{-\vec{e}})$ fit together to form a hyperbolic orbifold M with polyhedral boundary. M is a manifold with polyhedral boundary if $\Phi_f = 2\pi$ for all interior faces $f \in F$. The volume of M is*

$$V(M) = \frac{1}{2}\Big(\widehat{S}(\varphi) + \sum_{e \in E_{int}} \operatorname{Cl}_2(2\theta_e^*) \Big) = \frac{1}{2}\Big(S_{euc}(\rho) + \sum_{e \in E_{int}} \operatorname{Cl}_2(2\theta_e^*) \Big),$$

where $\rho \in \mathbb{R}^F$ is the corresponding critical point of S_{euc}.

4.4. The spherical functional

In the previous section, we defined $P_\theta(\varphi_1, \varphi_2)$ for $\varphi_1 + \varphi_2 = \pi - \theta$. If

$$\pi - \theta < \varphi_1 + \varphi_2 < \pi + \theta \quad \text{and} \quad \big|\varphi_1 - \varphi_2\big| < \pi - \theta,$$

let $P_\theta(\varphi_1, \varphi_2)$ be the hyperbolic polyhedron shown in figure 4.3 in the Poincaré ball model of hyperbolic space:

$$H^3 = \big\{ (x, y, z) \in \mathbb{R}^3 \mid x^2 + y^2 + z^2 < 1 \big\}$$

with metric

$$|ds| = \frac{2}{1 - x^2 - y^2 - z^2} \sqrt{dx^2 + dy^2 + dz^2}.$$

(If φ_1 or φ_2 are greater than $\frac{\pi}{2}$, then $P_\theta(\varphi_1, \varphi_2)$ is defined by an algebraic sum, as in the previous section. We will not dwell on this point.)

PROPOSITION. *Suppose $\varphi \in \mathbb{R}^{\vec{E}_{int}}$ is a spherical coherent angle system (see section 2.7). Then the functional $\widehat{S}(\varphi)$ of theorem 3.1 satisfies*

$$\widehat{S}(\varphi) = \sum_{e \in E_{int}} 2V\big(P_{\theta_e}(\varphi_{\vec{e}}, \varphi_{-\vec{e}})\big)$$

where V is the volume function, the sum is taken over all non-oriented interior edges e, and $\vec{e}$, $-\vec{e}$ are the two corresponding oriented edges.
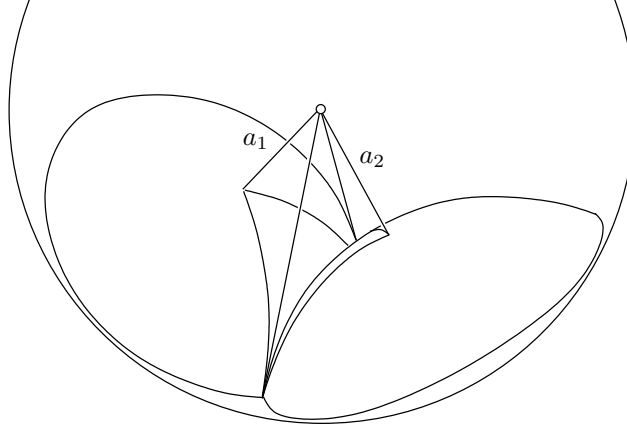
FIGURE 4.3. The hyperbolic polyhedron $P_\theta(\varphi_1, \varphi_2)$ for $\pi - \theta < \varphi_1 + \varphi_2 < \pi + \theta$ and $\left|\varphi_1 - \varphi_2\right| < \pi - \theta$, shown in the Poincaré ball model. The dihedral angles at the edges marked a_1 and a_2 are $2\varphi_1$ and $2\varphi_2$. The other two edges of the vertex marked '∘' (which is at $(x, y, z) = (0, 0, 0)$) have angle θ; and the faces opposite vertex '∘' intersect at the angle $\theta^* = \pi - \theta$. The four remaining edges have dihedral angle $\frac{\pi}{2}$. The polyhedron has two vertices in the infinite boundary.

COROLLARY. *If $\varphi \in \mathbb{R}^{\vec{E}_{int}}$ is a critical point of $\widehat{S}$ under variations in the space of spherical coherent angle systems, then the polyhedra $P_{\theta_e}(\varphi_{\vec{e}}, \varphi_{-\vec{e}})$ fit together to form a hyperbolic orbifold M with polyhedral boundary. M is a manifold with polyhedral boundary if $\Phi_f = 2\pi$ for all interior faces $f \in F$. The volume of M is*

$$V(M) = \tfrac{1}{2}\widehat{S}(\varphi) = \tfrac{1}{2}S_{sph}(\rho),$$

where $\rho \in \mathbb{R}^F$ is the corresponding critical point of S_{sph}.

The proposition follows directly from the following lemma.

LEMMA 4.3. *The volume of $P_\theta(\varphi_1, \varphi_2)$ is*

$$
V\big(P_\theta(\varphi_1, \varphi_2)\big) = \frac{1}{2}\Big(\mathrm{Cl}_2(\theta^* + \varphi_1 - \varphi_2) + \mathrm{Cl}_2(\theta^* - \varphi_1 + \varphi_2) \\
+ \mathrm{Cl}_2(\theta^* + \varphi_1 + \varphi_2) + \mathrm{Cl}_2(\theta^* - \varphi_1 - \varphi_2) - 2\,\mathrm{Cl}_2(2\theta^*)\Big).
\tag{4.5}
$$

PROOF OF LEMMA 4.3. We will show that the derivatives of both sides of equation (4.5) with respect to φ_1 and φ_2 are equal. Since both sides tend to 0 as $\varphi_1 \to 0$ and $\varphi_2 \to \theta^*$, equation (4.5) follows.

Consider deformations of $P_\theta(\varphi_1, \varphi_2)$ during which all dihedral angles except $2\varphi_1$ and $2\varphi_2$ remain constant. By Milnor's generalization of Schläfli's differential volume formula (lemma 4.1),

$$dV\big(P_\theta(\varphi_1, \varphi_2)\big) = -a_1\,d\varphi_1 - a_2\,d\varphi_2,$$

where a_1, a_2 are the lengths of the sides with dihedral angles $2\varphi_1$ and $2\varphi_2$. (And this is also true in the case where $P_\theta(\varphi_1, \varphi_2)$ is defined as an algebraic sum.) By equation (B.4), the differential of the right hand side of equation (4.5) is

$$\rho_1\,d\varphi_1 + \rho_2\,d\varphi_2,$$

where ρ_1 and ρ_2 are given by equation (3.4). Let r_1 and r_2 be the *spherical* radii of the circles in the infinite boundary shown in figure 4.3. Then r_1 and r_2 are related to ρ_1 and ρ_2 by equation (2.23). This implies $\rho_1 = -a_1$ and $\rho_2 = -a_2$; see figure 4.4. This completes the proof. ■
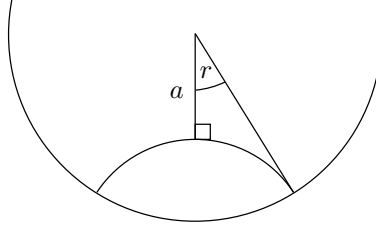
FIGURE 4.4. In a hyperbolic right-angled triangle with one vertex at infinity, the length a and the angle r satisfy the equation $a = -\log \tan \frac{r}{2}$.
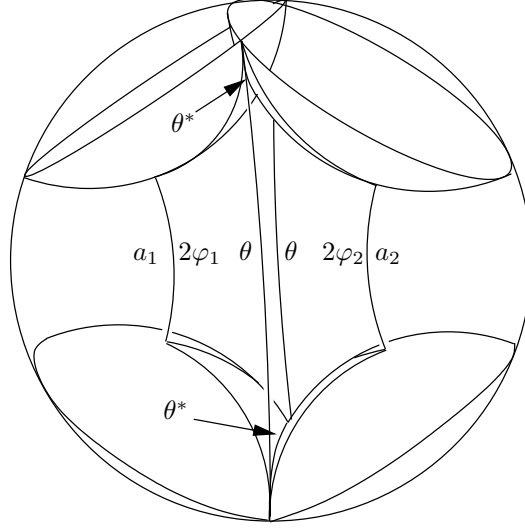

FIGURE 4.5. The hyperbolic polyhedron $P_\theta(\varphi_1, \varphi_2)$ for $\varphi_1 + \varphi_2 < \pi - \theta$, shown in the Poincaré ball model. The dihedral angles are as indicated, where $\theta^* = \pi - \theta$. The unmarked edges have dihedral angle $\frac{\pi}{2}$. The polyhedron has four vertices in the infinite boundary. It is symmetric with respect to reflection on the equatorial plane.

4.5. The hyperbolic functional

Now we define the hyperbolic polyhedron $P_\theta(\varphi_1, \varphi_2)$ for

$$\varphi_1 + \varphi_2 < \pi - \theta.$$

In this case, let $P_\theta(\varphi_1, \varphi_2)$ be the hyperbolic polyhedron shown in figure 4.5 in the Poincaré ball model of hyperbolic space. (If φ_1 or φ_2 are greater than $\frac{\pi}{2}$, then $P_\theta(\varphi_1, \varphi_2)$ is defined by an algebraic sum, as described in section 4.3. We will not dwell on this point.)

PROPOSITION. *Suppose* $\varphi \in \mathbb{R}^{\vec{E}_{int}}$ *is a hyperbolic coherent angle system (see section 2.7). Then the functional* $\widehat{S}(\varphi)$ *of theorem 3.1 satisfies*

$$\widehat{S}(\varphi) = \sum_{e \in E_{int}} V\big(P_{\theta_e}(\varphi_{\vec{e}}, \varphi_{-\vec{e}})\big)$$

where V *is the volume function, the sum is taken over all non-oriented interior edges* e, *and* $\vec{e}$, $-\vec{e}$ *are the two corresponding oriented edges.*

COROLLARY. *If* $\varphi \in \mathbb{R}^{\vec{E}_{int}}$ *is a critical point of* $\widehat{S}$ *under variations in the space of hyperbolic coherent angle systems, then the polyhedra* $P_{\theta_e}(\varphi_{\vec{e}}, \varphi_{-\vec{e}})$ *fit together*
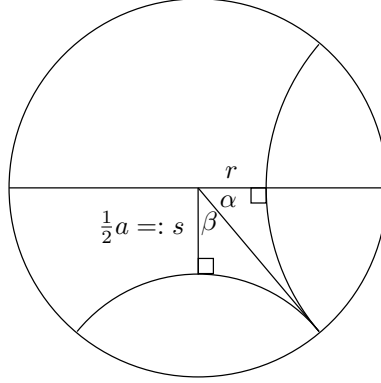
FIGURE 4.6. From $r = -\log\tan\frac{\alpha}{2}$ and $s = -\log\tan\frac{\beta}{2}$ with $\alpha+\beta = \frac{\pi}{2}$, one obtains $s = -\log\tanh\frac{r}{2}$. Hence, $s = -\rho$, with ρ given by equation (2.14).

to form a hyperbolic orbifold M with polyhedral boundary. M is a manifold with polyhedral boundary if $\Phi_f = 2\pi$ for all interior faces $f \in F$. The volume of M is

$$V(M) = \widehat{S}(\varphi) = S_{hyp}(\rho),$$

where $\rho \in \mathbb{R}^F$ is the corresponding critical point of S_{hyp}.

The proposition follows directly from the following lemma.

LEMMA 4.4. *The volume of $P_\theta(\varphi_1, \varphi_2)$ is*

$$\begin{aligned} V\big(P_\theta(\varphi_1,\varphi_2)\big) = {} & \mathrm{Cl}_2(\theta^* + \varphi_1 - \varphi_2) + \mathrm{Cl}_2(\theta^* - \varphi_1 + \varphi_2) \\ & + \mathrm{Cl}_2(\theta^* + \varphi_1 + \varphi_2) + \mathrm{Cl}_2(\theta^* - \varphi_1 - \varphi_2) - 2\,\mathrm{Cl}_2(2\theta^*). \end{aligned} \tag{4.6}$$

Lemma 4.4 is proved in the same way as lemma 4.3:

PROOF OF LEMMA 4.4. We will show that the derivatives of both sides of equation (4.6) with respect to φ_1 and φ_2 are equal. Since both sides tend to 0 as $\varphi_1 \to 0$ and $\varphi_2 \to \theta^*$, equation (4.5) follows.

Under deformations of $P_\theta(\varphi_1, \varphi_2)$ during which all dihedral angles except $2\varphi_1$ and $2\varphi_2$ remain constant, the volume differential is

$$dV\big(P_\theta(\varphi_1,\varphi_2)\big) = -a_1\,d\varphi_1 - a_2\,d\varphi_2,$$

where a_1, a_2 are the lengths of the sides with dihedral angles $2\varphi_1$ and $2\varphi_2$. (And this is also true in the case where $P_\theta(\varphi_1, \varphi_2)$ is defined as an algebraic sum.) By equation (B.4), the differential of the right hand side of equation (4.6) is

$$2\rho_1\,d\varphi_1 + 2\rho_2\,d\varphi_2,$$

where ρ_1 and ρ_2 are given by equation (3.3). The symmetry plane intersects $P_\theta(\varphi_1, \varphi_2)$ in a hyperbolic kite-shaped quadrilateral with angles θ, φ_1, φ_2. Let the hyperbolic side lengths of this quadrilateral be r_1 and r_2. Then r_1 and r_2 are related to ρ_1 and ρ_2 by equation (2.14) (see lemma 2.5). Furthermore, $a_j = -2\rho_j$ (see figure 4.6). This completes the proof. ∎

4.6. Leibon's functional

Schläfli's differential volume formula is the basis for Leibon's functional (see section 3.6) as well. Lemma 4.5 and Schläfli's differential volume formula provide another proof of Leibon's variational principle, lemma 3.4.

An *ideal triangular prism* is a convex hyperbolic polyhedron with six ideal vertices, which is symmetric with respect to a hyperbolic plane (see figure 4.7). An
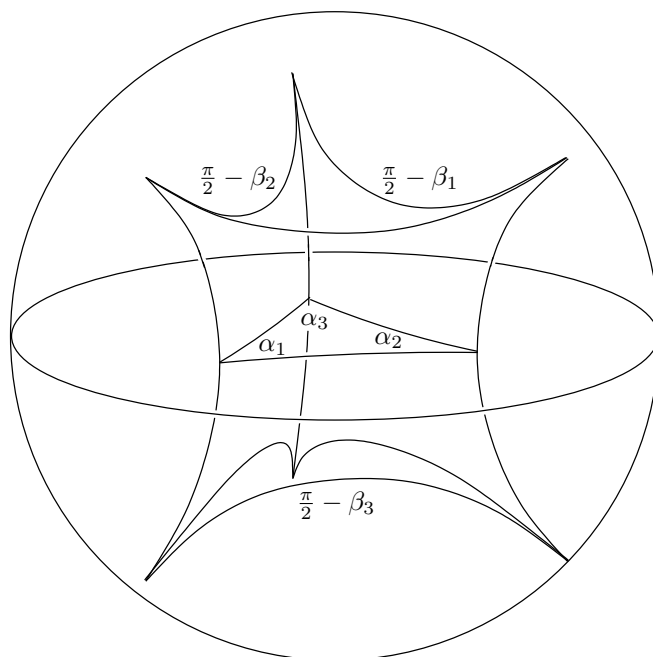
FIGURE 4.7. An ideal triangular prism, shown in the Poincaré ball model. The equatorial plane is the plane of symmetry.
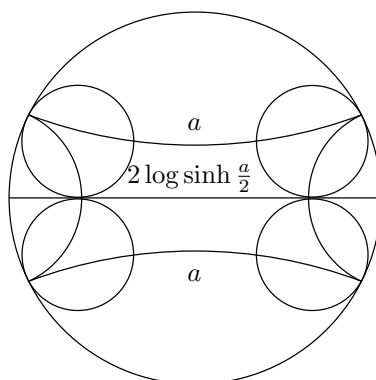
FIGURE 4.8. Truncated quadrilateral face of the ideal prism.

ideal triangular prism intersects the plane of symmetry in a hyperbolic triangle. The angles α_1, α_2, α_3 of this triangle determine the shape of the prism. They are also the dihedral angles of the three edges intersecting the symmetry plane. The other dihedral angles are $\frac{\pi}{2} - \beta_1$, $\frac{\pi}{2} - \beta_2$, and $\frac{\pi}{2} - \beta_3$, with the β_j defined by equations (3.19).

LEMMA 4.5 (Leibon [27][28]). *The hyperbolic volume of the ideal prism shown in figure 4.7 is $V(\alpha_1, \alpha_2, \alpha_3)$ as defined by equation (3.16).*

Truncate the ideal prism by horospheres which are centered at the ideal vertices and touch the symmetry plane. The truncated edge lengths are 0 for the edges which intersect the symmetry plane, and $2 \log \sinh \frac{a_j}{2}$ for the other edges, where a_j is the length of the corresponding side of the hyperbolic triangle with angles α_1, α_2, α_3. (See figure 4.8.)

FIGURE 4.9. *Left:* Schematic picture of one of the three pieces into which the ideal prism of figure 4.7 is decomposed. It has four ideal vertices, which are marked '∘'. The dihedral angles at four of the edges are $\frac{\pi}{2}$. The other dihedral angles are as indicated. *Right:* The triangular intersection with the symmetry plane is decomposed into three isosceles triangles.

4.7. A common ancestor of Leibon's and our functionals

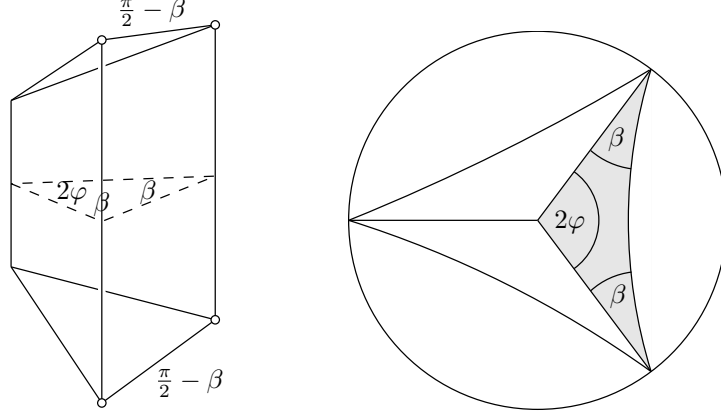The geometric interpretation of both Leibon's functional and the functional $\widehat{S}(\varphi)$ in terms of hyperbolic volume clarifies their mutual relationship. In this section, we construct another functional, $T(\varphi, \beta)$, from which both Leibon's functional and $\widehat{S}(\varphi)$ can be derived. Let Σ be a cell decomposition of a compact surface without boundary, let intersection angles be prescribed by a function $\theta : E \to (0, \pi)$ on the non-oriented edges, and let cone angles in the centers of the circles be prescribed by a function $\Phi : F \to (0, 2\pi)$ on the faces.

The ideal prism shown in figure 4.7 can be decomposed into three polyhedral pieces like the one shown in figure 4.9. The hyperbolic polyhedron $P_\theta(\varphi_1, \varphi_2)$ (see figure 4.5) can be decomposed into two pieces of this kind. Let $W(\varphi, \beta)$ be the hyperbolic volume of such a polyhedron.

A *coherent angle system* in this setting is a pair $\varphi \in \mathbb{R}^{\vec{E}}$, $\beta \in \mathbb{R}^{\vec{E}}$ of functions on the oriented edges satisfying

(i) For all $\vec{e} \in \vec{E}$,

$$\varphi_{\vec{e}} > 0, \quad \beta_{\vec{e}} > 0, \quad \text{and} \quad \varphi_{\vec{e}} + \beta_{\vec{e}} < \frac{\pi}{2}. \tag{4.7}$$

(ii) For all faces $f \in F$,

$$\sum 2\varphi_{\vec{e}} = \Phi_f, \tag{4.8}$$

where the sum is taken over all oriented edges in the oriented boundary of f.

(iii) For all $\vec{e} \in \vec{E}$,

$$\beta_{\vec{e}} + \beta_{-\vec{e}} = \theta_e. \tag{4.9}$$

For $\varphi \in \mathbb{R}^{\vec{E}}$, $\beta \in \mathbb{R}^{\vec{E}}$ which satisfy *(i)*, define the functional

$$T(\varphi, \beta) = \sum_{\vec{e} \in \vec{E}} W(\varphi_{\vec{e}}, \beta_{\vec{e}}).$$

(Condition *(i)* has to be fulfilled for the corresponding polyhedron of figure 4.9 *(left)* to exist.)

PROPOSITION. *A coherent angle system φ, β is a critical point of $T(\varphi, \beta)$ under variations in the space of coherent angle systems, if and only if the isosceles triangles*

with angles $2\varphi_{\vec{e}}$ and $\beta_{\vec{e}}$ as in figure 4.9 (right) fit together to form a circle pattern with intersection angles θ and cone angles Φ in the centers of circles.

PROOF. The tangent space to the space of of coherent angle systems is spanned by vectors of the form

$$\frac{\partial}{\partial \beta_{\vec{e}}} - \frac{\partial}{\partial \beta_{-\vec{e}}}$$

and

$$\frac{\partial}{\partial \varphi_{\vec{e}_1}} - \frac{\partial}{\partial \varphi_{\vec{e}_2}},$$

where $\vec{e}_1$ and $\vec{e}_2$ are two consecutive oriented edges in the oriented boundary of the same face. If and only if

$$\left(\frac{\partial}{\partial \beta_{\vec{e}}} - \frac{\partial}{\partial \beta_{-\vec{e}}} \right) T(\varphi, \beta) = 0,$$

then the polyhedral pieces corresponding to the edges $\vec{e}$ and $-\vec{e}$ fit together to form a polyhedron $P_{\theta_e}(\varphi_{\vec{e}_1}, \varphi_{\vec{e}_2})$ (see figure 4.5).

If and only if

$$\left(\frac{\partial}{\partial \varphi_{\vec{e}_j}} - \frac{\partial}{\partial \varphi_{\vec{e}_k}} \right) T(\varphi, \beta) = 0$$

for all pairs of consecutive edges $\vec{e}_j$, $\vec{e}_k$ in the oriented boundary of a face, then the corresponding polyhedral pieces fit together to form a (not necessarily triangular) ideal prism as shown in figure 4.7 (with a cone-like singular line if $\Phi_f \neq 2\pi$). ∎

The following two propositions explain how the functional $\widehat{S}(\varphi)$ and Leibon's functional can be obtained as two different reductions of $T(\varphi, \beta)$.

PROPOSITION. *If φ, β is a coherent angle system in the sense of this section, then φ is a hyperbolic coherent angle system in the sense of section 2.7.*

Suppose $\varphi \in \mathbb{R}^{\vec{E}}$ is a hyperbolic coherent angle system in the sense of section 2.7. Then there exists exactly one $\beta(\varphi) \in \mathbb{R}^{\vec{E}}$ which satisfies (4.7) and (4.9), such that φ, $\beta(\varphi)$ is a critical point of $T(\varphi, \beta)$ under variations with fixed φ, and with β constrained by equation (4.9). The hyperbolic circle pattern functional is

$$\widehat{S}(\varphi) = T(\varphi, \beta(\varphi)).$$

(SKETCH OF A) PROOF. The first claim about coherent angle systems follows directly from the definitions.

Now, suppose $\varphi \in \mathbb{R}^{\vec{E}}$ is a hyperbolic coherent angle system in the sense of section 2.7. For each non-oriented edge $e = \{\vec{e}, -\vec{e}\}$, construct the hyperbolic kite with angles $2\varphi_{\vec{e}}$, $2\varphi_{-\vec{e}}$, and θ_e, as in figure 2.3 *(left)*. The angle θ_e is divided by one of the diagonals into two angles $\beta_{\vec{e}}$ and $\beta_{-\vec{e}}$, such that φ, β form a coherent angle system in the sense of this section. This (φ, β) is the unique critical point of $T(\varphi, \beta)$ under variations with fixed φ, and with β constrained by equations (4.9). Indeed, it follows from Schläfli's formula, that for every such critical point, the polyhedra of figure 4.9 *(left)* fit together in pairs to form polyhedra as in figure 4.5. (This means that the isosceles triangles of figure 4.9 *(right)* fit together to form kites.) Equation $\widehat{S}(\varphi) = T(\varphi, \beta(\varphi))$ follows form the additivity of the volume function. ∎

PROPOSITION. *Suppose that Σ is a triangulation, θ sums to 2π around each vertex, and $\Phi_f = 2\pi$ for all faces f.*

If φ, β is a coherent angle system in the sense of this section, then $\alpha \in \mathbb{R}^{\vec{E}}$, defined by equations (3.19), is a coherent angle system in the sense of section 3.6.

Suppose $\alpha \in \mathbb{R}^{\vec{E}}$ is a coherent angle system in the sense of section 3.6, and $\beta \in \mathbb{R}^{\vec{E}}$ is defined by equations (3.19). Then there exists exactly one $\varphi(\beta) \in \mathbb{R}^{\vec{E}}$

which satisfies (4.7) and (4.8), such that φ, $\beta(\varphi)$ is a critical point of $T(\varphi, \beta)$ under variations with fixed β, and with φ constrained by equation (4.8). Leibon's circle pattern functional is

$$H(\beta) = T(\varphi(\beta), \beta).$$

The proof is similar to the proof of the last proposition.

CHAPTER 5

A computer implementation

The variational method of constructing circle patterns described in chapter 2 is well suited for computer implementation. Here, we present an implementation in Java. The classes in the `cellularSurface` and `circlePattern` package hierarchies were written by the author. The `mfc`, `numericalMethods`, and `moebiusViewer` package hierarchies are part of the jtem project [**24**]. Of these classes, the author has written `ChebyshevApproximation`, `Clausen`, and `HermitianCircle`.

The `render` package contains Ken Perlin's 3D renderer [**32**]. Originally, the author used Oorange, an experimental programming tool for Java and a part of the jtem project, to experiment with the circle pattern classes. Here, we use the BeanShell [**4**], a Java scripting tool, to illustrate how the classes work.

5.1. Getting started

Unix. Download the zip-file `circlepatternsoftware.zip` from the URL `http://www.math.tu-berlin.de/~springb/software` and unzip it. Change into the directory `circlepatternsoftware` and execute the shell script `bin/bsh` with one of the example BeanShell scripts in the `examples` directory as parameter:

```
> bin/bsh examples/cube.bsh
```

You should see some text output like this

```
Surface has 6 faces, 12 edges, and 8 vertices.
Minimizing ... Minimum found after 237ms.
Laying out circles ... Done.
```

and one or more windows displaying circle patterns should open (see figure 5.1).

Windows. Download the file `circlepatternsoftware.zip` and unzip it as above. Open the `circlepatternsoftware` folder and, in it, the folders `bin` and `examples`. Drag and drop an example BeanShell script (such as `cube.bsh`) from the `examples` folder onto the `bsh.bat` batch file in the `bin` folder.

Alternatively, you may start a command shell and invoke the batch file `bsh.bat` with one of the example BeanShell scripts as argument.

What the scripts do. The scripts `bsh` and `bsh.bat` only call the BeanShell interpreter with the right class path, passing on the argument. Should they not work properly—for example, because you have a Mac—here is what to do. Make sure that the directory `cls` and the jar-file(s) in the directory `lib` are in the class path. (Of course, no other versions of the BeanShell, Ken Perlin's renderer, or the jtem classes should be in the class path.) Invoke a Java virtual machine and run the class `bsh.Interpreter` with a BeanShell script as argument.

Running the BeanShell in interactive mode. If you execute the scripts `bsh` or `bsh.bat` without arguments, the BeanShell will run in interactive mode. You can run BeanShell scripts using the BeanShell command `source()`. Listing 1 shows an example session with the BeanShell in interactive mode. After the BeanShell is

invoked, it prompts the user to enter commands. In the example session, the script `cube.bsh` is run and then the gradient of the functional is printed out.

5.2. The example scripts

Figure 5.1 shows circle patterns produced by BeanShell scripts in the `examples` directory. The scripts `cube.bsh`, `dodecahedron.bsh` and `icosahedron.bsh` produce the obvious trivial circle patterns in the sphere. A slightly more interesting pattern is produced by `truncated_cube.bsh.` All circles intersect at right angles. Half the circles form a packing with the combinatorics of a truncated cube. The script `branched.bsh` produces two circle patterns. The first is the orthogonal pattern consisting of two packings with icosahedral and dodecahedral combinatorics. The second is a branched pattern with the same combinatorics and intersection angles. There are two opposite branched faces with cone angle 4π.

We will illustrate how the scripts work by taking a closer look at `cube.bsh`, see listing 2. First, the relevant classes are imported.

```
1 import cellularSurface.*;
2 import cellularSurface.examples.*;
3 import circlePattern.variational.*;
4 import circlePattern.viewer.perlin.*;
5 import circlePattern.viewer.moebius.*;
```

The package `cellularSurface` contains only one class, `CellularSurface`, which implements a combinatorial model for cell decompositions of surfaces. The package `cellularSurface.examples` contains classes like `Cube`, which inherit from `CellularSurface` but have different constructors. Thus,

```
7 CellularSurface surface = new Cube();
```

assigns to the variable *surface* a `CellularSurface` representing the combinatorial type of a cube.

The package `circlePattern.variational` contains the classes `SphericalData` and `SphericalLayout`. The class `SphericalData` holds the intersection angles, cone angles, and variables ρ for a spherical circle pattern. It can compute the correct ρ by minimizing the spherical circle pattern functional $S_{\mathrm{sph}}(\rho)$. Given an instance of `SphericalData`, the class `SphericalLayout` calculates the positions of the centers and intersection points of a spherical circle pattern. (To construct euclidean or hyperbolic circle patterns, use the analogous classes `EuclideanData`, `EuclideanLayout`, `HyperbolicData`, and `HyperbolicLayout`.)

```
8 GenericData data = new SphericalData();
9 GenericLayout layout = new SphericalLayout();
```

The next lines print out some information about the *surface*.

```
11 System.out.println("Surface has " + surface.getNumFaces()
12                     + " faces, " + surface.getNumEdges()
13                     + " edges, and " + surface.getNumVertices()
14                     + " vertices.");
```

Next, we set up the *data*. Since three edges meet at each vertex, the exterior intersection angles θ are set to $\frac{2}{3}\pi$. All Φ are set to 2π because there are no boundary faces and the pattern is unbranched.

```
16 data.setSurface(surface);
17 data.assignAllCapitalPhi(2.0*Math.PI);
18 data.assignAllTheta(2.0/3.0*Math.PI);
```

```
> bin/bsh
BeanShell 1.2.7 - by Pat Niemeyer (pat@pat.net)
bsh % source("examples/cube.bsh");
Surface has 6 faces, 12 edges, and 8 vertices.
Minimizing ...  Minimum found after 232ms.
Laying out circles ...  Done.
bsh % for (int i = 0; i < 6; i++) {
System.out.println(data.getGradient(i));
}
4.5469956688748425E-8
1.9296370279420216E-8
1.9296370279420216E-8
1.9296370279420216E-8
1.9296370279420216E-8
4.5469954468302376E-8
bsh % exit();
>
```

LISTING 1. Example session: Running the BeanShell interactively.

```
1  import cellularSurface.*;
2  import cellularSurface.examples.*;
3  import circlePattern.variational.*;
4  import circlePattern.viewer.perlin.*;
5  import circlePattern.viewer.moebius.*;
6
7  CellularSurface surface = new Cube();
8  GenericData data = new SphericalData();
9  GenericLayout layout = new SphericalLayout();
10
11 System.out.println("Surface has " + surface.getNumFaces()
12                 + " faces, " + surface.getNumEdges()
13                 + " edges, and " + surface.getNumVertices()
14                 + " vertices.");
15
16 data.setSurface(surface);
17 data.assignAllCapitalPhi(2.0*Math.PI);
18 data.assignAllTheta(2.0/3.0*Math.PI);
19
20 //data.setRho(0, 1.0);
21
22 System.out.print("Minimizing ... ");
23 data.adjustRho();
24
25 System.out.print("Laying out circles  ... ");
26 layout.layout(data);
27 System.out.println("Done.");
28
29 PerlinView.show(layout);
30 //MoebiusView.show(layout);
```
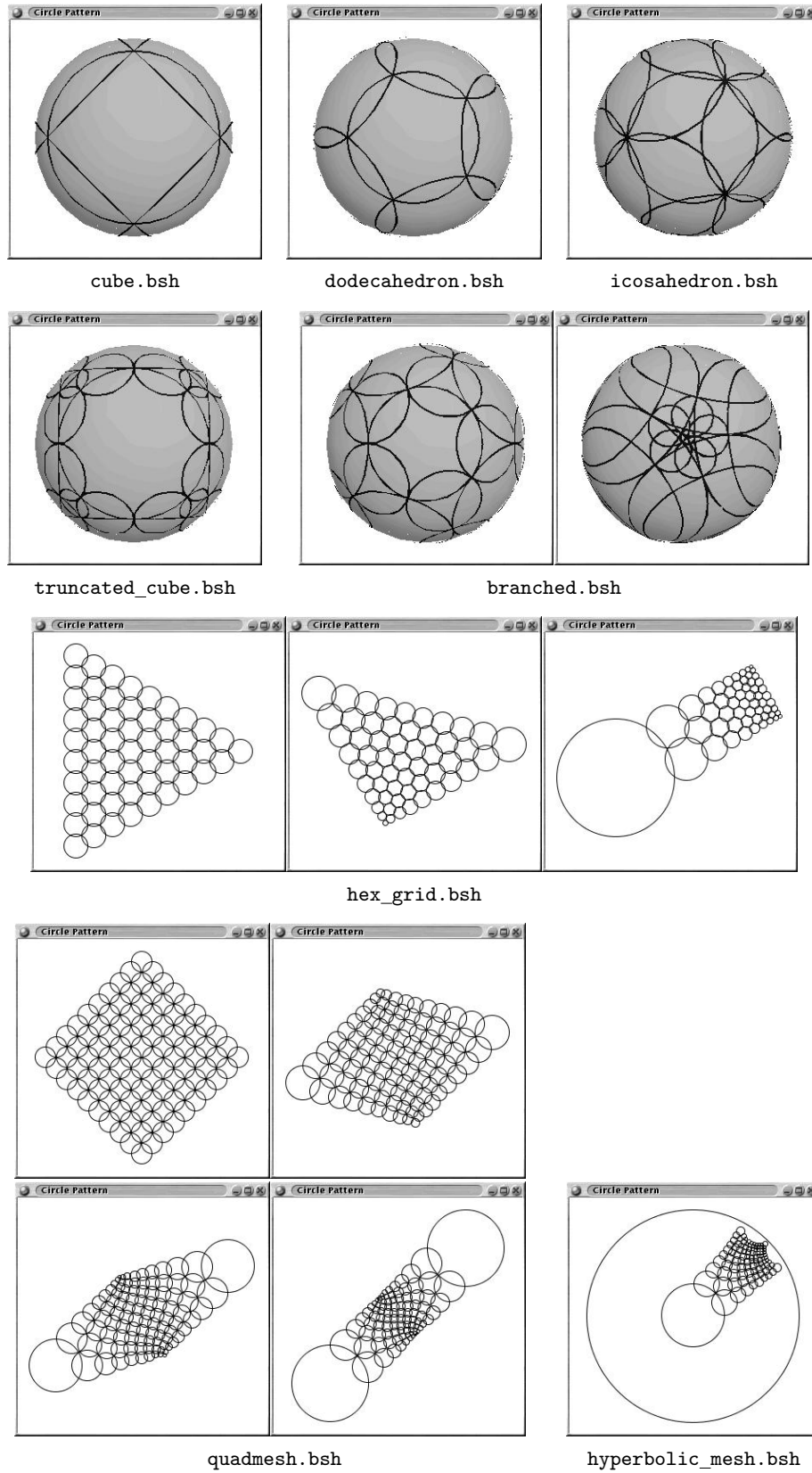
LISTING 2. `cube.bsh`

FIGURE 5.1. Circle patterns produced by the example BeanShell scripts.

Then, *data* calculates the correct ρ, and from this, *layout* calculates the coordinates of the centers and intersection points.

22 System.out.print("Minimizing ... ");
23 data.adjustRho();
24
25 System.out.print("Laying out circles ... ");
26 layout.layout (*data*);
27 System.out.println("Done.");

Finally, we display the resulting pattern in a 3-dimensional spherical view.

29 PerlinView.show(*layout*);

Dragging the mouse rotates the sphere.
     If you uncomment the last line,

30 //MoebiusView.show(layout);

another window will pop up with a view of the same circle pattern projected stereo-graphically to the plane. Dragging the mouse will translate the pattern. Shift click inside the window to select between translate, rotate, scale, info-coord, and three-point-transform mode. In three-point-transform mode, you can Möbius transform the image by dragging three points. Press the i-key to perform an inversion on the unit circle.

     The resulting circle pattern is fairly symmetric—all radii are about equal—even though the solution is only unique up to Möbius transformations. This is so because initially, before the spherical functional is minimized, all ρ are equal to 0. If you uncomment line 20,

20 //data.setRho (0, 1.0);

you will get a more unsymmetric solution.

5.3. Class overview

     Below, we list the packages and most important classes with some comments. For more detailed documentation, see sections 5.4 and 5.5, and the code documentation in the `javadocs` directory.

———————————— classes pertaining to cellular surfaces ————————————

package `cellularSurface` : contains only one class.
     class `CellularSurface` : implements a winged edge model for cell decompositions of surfaces.
package `cellularSurface.examples` : contains classes which inherit from the class `CellularSurface`. Their constructors create specific cell decompositions.
     class `Cube` **extends** `CellularSurface` : the combinatorial type of the cube.
     class `Dodecahedron` **extends** `CellularSurface` : the combinatorial type of the dodecahedron.
     class `ProjectivizedCube` **extends** `CellularSurface` : the combinatorial type of a cube with diametrically opposite points identified. A non-orientable cell decomposition with 3 faces, 6 edges, and 4 vertices.
     class `ProjectivizedDodecahedron` **extends** `CellularSurface` : the combinatorial type of a dodecahedron with diametrically opposite points identified. A non-orientable cell decomposition with 6 faces, 15 edges, and 10 vertices.

class QuadMesh extends `CellularSurface` : a cell decomposition of the disc consisting of a rectangular grid of quadrilateral faces. (No boundary edges.)

class HexGrid extends `CellularSurface` : a cell decomposition of the disc consisting of a triangular grid of hexagonal faces. (No boundary edges.)

———————————— classes pertaining to circle patterns ————————————

package `circlePattern.variational` :

class CPMath : provides static methods for mathematical functions that are used in different classes.

class EuclideanFunctional : provides a static method to compute the value of the euclidean functional $S_{\mathrm{euc}}(\rho)$ and its gradient, given a `CellularSurface`, intersection angles, cone angles, and ρ.

class HyperbolicFunctional : same for the hyperbolic functional $S_{\mathrm{hyp}}(\rho)$.

class SphericalFunctional : same for the spherical functional $S_{\mathrm{sph}}(\rho)$.

abstract class GenericData : abstract superclass of the following three classes. Properties: a `CellularSurface`, intersection angles, and cone angles.

class EuclideanData extends `GenericData` : minimizes the euclidean functional.

class HyperbolicData extends `GenericData` : minimizes the hyperbolic functional.

class SphericalData extends `GenericData` : minimizes the spherical functional.

abstract class GenericLayout : abstract superclass of the following three classes.

class EuclideanLayout extends `GenericLayout` : responsible for laying out the circles, given an instance of `EuclideanData` with correct ρ.

class HyperbolicLayout extends `GenericLayout` : same for `HyperbolicData`.

class SphericalLayout extends `GenericLayout` : same for `SphericalData`.

package `circlePattern.viewer.moebius` : helper classes to view circle patterns in the `MoebiusViewer`.

class CirclePatternShape : This is an adapter class to view circle patterns in the `MoebiusViewer`. Holds a reference to a `GenericLayout` and implements the interface `MoebiusShape`.

class MoebiusView : the static method show(`GenericLayout` *layout*) opens a frame with a `MoebiusViewer` displaying the circle pattern *layout*.

package `circlePattern.viewer.perlin` : contains only one class.

class PerlinView : The static method show(`GenericLayout` *layout*) opens a frame showing a 3-dimensional spherical view of the circle pattern *layout* in Ken Perlin's renderer.

———————————— mathematical foundation classes ————————————

package `mfc.number` : provides the class `Complex` for complex numbers.

package `mfc.vector` : provides the classes `Real3` and `Complex2` for real 3-vectors and complex 2-vectors.

package `mfc.matrix` : provides classes for different types of complex matrices.

abstract class AbstractComplex2By2 : abstract superclass of the other matrix classes. Provides functionality, but access is restricted.

class Complex2By2 extends `AbstractComplex2By2` : class for general complex 2×2 matrices.

class HermitianComplex2By2 extends `AbstractComplex2By2` : class for Hermitian complex 2×2 matrices.

package `mfc.group` : provides classes for matrix groups.

class `Moebius` **extends** `AbstractComplex2By2` : class for elements of the group of orientation preserving conformal self-maps of the Riemann sphere.

package `mfc.geometry` : provides classes for some geometric objects.

    class `ComplexProjective1` **extends** `Complex2` : homogeneous coordinates of 1-dimensional complex projective space.

    class `HermitianCircle` **extends** `HermitianComplex2By2` : Oriented circles in the Riemann sphere are described by Hermitian 2×2 matrices with negative determinant.

———————————— classes for numerical calculations ————————————

package `numericalMethods.function` : provides interfaces which compensate the lack of function pointers in Java.

    interface `DoubleParametrized`

    interface `DoubleValued`

    interface `DoubleArrayParametrized`

    interface `DoubleArrayValued`

package `numericalMethods.calculus.functionApproximation`

    class `ChebyshevApproximation` : provides static methods for Chebyshev interpolation and integration.

package `numericalMethods.calculus.specialFunctions`

    class `Clausen` : implements Clausen's integral.

package `numericalMethods.calculus.minimizing` : provides methods for the unconstrained minimization of functions of one or many variables.

———————————— the 2D Möbius viewer ————————————

package `moebiusViewer` (and sub-packages).

———————————— Ken Perlin's 3D renderer ————————————

package `render` : Some classes have been modified slightly by the author to allow resizing of the `RenderApplet`. The changes are documented in the code (search for "Springborn").

5.4. The class `CellularSurface`

In appendix D, *non-oriented cellular surfaces* were defined in terms of a finite set $\vec{E}$ of oriented edges and three permutations (ι, σ, and τ) of $\vec{E}$. The class `CellularSurface` is an implementation of this combinatorial model. Here, we describe its fundamental features. See also the documentation in the `javadocs` directory.

The oriented edges $\vec{e} \in \vec{E}$ are numbered consecutively, starting at 0. The edge numbering complies with the following convention: If edge $\vec{e}$ has number n, then $\iota\vec{e}$ has number $n \frown 2$ and $\tau\vec{e}$ has number $n \frown 1$, where $\frown$ denotes bitwise exclusive or. Hence, edge-numbers $4k$, $4k + 1$, $4k + 2$, and $4k + 3$ all belong to the same edge of the cell decomposition. The edges with numbers $4k$ and $4k + 2$ ($4k + 1$ and $4k + 3$) are images of each other under ι, that is, they correspond to the different orientations of the same unoriented edge. The edges with numbers $4k$ and $4k + 1$ ($4k + 2$ and $4k + 3$) are images of each other under τ, that is, they correspond to the two preimages in the oriented double cover of the same oriented edge in the non-oriented cell-decomposition.

The faces are also numbered consecutively, starting at 0, and such that if a face f has number n, then the oppositely oriented face τf has number $n \frown 1$.

The same is true for the vertices. If the vertex v has number n, then the vertex τv has number $n \frown 1$.

The default constructor of `CellularSurface` produces an 'empty' cell decomposition with 0 faces, 0 vertices, and 0 edges.

Figure 5.2 shows the edge numbers and face numbers of the cellular surfaces produced by the constructors of the classes `Cube` and `ProjectivizedCube` in the package `cellularSurface.examples`. The first represents the combinatorial type of the cube. Note that orientable surfaces may be defined using only even indices. On the other side of the surface, all elements have then odd indices. The second represents the combinatorial type of a 'projectivized cube', that is, a cube with diametrically opposite points identified. These two `CellularSurface` s are constructed with calls to the method

void buildFromFaceBoundaries(**int**[ ][ ] *faceBoundaries*) .

`Cube` is produced by a call of buildFromFaceBoundaries with the double **int** array

new int [ ][ ] {
    {0, 4, 8, 12},
    {2, 16, 32, 22},
    {6, 20, 36, 26},
    {10, 24, 40, 30},
    {14, 28, 44, 18},
    {34, 46, 42, 38}
}

as argument. The argument

new int [ ][ ] {
    {0, 4, 8, 12},
    {2, 16, 9, 22},
    {6, 20, 13, 17}
}

is passed to produce `ProjectivizedCube`. Each row defines a face by listing the oriented edge numbers of the boundary in cyclic order. The first row defines face number 0, the second row defines face number 2, the third row defines face number 4 and so forth. (This determines also the face boundaries of the oppositely oriented odd numbered faces.) The vertex indices are generated automatically.

The methods

int getNumFaces()
int getNumVertices()
int getNumEdges()

return the numbers of non-oriented faces, vertices and edges. The face indices and vertex indices range from 0 to

$2 * \text{getNumFaces}() - 1$

and from 0 to

$2 * \text{getNumVertices}() - 1$

while the edge indices range from 0 to

$4 * \text{getNumEdges}() - 1$

because four consecutive indices correspond to a single edge of the cell decomposition.

Often, one wants to loop over all non-oriented faces or all non-oriented edges of a cell decomposition represented by a `CellularSurface` surf. This is achieved by loops like

for (**int** $face = 0$, $max = 2 * \text{surf.getNumFaces}()$; $face < max$; $face \mathrel{+}= 2$) {

. . .

}

and

for (**int** $edge = 0$, $max = 4 * \text{surf.getNumEdges}()$; $edge < max$; $edge \mathrel{+}= 4$) {

. . .

}

while

for (**int** $edge = 0$, $max = 4 * \text{surf.getNumEdges}()$; $edge < max$; $edge \mathrel{+}= 2$) {

. . .

}

loops over all oriented edges of a non-oriented cell decomposition.

Suppose an oriented edge $\vec{e}$ has index i. When called with i as argument,

the method	returns the index of (see figure D.1)
int nextEdgeOfLeftFace(**int**)	the edge $\sigma\vec{e}$.
int previousEdgeOfLeftFace(**int** i)	the edge $\sigma^{-1}\vec{e}$.
int nextEdgeOfRightFace(**int**)	the edge $\iota\sigma^{-1}\iota\vec{e}$.
int previousEdgeOfRightFace(**int**)	the edge $\iota\sigma\iota\vec{e}$.
int leftEdgeOfInitialVertex(**int**)	the edge $\iota\sigma^{-1}\vec{e}$.
int rightEdgeOfInitialVertex(**int**)	the edge $\sigma\iota\vec{e}$.
int leftEdgeOfTerminalVertex(**int**)	the edge $\iota\sigma\vec{e}$.
int rightEdgeOfTerminalVertex(**int**)	the edge $\sigma^{-1}\iota\vec{e}$.
int leftFace(**int**)	the face on the left side of $\vec{e}$.
int rightFace(**int**)	the face on the right side of $\vec{e}$.
int initialVertex(**int**)	the initial vertex of $\vec{e}$.
int terminalVertex(**int**)	the terminal vertex of $\vec{e}$.

All these methods are fast, because they consist essentially in an array lookup. There are also methods like

int edgeWithLeftFace(**int** *face*)
int edgeWithTerminalVertex(**int** *vertex*)

which return an edge in the boundary of *face* and an edge ending in *vertex*, respectively. These are computationally more expensive, because they involve a looping over the edges and checking, say, whether leftFace(*edge*) returns *face*. The same holds for

int boundaryLength(**int** *face*).

To describe cell decompositions of surfaces with boundary, there is a special index

static final int NO_ELEMENT $= -1$

to indicate that there is no such edge/face/vertex. The class `CellularSurface` may be used to describe both *cellular surfaces with holes and punctures* and *cellular surfaces with boundary faces and boundary vertices*, as defined in section D.2. For example, after calling

buildFromFaceBoundaries(**new int**[ ][ ]{{0,4,8}})

the `CellularSurface` describes a cell decomposition of the disc with one face, three boundary edges, and three vertices. The methods leftFace(**int**) and rightFace(**int**)

return the following values:

i	0	1	2	3	4	5	6	7	8	9	10	11
leftFace (i)	0	-1	-1	1	0	-1	-1	1	0	-1	-1	1
rightFace(i)	-1	1	0	-1	-1	1	0	-1	-1	1	0	-1

The `circlePattern`-classes expect `CellularSurface`s which encode cellular surfaces with boundary faces and boundary vertices. In this case every edge has a left face and a right face and an initial and a terminal vertex. But some faces may have non-closed boundary. For example, consider the example `Cube` (see figure 5.2, *top*) with face number 10 and its boundary edges removed. Such a `CellularSurface` is produced by the method call

buildFromFaceBoundaries(**new int**[ ][ ] {
   {0, 4, 8, 12},
   {2, 16, −1, 22},
   {6, 20, −1, 26},
   {10, 24, −1, 30},
   {14, 28, −1, 18}
});

It has 5 faces, 8 edges, and 8 vertices. The method nextEdgeOfLeftFace(**int**) will return −1 when called with argument 16, 20, 24, or 28 (and also when called with 17, 21, 25, or 29).

The method

void copy(`CellularSurface` *surface*)

builds a copy of *surface* and the method

void buildPoincareDual(`CellularSurface` *surface*)

builds the Poincaré dual of *surface*. For example, a `CellularSurface` representing the combinatorial type of an icosahedron may be obtained in this way:

import cellularSurface.CellularSurface;
import cellularSurface.examples.Dodecahedron;
CellularSurface *surface* = **new** Dodecahedron();
surface.buildPoincareDual(*surface*);

There are several methods to modify a `CellularSurface`. Figure 5.3 illustrates the simple moves. The methods

void slideEdgeLeft(**int** *edge*)
void slideEdgeRight(**int** *edge*)

do not change the numbers of faces, edges and vertices, while

int splitEdgeAlong(**int** *edge*)

introduces a new edge and a new face, and

int splitEdgeAcross(**int** *edge*)

introduces a new edge and a new vertex. These last two methods return the index of the new edge. An edge may be contracted with

void contractEdge(**int** *edge*).

More complicated moves such as truncating a vertex with

void truncateVertex(**int** *vertex*)

and building the medial decomposition (see figure 2.8) with

void medialGraph()

are composed of many of the simple moves.

5.5. The `circlePattern`-classes

Here, we give a brief description of the classes which perform the construction of circle patterns. They are contained in the package `circlePattern.variational`. The construction proceeds in two steps. First, one of the classes `EuclideanData`, `HyperbolicData`, or `SphericalData` computes the radii of the circles, and then then corresponding class `EuclideanLayout`, `HyperbolicLayout`, or `SphericalLayout` computes the centers and intersection points of the circles in the respective constant curvature space.

The ——Data **classes.** The classes `EuclideanData`, `HyperbolicData`, and `SphericalData` perform the minimization of the respective functionals to compute the radii. They all inherit from the abstract superclass `GenericData` which provides the member variables with get/set methods.

The **protected** member variables, which can be accessed with get/set methods, are:

• `CellularSurface` *surface*. The cell decomposition which determines the combinatorics of the circle pattern. Faces of the decomposition correspond to circles of the pattern. The *surface* may be non-orientable. It may be closed or a cellular surface with boundary faces and boundary vertices (see sections 5.4 and D.2). Boundary edges are not allowed.

• **double**[ ] *capitalPhi*. The cone/boundary angles Φ. Before *surface* is set, *capitalPhi* may be **null**. When *surface* is set, *capitalPhi* is assigned and array with length surface.getNumFaces(). There is one angle Φ_f for each non-oriented face f. The oriented faces with indices $2n$ and $2n+1$ have the cone/boundary angle *capitalPhi*[n].

• **double**[ ] *theta*. The exterior intersection angles θ (see figure 1.3). Before *surface* is set, *theta* may be **null**. When *surface* is set, *theta* is assigned an array with length surface.getNumEdges(). There is one intersection angle θ_e for each non-oriented edge e. The oriented edges with indices $4n$, $4n+1$, $4n+2$ and $4n+3$ have the intersection angle *theta*[n].

• **double** *tolerance*. The error tolerance for the minimal value of the functional. The default is `DEFAULT_TOLERANCE`.

• **double**[ ] *rho*. The variables ρ. Before *surface* is set, *rho* may be **null**. When *surface* is set, ρ is assigned an array with length surface.getNumFaces(). There is one variable ρ_f for each non-oriented face f. To the oriented faces with indices $2n$ and $2n+1$ belongs the variable *rho*[n]. Apart from the set methods, the values *rho*[n] are changed by the method adjustRho().

• **double** *value*. The value of the respective circle pattern functional. This is set by evaluateFunctional() and adjustRho(). There is no set method.

• **double**[ ] *gradient*. The gradient of the respective circle pattern functional. Before *surface* is set, *rho* may be **null**. When *surface* is set, *rho* is assigned an array with length surface.getNumFaces(). To the oriented faces with indices $2n$ and $2n+1$ belongs the gradient entry *gradient*[n]. The values *gradient*[n] are set by the methods evaluateFunctional() and adjustRho(). There are no set methods.

The functionality is provided by the following methods, which are abstract in `GenericData`:

- **void** evaluateFunctional(). From the values of *surface*, *capitalPhi*, *theta*, and *rho*, this method calculates the value and gradient of the functional S_{euc}, S_{hyp}, or S_{sph} (depending on the subclass of `GenericData`) and sets *value* and *gradient* accordingly.

- **void** adjustRho(). Minimizes the functional S_{euc}, S_{hyp}, or S_{sph} (depending on the subclass of `GenericData`) using a conjugate gradient method. (In the case of the spherical functional S_{sph}, the minimax procedure described in section 2.6 is performed.) It attempts to determine the minimal value up to a maximal error of *tolerance*. If it returns successfully, the member variables *rho*, *value*, and *gradient* hold the approximated position of the minimum, the approximated minimal value and the gradient at the approximated minimum (which should be close to zero).

- **double** radius(**double** *rho*). Performs the variable transformation from the variables ρ to the radii r. The relation between r and ρ is given by equations (2.3), (2.14), or (2.23), depending on the subclass of `GenericData`.

The ——Layout classes. Once the radii of the circles have been computed, the classes `EuclideanLayout`, `HyperbolicLayout`, and `SphericalLayout` compute the centers and intersection points of the circles. They all inherit from the abstract superclass `GenericLayout`, which provides the member variables and almost all of the functionality.

The **protected** member variables, which can only be read with get methods, are:

- `ComplexProjective1[ ]` *centerPoint*. Complex homogeneous coordinates for the centers of the circles. After a call of the method layout(*data*) (see below), *centerPoint* is an array of length 2∗data.getNumFaces(). There is one entry for each oriented face. If the oriented double cover of the surface is not connected (for example, if the surface is orientable), then some entries of *centerPoint* will be null.

- `ComplexProjective1[ ]` *vertexPoint*. Complex homogeneous coordinates for the intersection points. After a call of the method layout(*data*), *vertexPoint* is an array of length 2∗data.getNumVertices(). There is one entry for each vertex of the oriented double cover. If the oriented double cover is not connected (for example, if the surface is orientable), then some entries of *vertexPoint* will be null.

- `HermitianCircle[ ]` *circle*. The circles of the circle pattern, described in a Möbius-invariant fashion as Hermitian (2×2)-matrices with negative determinant. After a call of the method layout(*data*), *circle* is an array of length 2∗data.getNumFaces(). There is one entry for each oriented face. If the oriented double cover of the surface is not connected (for example, if the surface is orientable), then some entries of *circle* will be null.

The member variables are set by the method

void layout(`GenericData` *data*)

of class `GenericLayout`. The member variables *surface*, *theta*, and *rho* of the argument *data* are expected to hold correct values for a circle pattern of the respective geometry. This means, the layout method of `EuclideanLayout` expects to be passed an instance of `EuclideanData` with *rho* set by a successful call of its method adjustRho(), etc.

The layout algorithm is fairly unsophisticated: Initialize member variables *centerPoint*, *vertexPoint*, and *circle* to arrays of the correct size with all entries equal to **null**. Then, place the first two points: set the *centerPoint* of the left face of the edge with index `INITIAL_EDGE` to the origin; and set the *vertexPoint* of the initial vertex of the same edge an appropriate distance away on the positive

real axis. After the initial points are placed, keep searching for more points whose position can be determined until no more can be found.

Almost all the work is done in the abstract superclass `GenericLayout`. Its layout method is not abstract. But internally, it calls the two abstract methods of `GenericLayout`:

abstract void assignOtherFixPoint(`ComplexProjective1` *center*,
$\qquad\qquad\qquad\qquad\qquad\qquad$ `ComplexProjective1` *otherFixPoint*);

abstract void assignCircle(`HermitianCircle` *circle*,
$\qquad\qquad\qquad\qquad$ `ComplexProjective1` *center*,
$\qquad\qquad\qquad\qquad$ **double** *radius*);

All the subclasses `EuclideanLayout`, `HyperbolicLayout`, and `SphericalLayout` do is to implement these two abstract methods:

The method assignOtherFixPoint assigns the argument *otherFixPoint* depending on the argument *center*. In the class `EuclideanFunctional`, the argument *otherFixPoint* is always set to the infinite point of the euclidean plane. In the class `HyperbolicFunctional`, *otherFixPoint* is set to image of *center* under an inversion on the circle which is the boundary of hyperbolic space. In the class `SphericalFunctional`, *otherFixPoint* is set to the point which is diametrically opposite to *center* on the Riemann sphere.

The method assignCircle assigns *circle* by the circle which, in the respective geometry, has center *center* and radius *radius*.

5.6. Computing Clausen's integral

In 1832, Clausen first tabulated the integral (B.3), which now bears his name [**15**]. He expands the functions

$$\mathrm{Cl}_2(\pi x) + \pi\left(2\log\frac{2+x}{2-x} + x\log\left((2+x)(2-x)|x|\right)\right)$$

and

$$\mathrm{Cl}_2(\pi(1-x)) - \pi\log\frac{1+x}{1-x} - \pi x\log\left((1+x)(1-x)\right)$$

into power series of x, which he uses to calculate $\mathrm{Cl}_2(x)$ in the intervals $[0, \frac{\pi}{2}]$ and $[\frac{\pi}{2}, \pi]$ to 16 decimals.

We proceed in a similar fashion, except that we use Chebyshev series. For $x \in [-\pi, \pi]$, the function

$$h(x) = -\log\left(\frac{2\sin\frac{x}{2}}{x}\right)$$

is analytic and

$$\mathrm{Cl}_2(x) = \int_0^x h(\xi)\,d\xi - x(\log|x| - 1).$$

The function $h(x)$ is approximated in the interval $[-\pi, \pi]$ by a Chebyshev series, which can easily be integrated.

The algorithms for fitting, integrating and evaluating Chebyshev series are described in the *Numerical Recipes* [**33**]. They are implemented in static methods of the class `ChebyshevApproximation`, which is contained in the package `numericalMethods.calculus.functionApproximation`.

Using these methods for Chebyshev approximation, the class `Clausen` in package `numericalMethods.calculus.specialFunctions` provides the static method

double cl2(**double** x)

to evaluate Clausen's integral. It also provides Catalan's constant $G = \mathrm{Cl}_2(\frac{\pi}{2})$:
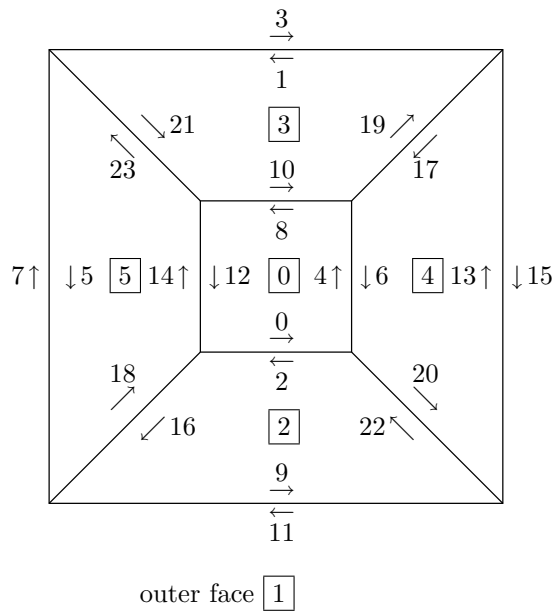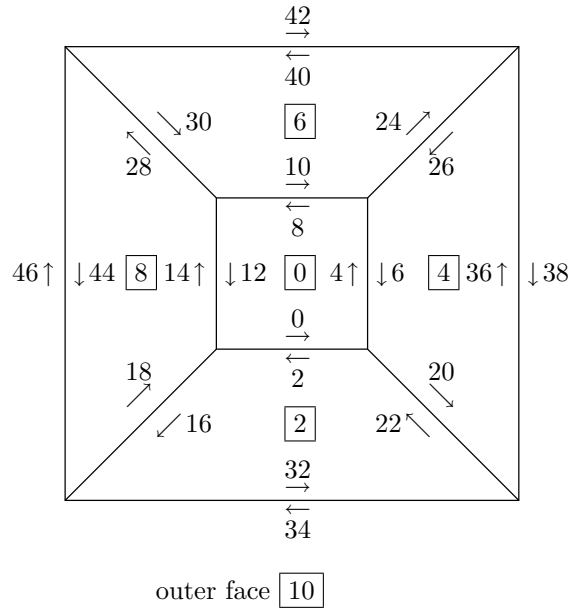
static final double CATALAN

$$\xrightarrow{42}$$
$$\xleftarrow{40}$$

↘30 $\boxed{6}$ 24↗

28         $\xrightarrow{10}$ 26

$\xleftarrow{8}$

46↑   ↓44 $\boxed{8}$ 14↑   ↓12 $\boxed{0}$ 4↑   ↓6 $\boxed{4}$ 36↑   ↓38

$\xrightarrow{0}$

18         $\xleftarrow{2}$ 20

↙16 $\boxed{2}$ 22↖

$$\xrightarrow{32}$$
$$\xleftarrow{34}$$

outer face $\boxed{10}$

$$\xrightarrow{3}$$
$$\xleftarrow{1}$$

↘21 $\boxed{3}$ 19↗

23         $\xrightarrow{10}$ 17

$\xleftarrow{8}$

7↑   ↓5 $\boxed{5}$ 14↑   ↓12 $\boxed{0}$ 4↑   ↓6 $\boxed{4}$ 13↑   ↓15

$\xrightarrow{0}$

18         $\xleftarrow{2}$ 20

↙16 $\boxed{2}$ 22↖

$$\xrightarrow{9}$$
$$\xleftarrow{11}$$

outer face $\boxed{1}$

FIGURE 5.2. `Cube` and `ProjectivizedCube`.

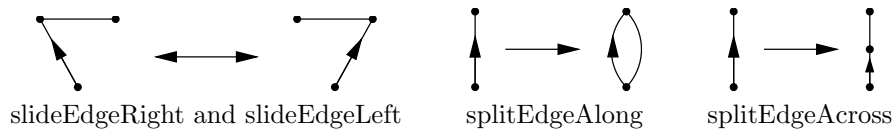slideEdgeRight and slideEdgeLeft   splitEdgeAlong   splitEdgeAcross

FIGURE 5.3. Simple moves.

Proof of the trigonometric relations of lemma 2.5 and lemma 2.10

In this appendix, we derive the below formulae for the remaining angles in a hyperbolic or spherical triangle when two sides and the enclosed angle between them are given. Suppose the given sides of the triangle are r_1 and r_2, the included angle between them is θ, its complement is $\theta^* = \pi - \theta$, and the remaining angles are φ_1 and φ_2, as shown in figure 2.4.

In the spherical case,

$$\varphi_1 = \frac{1}{2i} \log \frac{1 + e^{\rho_2 - \rho_1 + i\theta^*}}{1 + e^{\rho_2 - \rho_1 - i\theta^*}} - \frac{1}{2i} \log \frac{1 - e^{\rho_1 + \rho_2 + i\theta^*}}{1 - e^{\rho_1 + \rho_2 - i\theta^*}} , \qquad (A.1)$$

where we assume $0 < r_j < \pi$, and

$$\rho_j = \log \tan \frac{r_j}{2}.$$

In the hyperbolic case,

$$\varphi_1 = \frac{1}{2i} \log \frac{1 + e^{\rho_2 - \rho_1 + i\theta^*}}{1 + e^{\rho_2 - \rho_1 - i\theta^*}} - \frac{1}{2i} \log \frac{1 + e^{\rho_1 + \rho_2 + i\theta^*}}{1 + e^{\rho_1 + \rho_2 - i\theta^*}} , \qquad (A.2)$$

where

$$\rho_j = \log \tanh \frac{r_j}{2}.$$

These equations (A.1) and (A.2) imply equations (2.22) and (2.13).

To derive such formulae from known relations of non-euclidean trigonometry can be cumbersome. Instead, we present a method using Möbius transformations which has proved to be helpful. We identify the group of Möbius transformations of $\widehat{\mathbb{C}} = \mathbb{C} \cup \{\infty\}$ with the projectivized linear group $PGL(2, \mathbb{C})$. A Möbius transformation

$$z \mapsto \frac{az + b}{cz + d} , \quad ad - bc \neq 0$$

corresponds to

$$\begin{bmatrix} a & b \\ c & d \end{bmatrix} := \mathbb{C} \cdot \begin{pmatrix} a & b \\ c & d \end{pmatrix} \in PGL(2, \mathbb{C}).$$

A.1. The spherical case

The unit sphere $S^2 = \left\{ (x_1, x_2, x_3) \in \mathbb{R}^3 \mid x_1{}^2 + x_2{}^2 + x_3{}^2 = 1 \right\}$ is mapped to the extended complex plane $\widehat{\mathbb{C}} = \mathbb{C} \cup \{\infty\}$ by stereographic projection

$$(x_1, x_2, x_3) \mapsto z = \frac{x_1 + ix_2}{1 - x_3} .$$

The orientation preserving isometries of the sphere (the rotations) correspond to Möbius transformations $\begin{bmatrix} a & b \\ c & d \end{bmatrix}$ with $a = \bar{d}$ and $b = -\bar{c}$. Rotations around the x_1-,

x_2-, and x_3-axis by an angle α correspond to

$$R_1(\alpha) = \begin{bmatrix} \cos\frac{\alpha}{2} & i\sin\frac{\alpha}{2} \\ i\sin\frac{\alpha}{2} & \cos\frac{\alpha}{2} \end{bmatrix},$$

$$R_2(\alpha) = \begin{bmatrix} \cos\frac{\alpha}{2} & -\sin\frac{\alpha}{2} \\ \sin\frac{\alpha}{2} & \cos\frac{\alpha}{2} \end{bmatrix},$$

$$R_3(\alpha) = \begin{bmatrix} e^{i\alpha/2} & 0 \\ 0 & e^{-i\alpha/2} \end{bmatrix} = \begin{bmatrix} e^{i\alpha} & 0 \\ 0 & 1 \end{bmatrix},$$

respectively. If α is not an odd multiple of π, then

$$R_1(\alpha) = \begin{bmatrix} 1 & i\tan\frac{\alpha}{2} \\ i\tan\frac{\alpha}{2} & 1 \end{bmatrix},$$

$$R_2(\alpha) = \begin{bmatrix} 1 & -\tan\frac{\alpha}{2} \\ \tan\frac{\alpha}{2} & 1 \end{bmatrix}.$$

The quantities r_1, r_2, l, and φ_1, φ_2, $\theta = \pi - \theta^*$ are the sides and angles of a spherical triangle as in figure 2.4 if and only if

$$R_2(r_1)R_3(\theta^*)R_2(r_2) = R_3(\varphi_1)R_2(l)R_3(\varphi_2).$$

With $\rho_j = \log\tan(r_j/2)$, the left hand side of this equation equals

$$\mathrm{LHS} = \begin{bmatrix} 1 & -e^{\rho_1} \\ e^{\rho_1} & 1 \end{bmatrix}\begin{bmatrix} e^{i\theta^*} & 0 \\ 0 & 1 \end{bmatrix}\begin{bmatrix} 1 & -e^{\rho_2} \\ e^{\rho_2} & 1 \end{bmatrix}$$

$$= \begin{bmatrix} e^{i\theta^*} - e^{\rho_1+\rho_2} & -e^{\rho_2+i\theta^*} - e^{\rho_1} \\ e^{\rho_1+i\theta^*} + e^{\rho_2} & 1 - e^{\rho_1+\rho_2+i\theta^*} \end{bmatrix}$$

$$= \begin{bmatrix} \dfrac{e^{i\theta^*} - e^{\rho_1+\rho_2}}{1 - e^{\rho_1+\rho_2+i\theta^*}} & -\dfrac{e^{\rho_2+i\theta^*} + e^{\rho_1}}{1 - e^{\rho_1+\rho_2+i\theta^*}} \\ \dfrac{e^{\rho_1+i\theta^*} + e^{\rho_2}}{1 - e^{\rho_1+\rho_2+i\theta^*}} & 1 \end{bmatrix}.$$

With $\lambda = \log\tan(l/2)$, the right hand side equals

$$\mathrm{RHS} = \begin{bmatrix} e^{i\varphi_1} & 0 \\ 0 & 1 \end{bmatrix}\begin{bmatrix} 1 & -e^{\lambda} \\ e^{\lambda} & 1 \end{bmatrix}\begin{bmatrix} e^{i\varphi_2} & 0 \\ 0 & 1 \end{bmatrix}$$

$$= \begin{bmatrix} e^{i(\varphi_1+\varphi_2)} & -e^{\lambda+i\varphi_1} \\ e^{\lambda+i\varphi_2} & 1 \end{bmatrix}.$$

Hence,

$$\varphi_1 = \arg\frac{e^{\rho_2+i\theta^*} + e^{\rho_1}}{1 - e^{\rho_1+\rho_2+i\theta^*}},$$

which implies equation (A.1).

A.2. The hyperbolic case

We use the Poincaré disc model of hyperbolic 2-space: $H^2 = \{z \in \mathbb{C} \mid |z| < 1\}$ with metric $|ds| = 2|dz|/(1 - |z|^2)$. The orientation preserving isometries of H^2 are the Möbius transformations $\begin{bmatrix} a & b \\ c & d \end{bmatrix}$ with $a = \bar{d}$ and $b = \bar{c}$. Let

$$T(s) = \begin{bmatrix} \cosh\frac{s}{2} & \sinh\frac{s}{2} \\ \sinh\frac{s}{2} & \cosh\frac{s}{2} \end{bmatrix} = \begin{bmatrix} 1 & \tanh\frac{s}{2} \\ \tanh\frac{s}{2} & 1 \end{bmatrix},$$

$$R(\alpha) = \begin{bmatrix} e^{i\alpha/2} & 0 \\ 0 & e^{-i\alpha/2} \end{bmatrix} = \begin{bmatrix} e^{i\alpha} & 0 \\ 0 & 1 \end{bmatrix}.$$

The transformation $T(s)$ translates all points on the line $\{z \in H^2 \mid \operatorname{Im} z = 0\}$ towards $z = 1$ by the distance s. The transformation $R(\alpha)$ is a rotation around $z = 0$ by the angle α.

The quantities r_1, r_2, l, and φ_1, φ_2, $\theta = \pi - \theta^*$ are the sides and angles of a hyperbolic triangle as in figure 2.4 if and only if

$$T(r_1)R(\theta^*)T(r_2) = R(\varphi_1)T(l)R(\varphi_2).$$

With $\rho_j = \log\tanh(r_j/2)$, the left hand side of this equation equals

$$
\begin{aligned}
\text{LHS} &= \begin{bmatrix} 1 & e^{\rho_1} \\ e^{\rho_1} & 1 \end{bmatrix} \begin{bmatrix} e^{i\theta^*} & 0 \\ 0 & 1 \end{bmatrix} \begin{bmatrix} 1 & e^{\rho_2} \\ e^{\rho_2} & 1 \end{bmatrix} \\
&= \begin{bmatrix} e^{i\theta^*} + e^{\rho_1+\rho_2} & e^{\rho_2+i\theta^*} + e^{\rho_1} \\ e^{\rho_1+i\theta^*} + e^{\rho_2} & 1 + e^{\rho_1+\rho_2+i\theta^*} \end{bmatrix} \\
&= \begin{bmatrix} \dfrac{e^{i\theta^*} + e^{\rho_1+\rho_2}}{1 + e^{\rho_1+\rho_2+i\theta^*}} & \dfrac{e^{\rho_2+i\theta^*} + e^{\rho_1}}{1 + e^{\rho_1+\rho_2+i\theta^*}} \\ \dfrac{e^{\rho_1+i\theta^*} + e^{\rho_2}}{1 + e^{\rho_1+\rho_2+i\theta^*}} & 1 \end{bmatrix}.
\end{aligned}
$$

With $\lambda = \log\tanh(l/2)$, the right hand side equals

$$
\begin{aligned}
\text{RHS} &= \begin{bmatrix} e^{i\varphi_1} & 0 \\ 0 & 1 \end{bmatrix} \begin{bmatrix} 1 & e^{\lambda} \\ e^{\lambda} & 1 \end{bmatrix} \begin{bmatrix} e^{i\varphi_2} & 0 \\ 0 & 1 \end{bmatrix} \\
&= \begin{bmatrix} e^{i(\varphi_1+\varphi_2)} & e^{\lambda+i\varphi_1} \\ e^{\lambda+i\varphi_2} & 1 \end{bmatrix}.
\end{aligned}
$$

Hence,

$$\varphi_1 = \arg \frac{e^{\rho_2+i\theta^*} + e^{\rho_1}}{1 + e^{\rho_1+\rho_2+i\theta^*}},$$

which implies equation (A.2).

The dilogarithm function and Clausen's integral

In this appendix, we collect all relevant facts about the dilogarithm function and Clausen's integral that is relevant for this paper. A more thorough treatment and an extensive bibliography are contained in Lewin's monograph [**29**].

For $|z| \leq 1$, the dilogarithm function is defined by the power series

$$\mathrm{Li}_2(z) = \frac{z}{1^2} + \frac{z^2}{2^2} + \frac{z^3}{3^2} + \dots .$$

For $|z| < 1$,

$$-\log(1-z) = \frac{z}{1} + \frac{z^2}{2} + \frac{z^3}{3} + \dots,$$

and hence

$$\mathrm{Li}_2(z) = -\int_0^z \frac{\log(1-\zeta)}{\zeta} \, d\zeta . \tag{B.1}$$

In the light of this integral representation, one sees that the dilogarithm can be continued analytically to the complex plane cut from 1 to ∞ along the positive real axis.

Take logarithms on both sides of the identity

$$1 - z^n = (1-z)(1-\omega z)(1-\omega^2 z) \dots (1-\omega^{n-1} z),$$

where $\omega = e^{2\pi i/n}$ is the fundamental n^{th} root of unity, then divide by z and integrate to obtain

$$\frac{1}{n} \, \mathrm{Li}_2(z^n) = \mathrm{Li}_2(z) + \mathrm{Li}_2(\omega z) + \mathrm{Li}_2(\omega^2 z) + \dots \mathrm{Li}_2(\omega^{n-1} z) \tag{B.2}$$

for $|z| \leq 1$. Both sides of the equation can be continued analytically to the complex plane with radial cuts outward from the nth roots of unity to infinity.

Clausen's integral $\mathrm{Cl}_2(x)$ can be defined by the imaginary part of the dilogarithm on the unit circle:

$$\mathrm{Cl}_2(x) = \mathrm{Im} \, \mathrm{Li}_2(e^{ix})$$

$$= \frac{1}{2i} \big(\mathrm{Li}_2(e^{ix}) - \mathrm{Li}_2(e^{-ix}) \big).$$

(The name "Clausen's *integral*" comes from the integral representation (B.3).) We consider Clausen's integral as a real valued function of a real variable. It is 2π-periodic and odd. The power series representation of the dilogarithm yields the Fourier series representation for Clausen's integral,

$$\mathrm{Cl}_2(x) = \sum_{n=1}^{\infty} \frac{\sin(nx)}{n^2} .$$

Substitute $\zeta = e^{i\xi}$ in the integral representation of the dilogarithm (B.1) to obtain, for $0 \leq x \leq 2\pi$,

$$\mathrm{Cl}_2(x) = -\int_0^x \log\left(2\sin\frac{\xi}{2}\right) d\xi . \tag{B.3}$$

By periodicity, for all $x \in \mathbb{R}$,

$$\frac{d}{dx} \operatorname{Cl}_2(x) = -\log \left| 2 \sin \tfrac{x}{2} \right|. \tag{B.4}$$

Clausen's integral is almost the same as Milnor's Lobachevski function [**31**]

$$\text{Л}(x) = -\int_0^x \log |2 \sin \xi| \, d\xi = \frac{1}{2} \operatorname{Cl}_2(2x) \, .$$

Lobachevski [**30**] himself defined a function $L(x)$ (Lobachevski's Lobachevski function) by

$$L(x) = -\int_0^x \log(\cos \xi) \, d\xi \, ,$$

such that

$$L(x) = \frac{1}{2} \operatorname{Cl}_2(2x - \pi) + x \log 2 \, .$$

From equation (B.2) one obtains

$$\frac{1}{n} \operatorname{Cl}_2(nx) = \sum_{k=0}^{n-1} \operatorname{Cl}_2(x + 2\pi k/n) \, .$$

In particular, using that $\operatorname{Cl}_2(x)$ is 2π-periodic and odd, one obtains the double-angle formula for Clausen's integral:

$$\frac{1}{2} \operatorname{Cl}_2(2x) = \operatorname{Cl}_2(x) - \operatorname{Cl}_2(\pi - x) \, . \tag{B.5}$$

We will now derive a formula expressing the imaginary part of the dilogarithm in terms of Clausen's integral not only on the unit circle, but anywhere in the complex plane. Suppose x is real and $0 < \theta < 2\pi$. Substitute $\zeta = e^{\xi + i\theta}$ in (B.1), to obtain

$$\begin{aligned}
\operatorname{Im} \operatorname{Li}_2(e^{x+i\theta}) &= \frac{1}{2i} \left(\operatorname{Li}_2(e^{x+i\theta}) - \operatorname{Li}_2(e^{x-i\theta}) \right) \\
&= \frac{1}{2i} \int_{-\infty}^x \log \left(\frac{1 - e^{\xi - i\theta}}{1 - e^{\xi + i\theta}} \right) d\xi \, .
\end{aligned} \tag{B.6}$$

Now substitute

$$\eta = \frac{1}{2i} \log \left(\frac{1 - e^{\xi - i\theta}}{1 - e^{\xi + i\theta}} \right) ,$$

and note that inversely

$$\xi = \log \left(\frac{2 \sin \eta}{2 \sin(\eta + \theta)} \right) \, .$$

Finally, one obtains

$$\operatorname{Im} \operatorname{Li}_2(e^{x+i\theta}) = yx + \frac{1}{2} \operatorname{Cl}_2(2y) - \frac{1}{2} \operatorname{Cl}_2(2y + 2\theta) + \frac{1}{2} \operatorname{Cl}_2(2\theta) \, , \tag{B.7}$$

where

$$y = \frac{1}{2i} \log \left(\frac{1 - e^{x - i\theta}}{1 - e^{x + i\theta}} \right) \, .$$

From this, we derive the formula

$$\operatorname{Im} \operatorname{Li}_2(e^{x+i\theta}) + \operatorname{Im} \operatorname{Li}_2(e^{-x+i\theta}) =$$
$$px + \operatorname{Cl}_2(p + \theta^*) + \operatorname{Cl}_2(-p + \theta^*) - \operatorname{Cl}_2(2\theta^*) \, , \tag{B.8}$$

where $\theta^* = \pi - \theta$, and

$$p = \frac{1}{2i} \log \frac{(1 + e^{x + i\theta^*})(1 + e^{-x - i\theta^*})}{(1 + e^{x - i\theta^*})(1 + e^{-x + i\theta^*})} \, .$$

Finally, p and x are related by

$$\tan\left(\frac{p}{2}\right) = \tanh\left(\frac{x}{2}\right)\tan\left(\frac{\theta^*}{2}\right).$$

APPENDIX C

The volume of a triply orthogonal hyperbolic tetrahedron with a vertex at infinity

Milnor [**31**, pp. 19f] calculated the volume of a triply orthogonal hyperbolic tetrahedron (three-dimensional hyperbolic orthoscheme) with *two* vertices at infinity by a straightforward integration. By the same computation, one derives a formula for the volume of a triply orthogonal hyperbolic tetrahedron with one vertex at infinity. For reference, we present this computation here.

Figure C.1 shows a triply orthogonal tetrahedron with one vertex at infinity in the Poincaré half-space model of hyperbolic space. In the figure, the tetrahedron is truncated by a horosphere centered at the infinite vertex. Three of the six dihedral angles are $\frac{\pi}{2}$. Because the sum of dihedral angles is π at an infinite vertex and larger than π at a finite vertex, the three remaining angles are α, $\frac{\pi}{2} - \alpha$, and β, as shown in the figure, where

$$0 < \alpha \leq \beta < \frac{\pi}{2}.$$

If $\alpha = \beta$, the tetrahedron has two infinite vertices.

PROPOSITION. *The hyperbolic volume of the triply orthogonal hyperbolic tetrahedron with a vertex at infinity is*

$$V = \frac{1}{8}\Big(2\,\mathrm{Cl}_2(\pi - 2\alpha) + \mathrm{Cl}_2(2\alpha - 2\beta) + \mathrm{Cl}_2(2\alpha + 2\beta)\Big). \qquad \text{(C.1)}$$

Setting $\alpha = \beta$ and using the double-angle formula for Clausen's integral (B.5), one obtains the formula for the volume of a triply orthogonal hyperbolic tetrahedron
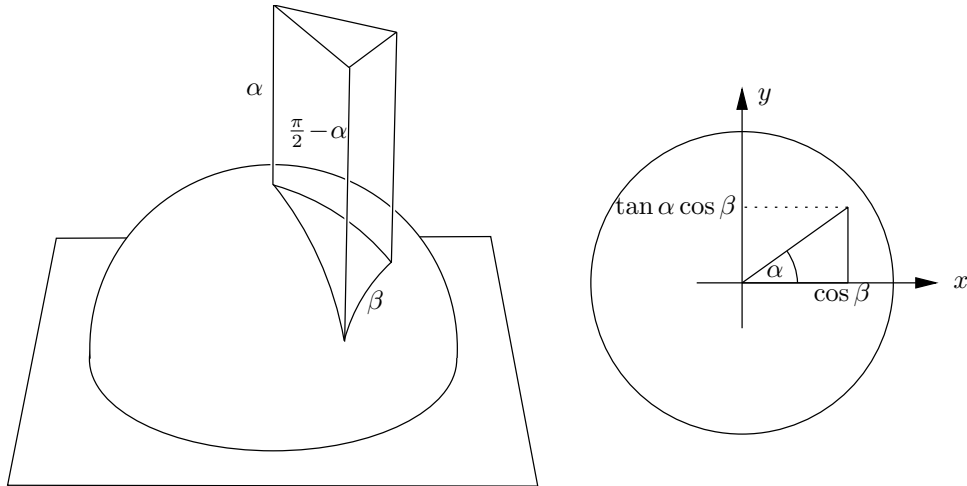

FIGURE C.1. *Left:* A triply orthogonal hyperbolic tetrahedron with one vertex at infinity (truncated at a horosphere). *Right:* The domain of integration in the xy-plane.

with *two* vertices at infinity and *characteristic angle* α:

$$V = \frac{1}{4}\,\mathrm{Cl}_2(2\alpha). \tag{C.2}$$

PROOF OF THE PROPOSITION. In the Poincaré half-space model, hyperbolic space is $H^3 = \{(x, y, z) \in \mathbb{R}^3 \,|\, z > 0\}$ with metric $ds^2 = \frac{1}{z^2}(dx^2 + dy^2 + dz^2)$. The volume form is therefore $\frac{1}{z^3}dx\,dy\,dz$. Hence,

$$V = \int_{x=0}^{\cos\beta} \int_{y=0}^{x\tan\alpha} \int_{z=\sqrt{1-x^2-y^2}}^{\infty} \frac{1}{z^3}\,dz\,dy\,dx,$$

see figure C.1 *(right)*. The first two integrations are readily performed:

$$V = \frac{1}{2}\int_{x=0}^{\cos\beta} \int_{y=0}^{x\tan\alpha} \frac{1}{1-x^2-y^2}\,dy\,dx$$

$$= \frac{1}{2}\int_{x=0}^{\cos\beta} \frac{1}{\sqrt{1-x^2}}\,\mathrm{artanh}\left(\frac{x\tan\alpha}{\sqrt{1-x^2}}\right)dx.$$

Substitute $x = \cos t$, and note that

$$\mathrm{artanh}\left(\frac{\tan\alpha}{\tan t}\right) = \frac{1}{2}\log\frac{1 + \frac{\sin\alpha}{\cos\alpha}\frac{\cos t}{\sin t}}{1 - \frac{\sin\alpha}{\cos\alpha}\frac{\cos t}{\sin t}}$$

$$= \frac{1}{2}\log\frac{\cos\alpha\sin t + \sin\alpha\sin t}{\cos\alpha\sin t - \sin\alpha\sin t}$$

$$= \frac{1}{2}\log\frac{\sin(t+\alpha)}{\sin(t-\alpha)}.$$

Using equation (B.3), one obtains

$$V = -\frac{1}{4}\int_{t=\frac{\pi}{2}}^{\beta} \log\frac{\sin(t+\alpha)}{\sin(t-\alpha)}$$

$$= \frac{1}{8}\Big[\mathrm{Cl}_2(2t+2\alpha) - \mathrm{Cl}_2(2t-2\alpha)\Big]_{t=\frac{\pi}{2}}^{\beta},$$

and hence equation (C.1). ∎

The combinatorial topology and homology of cellular surfaces

This appendix is concerned with a combinatorial model for finite cell decompositions of surfaces, and with their $\mathbb{Z}_2$-homology. Equivalent combinatorial models were described by Jacques [**23**], Tutte [**46**], and Jackson and Visentin [**22**]. They are sometimes called 'winged-edge models'. We present as much of the $\mathbb{Z}_2$-homology theory as needed in the proof of lemma 2.14 in section D.3.5. Of course, all of this is well known.

D.1. Cellular surfaces

Consider cell decompositions of a compact oriented 2-manifold without boundary. There is one such cell decomposition with no edges: The sphere with one face and one vertex. The others can be described by two permutations of the oriented edges: The first, ι, reverses the orientation of an edge. The second, σ, maps each oriented edge to the next oriented edge in the boundary of the face on its left side. (See figure D.1.)

DEFINITION. An *oriented cellular surface* $\Sigma = (\vec{E}, \iota, \sigma)$ is a finite set $\vec{E}$ together with an involution $\iota : \vec{E} \to \vec{E}$ without fixed points (that is, $\iota^2 = \mathrm{id}$ and $\iota\vec{e} \neq \vec{e}$ for all $\vec{e} \in \vec{E}$) and a permutation $\sigma : \vec{E} \to \vec{E}$.

The elements $\vec{e} \in \vec{E}$ are the *oriented edges* of Σ. The *unoriented edges* are unordered pairs $|\vec{e}| = \{\vec{e}, \iota\vec{e}\}$.

The *faces* of Σ are the orbits in $\vec{E}$ of the group generated by σ. The *face on the left side* of an oriented edge $\vec{e} \in \vec{E}$ is the orbit of $\vec{e}$. The *face on the right side* of $\vec{e}$ is the orbit of $\iota\vec{e}$.

The *vertices* of Σ are the orbits in $\vec{E}$ of the group generated by $\iota\sigma^{-1}$. The *initial vertex* of an oriented edge $\vec{e} \in \vec{E}$ is the orbit of $\vec{e}$. The *terminal vertex* of $\vec{e}$ is the orbit of $\iota\vec{e}$.

An oriented cellular surface is *connected* if the group generated by ι and σ acts transitively on $\vec{e}$.
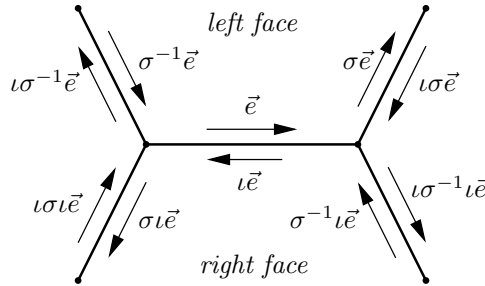

FIGURE D.1. Elements of the group generated by the permutations ι and τ acting on an oriented edge $\vec{e}$.
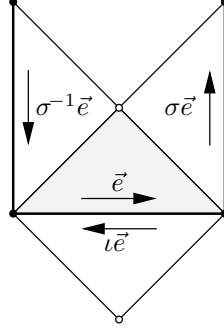
FIGURE D.2. How the 'winged edges' are glued together.

Every oriented cellular surface corresponds to a cell decomposition of a compact oriented 2-manifold without boundary. Indeed, the cell decomposition can be constructed from the cellular surface as follows. For each oriented edge $\vec{e} \in \vec{E}$, take one triangle (a 'winged edge') and glue them together as shown in figure D.2.

DEFINITION. Let $\Sigma_1 = (\vec{E}_1, \iota_1, \sigma_1)$ and $\Sigma_2 = (\vec{E}_2, \iota_2, \sigma_2)$ be two oriented cellular surfaces. An *orientation preserving homeomorphism* f from Σ_1 to Σ_2 is a bijection $f : \vec{E}_1 \to \vec{E}_2$ with

$$f \circ \iota_1 = \iota_2 \circ f \quad \text{and} \quad f \circ \sigma_1 = \sigma_2 \circ f.$$

An *orientation reversing homeomorphism* f from Σ_1 to Σ_2 is a bijection $f : \vec{E}_1 \to \vec{E}_2$ with

$$f \circ \iota_1 = \iota_2 \circ f \quad \text{and} \quad f \circ \iota_1 \sigma_1^{-1} \iota_1 = \sigma_2 \circ f.$$

An orientation preserving homeomorphism f maps the orbits of ι_1, σ_1, and $\iota_1 \circ \sigma_1^{-1}$ to the orbits of ι_2, σ_2, and $\iota_2 \circ \sigma_2^{-1}$. Hence, it induces bijections between the non-oriented edges, the faces, and the vertices of Σ_1 and Σ_2. The face on the left side of $\vec{e} \in \vec{E}_1$ is mapped to the face on the left side of $f(\vec{e})$, and the initial vertex of $\vec{e}$ is mapped to the initial vertex of $f(\vec{e})$.

An orientation reversing homeomorphism f also induces bijections between the non-oriented edges, the faces, and the vertices of the two cellular surfaces. The orbits of ι_1 and $\iota_1 \circ \sigma_1^{-1}$ are mapped to the orbits of ι_2 and $\iota_2 \circ \sigma_2^{-1}$ (although the latter are traversed in the opposite direction). The orbits of σ_1 are not mapped to orbits of σ_2, but to the images of such orbits under ι_2. Nonetheless, this puts the faces in a one-to-one correspondence: The orientation reversing homeomorphism f maps the face on the left side of $\vec{e} \in \vec{E}_1$ to the face on the right side of $f(\vec{e})$.

Cell decompositions of non-oriented (and possibly non-orientable) 2-manifolds are described in terms of their orientable double cover.

DEFINITION. A *non-oriented cellular surface* $\Sigma = (\vec{E}, \iota, \sigma, \tau)$ is an oriented cellular surface $\Sigma_0 = (\vec{E}, \iota, \sigma)$ together with an orientation reversing homeomorphism τ from Σ_0 onto itself, which is an involution without fixed oriented edges. The *faces*, *oriented edges*, and *vertices* of Σ are pairs of faces, oriented edges, and vertices of Σ_0, which are mapped to each other by τ.

In other words, $\tau : \vec{E} \to \vec{E}$ is another permutation with $\tau^2 = \text{id}$, $\tau(\vec{e}) \neq \vec{e}$ for all $\vec{e} \in \vec{E}$, $\tau\iota = \iota\tau$, and $\tau\iota\sigma^{-1}\iota = \sigma\tau$.

DEFINITION. The *Poincaré dual cellular surface* of an oriented cellular surface $\Sigma = (\vec{E}, \iota, \sigma)$ is the oriented cellular surface $\Sigma^* = (\vec{E}, \iota, \sigma^*)$ with $\sigma^* = \iota\sigma^{-1}$. The Poincaré dual cellular surface of a non-oriented cellular surface $\Sigma = (\vec{E}, \iota, \sigma, \tau)$ is

the non-oriented cellular surface $\Sigma^* = (\vec{E}, \iota, \sigma^*, \tau^*)$ with σ^* as in the oriented case and $\tau^* = \iota\tau$.

There is a one-to-one correspondence between the unoriented edges of Σ and Σ^*, between the vertices of Σ and the faces of Σ^*, and between the the faces of Σ and the vertices of Σ^*. The Poincaré dual of the Poincaré dual is essentially the same cellular surface. The map $\vec{e} \mapsto \iota\vec{e}$ is an orientation preserving homeomorphism from Σ to Σ^{**}.

D.2. Surfaces with boundary

Combinatorial models for cell decompositions of surfaces with boundary are less canonical. In this section we describe a few ways in which the above definition for cellular surfaces may be adapted to deal with bounded surfaces. We treat only the oriented case; unoriented surfaces may be described in terms of their oriented double cover, as in the previous section.

The most straightforward way to define oriented cellular surfaces with boundary is to mark some faces as holes:

DEFINITION. An *oriented cellular surface with holes* $\Sigma = (\vec{E}, \iota, \sigma, H)$ is an oriented cellular surface $(\vec{E}, \iota, \sigma)$ together with a subset H of the set of faces, such that, if an oriented edge $\vec{e} \in \vec{E}$ is contained in a face of H, then $\iota\vec{e}$ is not contained in a face of H.

There is no Poincaré duality for cellular surfaces with boundary by this definition. As a remedy, one may consider surfaces with holes and punctures:

DEFINITION. An *oriented cellular surface with holes and punctures*

$$\Sigma = (\vec{E}, \iota, \sigma, H, P)$$

is an oriented cellular surface $(\vec{E}, \iota, \sigma)$ together with a subset H of the set of faces and a subset P of the set of vertices, such that, if an oriented edge $\vec{e} \in \vec{E}$ is contained in a face of H or a vertex of P, then $\iota\vec{e}$ is not contained in a face of H or a vertex in P.

(If Poincaré duality is to be upheld, and adjacent holes are not allowed, then adjacent punctures must be forbidden, too. Alternatively, one may allow adjacent holes and punctures.)

In the computer implementation described in chapter 5, a slightly more exotic combinatorial model is used. It is obtained by deleting all boundary edges. As a consequence, some faces have non-closed boundary; and therefore, for some oriented edges, there *is no* next edge in the boundary of the left face. This model is well suited for applications where one is not interested in boundary edges at all, as in the case of circle patterns.

DEFINITION. An *oriented cellular surface with boundary faces and boundary vertices* $\Sigma = (\vec{E}, \iota, \sigma)$ is a finite set $\vec{E}$ together with an involution $\iota : \vec{E} \to \vec{E}$ without fixed points and a map $\sigma : \vec{E} \to \vec{E} \cup \{\emptyset\}$ which satisfies the following condition:
$$\forall \, \vec{e}_1, \vec{e}_2 \in \vec{E}: \quad \sigma(\vec{e}_1) = \sigma(\vec{e}_2) \neq \emptyset \quad \implies \quad \vec{e}_1 = \vec{e}_2.$$

Although σ is not invertible, there is a 'pseudo-inverse' $\sigma^{-1} : \vec{E} \to \vec{E} \cup \{\emptyset\}$ which satisfies $\sigma^{-1}(\sigma(\vec{e})) = \vec{e}$ for all $\vec{e} \in \vec{E}$ with $\sigma(\vec{e}) \neq \emptyset$, and $\sigma(\sigma^{-1}(\vec{e})) = \vec{e}$ for all $\vec{e} \in \vec{E}$ with $\sigma^{-1}(\vec{e}) \neq \emptyset$. Faces and vertices are defined as 'orbits' of σ and $\iota\sigma^{-1}$ as in the case of ordinary oriented cellular surfaces. Every edge has a left and a right face and an initial and a terminal vertex, and the Poincaré dual cellular surface is well defined.

D.3. $\mathbb{Z}_2$-Homology

Let Σ be an oriented cellular surface, or, equivalently, a cell decomposition of a compact 2-manifold without boundary. Let F, E, and V be the sets of faces, non-oriented edges, and vertices.

D.3.1. Homology groups. The *chain-spaces* $C_0(\Sigma)$, $C_1(\Sigma)$, and $C_2(\Sigma)$ are the $\mathbb{Z}_2$ vector spaces generated by V, E, and F; that is, they are the vector spaces of formal sums of vertices, edges, and faces with coefficients in the field $\mathbb{Z}_2 = \mathbb{Z}/2\mathbb{Z}$. The *boundary operators* $\partial : C_2(\Sigma) \to C_1(\Sigma)$ and $\partial : C_1(\Sigma) \to C_0(\Sigma)$ are the $\mathbb{Z}_2$-linear maps which are defined as follows. A face $f \in F$ of a cellular surface was defined as an orbit $f = \{\vec{e}_1, \dots, \vec{e}_n\}$ of oriented edges. The boundary of f is $\partial f = |\vec{e}_1| + \dots + |\vec{e}_n|$, where $|\vec{e}|$ is the non-oriented edge corresponding to $\vec{e}$. For an edge $e \in E$ with end vertices $v_1, v_2 \in V$, $\partial e = v_1 + v_2$.

The *chain complex* $C_*(\Sigma)$ is the following sequence of chain spaces and linear maps:

$$0 \overset{\partial}{\longrightarrow} C_2(\Sigma) \overset{\partial}{\longrightarrow} C_1(\Sigma) \overset{\partial}{\longrightarrow} C_0(\Sigma) \overset{\partial}{\longrightarrow} 0$$

The *cycle spaces* are the kernels $Z_n(\Sigma) = \{c \in C_n(\Sigma) \,|\, \partial c = 0\}$ for $n \in \{0, 1, 2\}$. The *boundary spaces* are the images $B_2(\Sigma) = 0$ and $B_n(\Sigma) = \partial C_{n+1}(\Sigma)$ for $n \in \{0, 1\}$. The *homology groups* are the quotient spaces $H_n(\Sigma) = Z_n(\Sigma)/B_n(\Sigma)$ and their dimensions are the *Betti numbers* $h_n(\Sigma) = \dim_{\mathbb{Z}_2} H_n(\Sigma)$.

The second Betti number $h_2(\Sigma)$ is the number of equivalence classes of faces under the equivalence relation

$$f_1 \sim f_2 \quad \Longleftrightarrow \quad \begin{array}{l} \text{Every closed 2-chain which} \\ \text{contains } f_1 \text{ also contains } f_2. \end{array}$$

The zeroth Betti number $h_0(\Sigma)$ is the number of equivalence classes of vertices under the equivalence relation

$$v_1 \sim v_2 \quad \Longleftrightarrow \quad \begin{array}{l} \text{The vertices } v_1 \text{ and } v_2 \text{ can be} \\ \text{joined by a path.} \end{array}$$

Using subdivision arguments one can show that $h_2(\Sigma) = h_0(\Sigma)$. Of course, this is just the number of connected components of Σ.

D.3.2. Poincaré duality. The Poincaré dual cellular surface Σ^* has face set $F^* = V$, edge set $E^* = E$, and vertex set $V^* = F$. The chain spaces are therefore $C_n(\Sigma^*) = C_{2-n}(\Sigma)$ for $n \in \{0, 1, 2\}$. Denote the boundary operators of the chain complex $C_*(\Sigma^*)$ by ∂^*. Let the chain spaces be equipped with scalar products $\langle \cdot, \cdot \rangle$ such that F, E, and V are orthonormal bases.

LEMMA D.1 (Poincaré duality). *The boundary operators ∂^* of the chain complex $C_*(\Sigma^*)$ are the adjoint operators of the boundary operators ∂ of the chain complex $C_*(\Sigma)$ with respect to the scalar product $\langle \cdot, \cdot \rangle$.*

This means, for $f \in F = V^*$, $e \in E = E^*$, and $v \in V = F^*$,

$$\langle \partial f, e \rangle = \langle f, \partial^* e \rangle \quad \text{and} \quad \langle \partial e, v \rangle = \langle e, \partial^* v \rangle.$$

PROPOSITION (Poincaré duality for cellular surfaces). *The Betti numbers of Σ and Σ^* satisfy*

$$h_n(\Sigma^*) = h_{2-n}(\Sigma).$$

PROOF. The dimensions of $H_n(\Sigma^*)$ and $H_{2-n}(\Sigma)$ are equal because they are dual vector spaces. This follows from the following facts from linear algebra.

Let V be a vector space, and let U and W be subspaces such that $W \subset U \subset V$. Then the dual space of the quotient U/W is

$$(U/W)^* = W^\perp / U^\perp,$$

$$
\begin{array}{ccccccccc}
& & 0 & & 0 & & 0 & & \\
& & \downarrow & & \downarrow & & \downarrow & & \\
0 & \longrightarrow & C_2(\Upsilon) & \xrightarrow{\partial} & C_1(\Upsilon) & \xrightarrow{\partial} & C_0(\Upsilon) & \longrightarrow & 0 \\
& & \downarrow & & \downarrow & & \downarrow & & \\
0 & \longrightarrow & C_2(\Sigma) & \xrightarrow{\partial} & C_1(\Sigma) & \xrightarrow{\partial} & C_0(\Sigma) & \longrightarrow & 0 \\
& & \downarrow & & \downarrow & & \downarrow & & \\
0 & \longrightarrow & C_2(\Sigma, \Upsilon) & \xrightarrow{\partial} & C_1(\Sigma, \Upsilon) & \xrightarrow{\partial} & C_0(\Sigma, \Upsilon) & \longrightarrow & 0 \\
& & \downarrow & & \downarrow & & \downarrow & & \\
& & 0 & & 0 & & 0 & &
\end{array}
$$

FIGURE D.3. The short exact sequence $0 \to C_*(\Upsilon) \to C_*(\Sigma) \to C_*(\Sigma, \Upsilon) \to 0$ of chain complexes.

where $W^\perp \subset V^*$ and $U^\perp \subset V^*$ are the spaces of linear functionals on V which vanish on W and U, respectively.

Let $f : V \longrightarrow W$ be a linear map between two vector spaces, and let $f^* : W^* \longrightarrow V^*$ be the adjoint map. Then the kernels and images of f and f^* are related by

$$
\operatorname{Im} f^* = (\operatorname{Ker} f)^\perp, \qquad \operatorname{Ker} f^* = (\operatorname{Im} f)^\perp.
$$

Hence,

$$
H_n(\Sigma)^* = \left(Z_n(\Sigma)/B_n(\Sigma) \right)^* = B_n(\Sigma)^\perp / Z_n(\Sigma)^\perp =
$$
$$
= Z_{2-n}(\Sigma^*)/B_{2-n}(\Sigma^*) = H_{2-n}(\Sigma^*).
$$

∎

D.3.3. Relative homology. Define a *subcomplex* Υ of a cellular surface Σ as a triple $\Upsilon = (F_\Upsilon, E_\Upsilon, V_\Upsilon)$ of subsets $F_\Upsilon \subset F$, $E_\Upsilon \subset E$, and $V_\Upsilon \subset V$, such that the following holds: If a face in F_Υ contains an oriented edge $\vec{e}$, then the corresponding unoriented edge $|\vec{e}| \in E_\Upsilon$; and the end-vertices of any edge in E_Υ are contained in V_Υ.

The *relative chain complex* $C_*(\Sigma, \Upsilon)$ consists of the quotient spaces $C_n(\Sigma, \Upsilon) = C_n(\Sigma)/C_n(\Upsilon)$ and the boundary operators induced by the boundary operators of $C_*(\Sigma)$. The corresponding homology groups $H_n(\Sigma, \Upsilon)$ are the *relative homology groups* of the pair (Σ, Υ).

The composition of the inclusion map $C_n(\Upsilon) \to C_n(\Sigma)$, followed by the natural projection $C_n(\Sigma) \to C_n(\Sigma, \Upsilon)$ is the zero map. Hence, the short sequence

$$
0 \longrightarrow C_*(\Upsilon) \longrightarrow C_*(\Sigma) \longrightarrow C_*(\Sigma, \Upsilon) \longrightarrow 0
$$

is exact. This means that the columns of the commutative diagram shown in figure D.3 are exact. By the zigzag-lemma, there is a long exact sequence of homology groups

$$
\begin{aligned}
0 \longrightarrow H_2(\Upsilon) \longrightarrow H_2(\Sigma) \longrightarrow H_2(\Sigma, \Upsilon) \longrightarrow \\
\longrightarrow H_1(\Upsilon) \longrightarrow H_1(\Sigma) \longrightarrow H_1(\Sigma, \Upsilon) \longrightarrow \\
\longrightarrow H_0(\Upsilon) \longrightarrow H_0(\Sigma) \longrightarrow H_0(\Sigma, \Upsilon) \longrightarrow 0.
\end{aligned}
$$

$$
\begin{array}{ccccccc}
& & 0 & & 0 & & \\
& & \downarrow & & \downarrow & & \\
0 & \xrightarrow{\partial} & C_1(\Gamma) & \xrightarrow{\partial} & C_0(\Gamma) & \longrightarrow & 0 \\
& & \downarrow & & \downarrow & & \\
0 \longrightarrow C_2(\Sigma) & \xrightarrow{\partial} & C_1(\Sigma) & \xrightarrow{\partial} & C_0(\Sigma) & \longrightarrow & 0 \\
& & \downarrow & & \downarrow & & \\
0 \longrightarrow C_2(\Sigma,\Gamma) & \xrightarrow{\partial} & C_1(\Sigma,\Gamma) & \xrightarrow{\partial} & C_0(\Sigma,\Gamma) & \longrightarrow & 0 \\
& & \downarrow & & \downarrow & & \\
& & 0 & & 0 & & 0 \\
\end{array}
$$

FIGURE D.4. The short exact sequence $0 \to C_*(\Gamma) \to C_*(\Sigma) \to C_*(\Sigma,\Gamma) \to 0$.

D.3.4. Lefschetz duality. Let $\Upsilon = (F_\Upsilon, E_\Upsilon, V_\Upsilon)$ be a subcomplex of the cellular surface Σ as in the previous section. Then the complement of Υ in Σ^*,

$$\Sigma^* \setminus \Upsilon := (F^* \setminus V_\Upsilon, E^* \setminus E_\Upsilon, V^* \setminus F_\Upsilon),$$

is a subcomplex of Σ^*.

PROPOSITION (Lefschetz duality for cellular surfaces). *The Betti numbers of the subcomplex $\Sigma^* \setminus \Upsilon$ and the pair (Σ, Υ) satisfy*

$$h_n(\Sigma^* \setminus \Upsilon) = h_{2-n}(\Sigma, \Upsilon).$$

PROOF. As in the case of Poincaré duality, the dimensions of the homology groups $H_n(\Sigma^* \setminus \Upsilon)$ and $H_{2-n}(\Sigma, \Upsilon)$ are equal because they are dual vector spaces. This is proved in the same way. ∎

D.3.5. Proof of lemma 2.14. Consider the long exact homology sequence of relative homology for a 1-dimensional subcomplex Γ, that is, a cellularly embedded graph. Let $E_\Gamma \subset E$ and $V_\Gamma \subset V$ be the edge and vertex sets of Γ. Since $C_2(\Gamma)$ is zero, the short exact sequence

$$0 \longrightarrow C_*(\Gamma) \longrightarrow C_*(\Sigma) \longrightarrow C_*(\Sigma,\Gamma) \longrightarrow 0$$

of chain-complexes is equivalent to the commutative diagram shown in figure D.4, in which the columns are exact. This gives rise to the following long exact homology sequence.

$$0 \longrightarrow H_2(\Sigma) \longrightarrow H_2(\Sigma,\Gamma) \longrightarrow H_1(\Gamma) \longrightarrow H_1(\Sigma) \longrightarrow H_1(\Sigma,\Gamma) \longrightarrow$$
$$\longrightarrow H_0(\Gamma) \longrightarrow H_0(\Sigma) \longrightarrow H_0(\Sigma,\Gamma) \longrightarrow 0$$

Since the sequence is exact, the corresponding dimensions satisfy

$$h_2(\Sigma) - h_2(\Sigma,\Gamma) + h_1(\Gamma) - h_1(\Sigma) + h_1(\Sigma,\Gamma) - h_0(\Gamma) + h_0(\Sigma) - h_0(\Sigma,\Gamma) = 0.$$

Now assume that Σ is connected and Γ is non-empty, that is, $V_\Gamma \neq \emptyset$. Then $h_0(\Sigma,\Gamma) = 0$, because from every vertex of Σ there is a path to a vertex of the graph Γ. Also,

$$h_1(\Gamma) - h_0(\Gamma) = |E_\Gamma| - |V_\Gamma|$$

and

$$h_2(\Sigma) - h_1(\Sigma) + h_0(\Sigma) = |F| - |E| + |V|,$$

and hence,
$$h_2(\Sigma, \Gamma) - |E_\Gamma| + |V_\Gamma| = |F| - |E| + |V| + h_1(\Sigma, \Gamma).$$
Now, $h_2(\Sigma, \Gamma)$ is the number of regions into which the graph Γ separates the cellular surface Σ. By Lefschetz-duality $h_1(\Sigma, \Gamma) = h_1(\Sigma^* \setminus \Gamma)$. Suppose Γ separates Σ^* into the components $\Pi_1, \ldots, \Pi_n$; then $h_1(\Sigma^* \setminus \Gamma) = \sum h_1(\Pi_j)$.

This completes the proof of lemma 2.14.

Bibliography

[1] E. M. Andreev. On convex polyhedra in Lobačevskiĭ spaces. *Math. USSR, Sb.*, 10:413–440, 1970.

[2] E. M. Andreev. On convex polyhedra of finite volume in Lobačevskiĭ spaces. *Math. USSR, Sb.*, 12:255–259, 1970.

[3] V. I. Arnold. *Mathematical Methods of Classical Mechanics*. Springer-Verlag, New York, 1978.

[4] BeanShell. Lightweight scripting for Java. `http://www.beanshell.org/`.

[5] A. F. Beardon. *The Geometry of Discrete Groups*, volume 91 of *Graduate Texts in Mathematics*. Springer-Verlag, New York, 1983.

[6] A. I. Bobenko, T. Hoffmann, and B. A. Springborn. Minimal surfaces from circle patterns: Geometry from combinatorics. `arXiv:math.DG/0305184`, May 2003.

[7] A. I. Bobenko and B. A. Springborn. Variational principles for circle patterns and Koebe's theorem. *Trans. Amer. Math. Soc.*, 356:659–689, 2004.

[8] A. I. Bobenko and Yu. B. Suris. Integrable systems on quad-graphs. *Int. Math. Res. Not.*, 2002(11):573–611, 2002.

[9] B. H. Bowditch. Singular euclidean structures on surfaces. *J. London Math. Soc. (2)*, 44:553–565, 1991.

[10] Ph. L. Bowers and M. K. Hurdal. Planar conformal mappings of piecewise flat surfaces. In H.-C. Hege and K. Polthier, editors, *Visualization and Mathematics III*, pages 3–34. Springer-Verlag, New York, 2003.

[11] Ph. L. Bowers and K. Stephenson. A branched Andreev-Thurston theorem for circle packings of the sphere. *Proc. London. Math. Soc.*, 73:185–215, 1996.

[12] W. Brägger. Kreispackungen und Triangulierungen. *Enseign. Math.*, 38:201–217, 1992.

[13] G. R. Brightwell and E. R. Scheinerman. Representations of planar graphs. *SIAM J. Disc. Math.*, 6(2):214–229, 1993.

[14] B. Chow and F. Luo. Combinatorial Ricci flows on surfaces. `arXiv:math.DG/0211256`, Nov. 2002.

[15] Th. Clausen. Ueber die Function $\sin \varphi + \frac{1}{2^2} \sin 2\varphi + \frac{1}{3^2} \sin 3\varphi +$ etc. *J. Reine Angew. Math.*, 8:298–300, 1832.

[16] Y. Colin de Verdière. Un principe variationnel pour les empilements de cercles. *Invent. Math.*, 104:655–669, 1991.

[17] C. R. Collins and K. Stephenson. A circle packing algorithm. *Comput. Geom.*, 25:233–256, 2003.

[18] L. R. Ford, Jr. and D. R. Fulkerson. *Flows in Networks*. Princeton University Press, Princeton, 1962.

[19] B. T. Garrett. Circle packings and polyhedral surfaces. *Discrete Comput. Geom.*, 8:429–440, 1992.

[20] P. J. Giblin. *Graphs, Surfaces and Homology*. Chapman and Hall, London, 1977.

[21] Zh. He and O. Schramm. The C^∞-convergence of hexagonal disk packings to the Riemann map. *Acta Math.*, 180:219–245, 1998.

[22] D. M. Jackson and T. I. Visentin. *An Atlas of the Smaller Maps in Orientable and Nonorientable Surfaces*. CRC Press Series on Discrete Mathematics and its Applications. Chapman & Hall/CRC, 2001.

[23] A. Jacques. Constellations et graphes topologiques. In P. Erdős, A. Rényi, and V. T. Sós, editors, *Colloquia Mathematica Societatis János Bolyai 4, Combinatorial Theory and its Applications*, pages 657–673. North-Holland, 1970.

[24] jtem: Java Tools for Experimental Mathematics. `http://www.jtem.de/`.

[25] H. Kneser. Der Simplexinhalt in der nichteuklidischen Geometrie. *Deutsche Math.*, 1:337–340, 1936.

[26] P. Koebe. Kontaktprobleme der konformen Abbildung. *Abh. Sächs. Akad. Wiss. Leipzig Math.-Natur. Kl.*, 88:141–164, 1936.

[27] G. Leibon. *Random Delaunay Triangulations, the Thurston-Andreev Theorem, and Metric Uniformization*. Ph.D. thesis, University of California, San Diego, 1999. `arXiv:math.DG/0011016`, Nov. 2000.

[28] G. Leibon. Characterizing the Delaunay decompositions of compact hyperbolic surfaces. *Geom. Topol.*, 6:361–391, 2002.

[29] L. Lewin. *Polylogarithms and Associated Functions*. North Holland, New York, 1981.

[30] N. J. Lobatschefskij. Anwendung der imaginären Geometrie auf einige Integrale. In H. Liebmann, editor, *N. J. Lobatschefskijs imaginäre Geometrie und Anwendung der imaginären Geometrie auf einige Integrale*, number 19 in Abhandlungen zur Geschichte der mathematischen Wissenschaften mit Einschluss ihrer Anwendungen. B. G. Teubner Verlag, Leipzig, 1904. German translation from the Russian original by the editor.

[31] J. Milnor. Hyperbolic geometry: the first 150 years. *Bull. Amer. Math. Soc.*, 6(1):9–24, 1982.

[32] K. Perlin. Java 1.1 3D renderer. `http://mrl.nyu.edu/~perlin/render`.

[33] W. H. Press, S. A. Teukolsky, W. T. Vetterling, and B. P. Flannery. *Numerical recipes in C*. Cambridge University Press, Cambridge, 2nd edition, 1992.

[34] I. Rivin. Euclidean structures of simplicial surfaces and hyperbolic volume. *Ann. of Math.*, 139:553–580, 1994.

[35] I. Rivin. A characterization of ideal polyhedra in hyperbolic 3-space. *Ann. of Math.*, 143:51–70, 1996.

[36] I. Rivin. Combinatorial optimization in geometry. *Adv. in Appl. Math.*, 31(1):242–271, 2003.

[37] B. Rodin and D. Sullivan. The convergence of circle packings to the Riemann mapping. *J. Differential Geom.*, 26:349–360, 1987.

[38] L. Schläfli. Theorie der vielfachen Kontinuität. In *Gesammelte mathematische Abhandlungen*, volume I. Verlag Birkhäuser, Basel, 1950.

[39] J.-M. Schlenker. Hyperbolic manifolds with polyhedral boundary. `arXiv:math.GT/0111136`, Nov. 2001.

[40] O. Schramm. How to cage an egg. *Invent. Math.*, 107(3):543–560, 1992.

[41] O. Schramm. Circle patterns with the combinatorics of the square grid. *Duke Math. J.*, 86:347–389, 1997.

[42] B. A. Springborn. Consticting circle patterns using a new functional. In H.-C. Hege and K. Polthier, editors, *Visualization and Mathematics III*, pages 59–68. Springer-Verlag, Berlin, 2003.

[43] E. Steinitz. Polyeder und Raumeinteilungen. In *Encyclopädie der mathematischen Wissenschaften*, volume III (Geometrie), pages 1–139. B. G. Teubner, Leipzig, 1922. Part IIIAB12.

[44] E. Steinitz and H. Rademacher. *Vorlesungen über die Theorie der Polyeder*. Springer, Berlin, 1934.

[45] W. P. Thurston. The geometry and topology of three-manifolds. Electronic version 1.0 of 1997. A version is currently available from the MSRI at the URL `http://www.msri.org/publications/books/gt3m/`.

[46] W. T. Tutte. What is a map? In F. Harary, editor, *New Directions in the Theory of Graphs (Proc. Third Ann Arbor Conf., Univ. Michigan, Ann Arbor, Mich., 1971)*, pages 309–325, New York, 1973. Academic Press.

[47] G. M. Ziegler. *Lectures on Polytopes*. Springer-Verlag, Berlin, 1995.